SUBSTRATE EXCHANGE IN THE WATER-OXIDISING COMPLEX OF PHOTOSYSTEM II

BY WARWICK HILLIER

PHD

THE AUSTRALIAN NATIONAL UNIVERSITY, 1998

A THESIS SUBMITTED FOR THE DEGREE OF DOCTOR OF PHILOSOPHY OF THE AUSTRALIAN NATIONAL UNIVERSITY.

FEBRUARY, 1999.

Declaration

Except where otherwise acknowledged,
the work in this thesis is my own

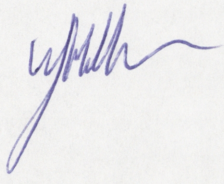

Warwick Hillier
February, 1999

Publications

Hillier, W., Messinger, J., & Wydrzynski, T. (1998) Kinetic determination of the fast exchanging substrate water molecule in the S_3 state of photosystem II. Biochemistry 37, 16908-16914.

Hillier, W., Messinger, J., & Wydrzynski, T. (1998) Substrate water ^{18}O exchange kinetics in the S_2 state of photosystem II. In *Proceedings of the 11th International Conference in Photosynthesis*, (G. Gareb ed.) Kluwer Academic Publishers, The Netherlands.

Acknowledgments

A sincere thank you to all of the following:

Tom Wydrzynski for encouragement, guidance and support over the years. I hope to one day attain your creativity and ability to explore and develop new areas of research.

Ron Pace for many solid (thermo)dynamic discussions. I aspire to one day emulate your inquiring mind.

Johannes Messinger for advice and recommendations on details of the Kok cycle that only he can know.

Murray Badger for his technical advice and assistance in the often daily struggle to keep the vacuum pumping and the data recording.

Alan Sargeson for advice on when a ligand is not a ligand.

Barry Osmond, not least of all for providing a pleasant and enlightening work place, but also for his enthusiasm in science.

Synopsis

The objectives of my thesis research were to develop kinetically faster and multi-flash techniques to measure the exchange kinetics of the two substrate water molecules during the photosynthetic water oxidation reaction sequence. This was performed using time-resolved mass spectrometry and a custom-built, rapid-mixing injection system for the addition of ^{18}O labelled water.

Measurements of ^{18}O exchange were performed on spinach thylakoid membranes as a function of S-states: S_0, S_1, S_2 and S_3. The exchange of one substrate water molecule was resolved from S_0 through to the S_3 state. The second substrate water molecule was resolved only in the S_3 state. The marked S-state dependence of the first substrate water molecule revealed exchange rates of 14 s^{-1} for S_0, 0.02 s^{-1} for S_1, 2.2 s^{-1} for S_2 and 2.2 s^{-1} for S_3 at 10°C. The second substrate water undergoes rapid exchange and was only resolved in the S_3 state, with an exchange rate of 37 s^{-1}. The exchange measurements show conclusively that one substrate water molecule is bound to the catalytic site beginning in S_0 while the second substrate water molecules is bound at least in the S_3 state. It is possible that the second substrate is either in very fast exchange in the S_0, S_1, and S_2 states or it enters into the catalytic site during the transition prior to the S_3 state.

A range of biochemically modified PSII sample preparations were used to investigate the details of ^{18}O exchange in the S_3 state. Treatments were undertaken to remove the extrinsic 16, 23 and 33 kDa proteins and to deplete/reconstitute the sample with Ca^{2+} and anion cofactors. The success of these procedures was determined with steady-state and flash-induced O_2 yield measurements. Two phases of ^{18}O exchange were consistently found in all treated samples; yet, surprisingly, there were only relatively small effects on the magnitude of the kinetics indicating that the two substrate binding sites are affected by relatively minor structural covering energies of ~2 kJ mol^{-1}. Measurements of the ^{18}O exchange in the S_3 state of spinach thylakoid membranes were also undertaken with non-invasive treatments to examine the dependence on pH, solvent effects by ethylene glycol, and the secondary isotope effects of D_2O. The results from the ethylene glycol treatment indicate that small, apparent structural changes to the catalytic site are not necessarily linked to changes in O_2 evolution activity. The pH dependence indicate that the exchange reactions were not limited by protonation and the D_2O effects indicate that the substrate water molecule in fast exchange in the S_3 state is H-bonded. The results are discussed in terms of various exchange mechanisms for water bound at a metal site and a phenomenological scheme is presented to account for the observed effects.

TABLE OF CONTENTS

LIST OF FIGURES

LIST OF TABLES

LIST OF EQUATIONS

ABBREVIATIONS

CCP	cytochrome *c* peroxidase
Chl	chlorophyll
EDTA	ethylenediaminetetraacetic acid
EGTA	ethylene glycol bis(β-aminoethyl ether)-N,N,N',N'-tetraacetic acid
EPR	electron paramagnetic resonance
EXAFS	extended X-ray absorption edge fine structure
HEPES	4-(2-hydroxyethyl)-1-piperazinesulfonic acid
HRP	horseradish peroxidase
MES	4-morpholinoethanesulfonic acid
NMR	nuclear magnetic resonance
P680	primary electron donor chlorophyll molecule in PSII
PAGE	polyacrylamide gel electrophoresis
Pheo	primary electron acceptor pheophytin molecule in PSII
PPBQ	p-phenylbenzoquinone
PRE	proton relaxation enhancement
PSI	photosystem I
PSII	photosystem II
Q_A	primary quinone acceptor molecule
Q_B	secondary quinone acceptor molecule
SDS	sodium dodecylsulfate
WOC	water oxidising complex
XANES	X-ray absorption near edge structure
Y_{2x}	oxygen yield due to a double hit
Y_3	oxygen yield on the third flash
Y_D	oxidisable tyrosine residue
Y_{inj}	oxygen yield from $H_2{}^{18}O$ injection.
Y_Z	tyrosine electron donor to $P680^+$

CHAPTER 1

1. INTRODUCTION TO PHOTOSYNTHETIC WATER OXIDATION

1.1 Evolution of Oxygenic Photosynthesis

Molecular oxygen began to accumulate in the earth's atmosphere about 3.5 billion years ago and it is widely believed that it had a photosynthetic origin. The accumulation of O_2 in the atmosphere marked the single most dramatic event in the earth's biosphere when the atmosphere underwent conversion from an initial reducing condition to an oxidising one. All pre-existing lifeforms had at that point either to find an anaerobic ecological niche or adapt to the ever increasing levels of O_2. Those that adapted, developed a diverse series of defensive and radical scavenging mechanisms to combat the general thermodynamic reactivity of oxygen.

Today on earth the photosynthetic O_2 generators (some might argue polluters) are widely distributed on the land as well as in the oceans and form an essential link in the biosphere. The enzyme performing oxygen evolution is called photosystem II (PSII) and is a photosynthetic reaction present in all plants and algae that contain the pigment chlorophyll *a*. The PSII reaction centre is not the only photosynthetic reaction centre - at least four other types exist - but it is the only reaction centre capable of generating redox potentials of > +1 V and coupling this potential via a unique protein motif comprising a redox active tyrosine residue and cluster of 4 Mn ions to oxidise water (Hansson & Wydrzynski, 1990; Debus, 1992; Rutherford, 1992; Britt, 1996). This protein motif is often simply termed the water oxidising complex (WOC) and is the site of the four electron water oxidation chemistry. The uniqueness of this site is a clear indication of the specificity and difficulty to catalyse water oxidation.

The incorporation of manganese as the metallo site for water oxidation is not just coincidence. Manganese can have a number of redox states and turns out to be one of earth's more abundant elements (12^{th}). The involvement of Mn in redox-active proteins is not limited to PSII. Indeed, Mn is found in several enzymes that participate in the chemistry of reactive oxygen species, eg. the Mn catalase which contains a binuclear Mn site that cycles between $Mn^{II}Mn^{II}$ and $Mn^{III}Mn^{III}$, a Mn superoxidase dismutase, a Mn peroxidase, and a Mn ribonucleotide reductase [for a review see Dismukes, 1996]. The uniqueness of the PSII WOC is that 4 Mn ions are involved and that the Mn is suggested to cycle through the Mn^{IV} oxidation state.

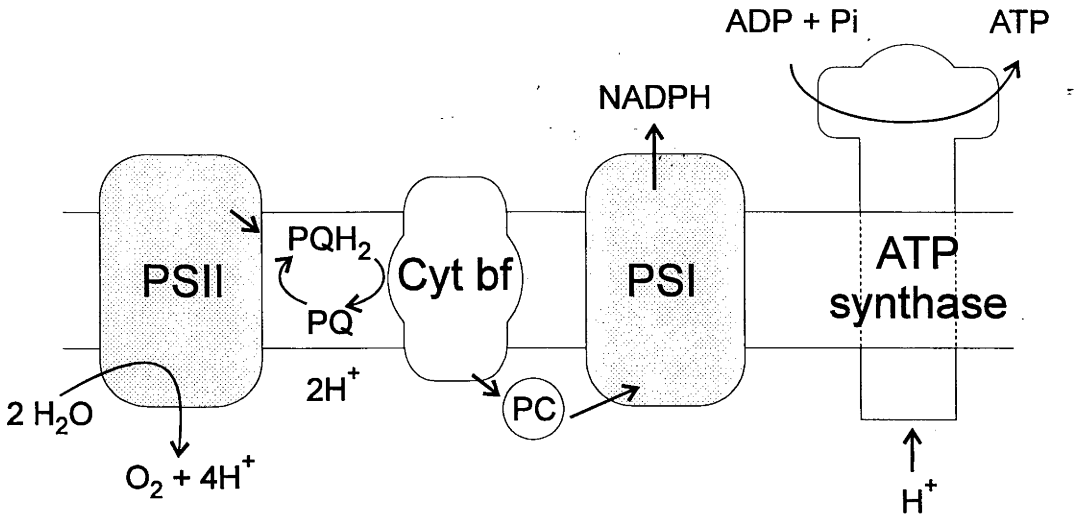

Figure 1-1 **The linear photosynthetic electron transport chain in higher plants.**

1.2 The Photosynthetic Electron Transport Chain

Photosystem II (PSII) where the oxidation of water occurs is the first integral component in the linear photosynthetic electron transport chain of higher plants which provides electrons for the reduction of $NADP^+$. The photosynthetic electron transport chain contains three additional integral membrane components: the cytochrome bf complex (cyt bf), photosystem I (PSI) and an ATP synthase. Electron transfer between the two photosystems and cyt bf is mediated by two pools of mobile electron carriers: plastoquinone (PQ), which links PSII to cyt bf, and plastocyanin (PC) which links cyt bf to PSI. The two photosystems act together in the net oxidation of water and reduction of $NADP^+$. During electron transport a proton gradient is generated across the thylakoid membrane through release of protons from water oxidation and plastoquinol (PQH_2) oxidation. The proton gradient is dissipated by the rotary F_0-F_1 ATP synthase. A diagram of the linear electron transport chain is given in Figure 1.1.

Photosystem II itself is a multiprotein complex that contains at least 25 polypeptides. Central to the function and structure of PSII are the D1 and D2 heterodimeric polypeptides which bind the special primary electron donor P680 chlorophyll and the pheophytin (Pheo) acceptor molecules. The D1/D2 heterodimer appears to be structurally related to the photosynthetic purple bacterial reaction centre, particularly around the acceptor side components (Michel & Deisenhofer, 1988) although additional protein(s) (eg. *psb* L) appear to be also required for the *in vitro* coordination of the quinone acceptor molecules (Q_A and Q_B) (Nagatsuka *et al.*, 1991; Araga *et al.*, 1993; Kitamura *et al.*, 1994). Current structural models of PSII are derived primarily from

Table 1-1 Polypeptides found in the PSII complex

Gene	Polypeptide	Mr. (kDa)	Location: Function
psb A[1]	D1	32	RC: Y_Z, binds P680, Pheo, Q_B & Mn
psb B[1]	CP47	47-51	RC:Chl *a* binding inner antenna
psb C[1]	CP43	43-47	RC:Chl *a* binding inner antenna
psb D[1]	D2	34	RC: Y_D, binds P680, Pheo, Q_A & Mn
psb E[1]	Cyt b559 α	9	RC
psb F[1]	Cyt b559 β	4	RC
psb H[1]	H	7.6	Phosphoprotein
psb I[1]	I	4.2	RC:
psb J[1,4]	J	<5	Intrinsic
psb K[1]	K	4.3	RCC
psb L[1]	L	4.3	RCC
psb M[1,4]	M	3.8	RCC
psb N[1,4]	N	4.7	RCC
psb O[2]	33 kDa	33	Extrinsic
psb P[2,3]	23 kDa	23	Extrinsic
psb Q[2,3]	16 kDa	16	Extrinsic
psb R[2,3]	10 kDa	10	Extrinsic
psb S[2]	CP22, S	22	Inner antenna
psb T[2]	T	11	
psb U[1,4]	V	9-12	Extrinsic
psb V[1,4]	Cyt c_{550}	16	Extrinsic
psb W[2]	W	6.1	RC
psb X	X	4.1	
psb Y	Y	20	
Lhcb 1[2]	LHCIII	28	Antenna
Lhcb 2[2]	LHCIII	27	Antenna
Lhcb 3[2]	LHCIII	25	Antenna
Lhcb 4[2]	CP29	30	Antenna
Lhcb 5[2]	CP26	29	Antenna
Lhcb 6[2]	CP24	20	Antenna

(1) chloroplast encoded gene; (2) nuclear encoded gene; (3) polypeptide found only in plants; (4) polypeptide found only in cyanobacteria; (RC) reaction centre and (RCC) reaction centre core location.

spectroscopy (Diner & Babcock, 1996) and sequence comparisons between the D1/D2 heterodimer and the bacterial reaction centre (Svensson *et al.*, 1996; Xiong *et al.*, 1998). Recently there has there been some low resolution 3D structural information (8 Å) to support the prevailing models (Rhee *et al.*, 1998). The donor side and the unique WOC has the least structural information available. A list of PSII associated polypeptides is given in Table 1.1.

The biochemistry, spectroscopy and activity measurements of PSII were initially limited to either chloroplast or thylakoid membrane samples. Subsequent isolation techniques incorporating detergents were used to prepare PSII-enriched membrane fragments from thylakoids (Berthold *et al.*, 1981; Kuwabara & Murata, 1982). Such sample preparations resulted in enormous advances in the understanding of PSII but aspects of

optical spectroscopy required better samples. Further purification of discrete PSII core complexes was made possible by employing non-ionic detergents and ion exchange chromatography or density centrifugation (Ikeuchi *et al.,* 1985; Satoh *et al.,* 1985; Tang & Satoh, 1985; Ghanotakis *et al.,* 1987; van Leeuwen *et al.,* 1991). These core preparations constitute the minimal PSII complex capable of O_2 evolving activity and contain the D1, D2, cyt b559, the chl *a* binding proteins CP43 and CP47, varying degrees of the chl *a/b* proteins CP24, CP26 and CP29 as well as several low molecular weight proteins including *psb* I, *psb* W and *psb* L. Further detergent solubilisation can be undertaken to isolate PSII reaction centre preparations (Namba & Satoh, 1987) which contain only the D1, D2, cyt b559 and *psb* I/*psb* W polypeptides [also see Satoh, 1996]. The reaction centre preparations contain 6 Chl *a* molecules per 2 pheophytins and can undergo the primary photochemical events. The pigments for the primary photochemistry are apparently bound only to the D1/D2 complex as the *psb* I and cyt b559 components can be removed without destroying photochemistry (Tang *et al.,* 1990). An important point for the understanding of PSII is that the vast majority of the PSII polypeptides appear only peripheral to D1 and D2. Some are obviously involved in light harvesting but many are enigmatic and their precise functional role remains undetermined.

1.3 Photosystem II Photochemistry and Charge Separation

The PSII water oxidation reaction is driven photochemically by the capture of light quanta. The surrounding chl *a/b* binding proteins serve as a light-harvesting antenna and deliver spectrally diverse quanta to the reaction centre chlorophyll molecule P680. Excitation of P680 generates an excited state (P680-Pheo)* which is in equilibrium with the exciton in the antenna and the charge separated state ($P680^+$ $Pheo^-$) (Dau, 1994). The time course of this reaction is under some contention with one group reporting times in the order of 3-8 ps (Wasielewski *et al.,* 1989; Greenfield *et al.,* 1997) and another reporting a longer time of ~20 ps (Hastings *et al.,* 1993; Klug *et al.,* 1995). The primary charge separation is rapidly followed by a charge stabilisation reaction in 300-500 ps resulting in the formation of $P680^+$ Q_A^- (Nuijs *et al.,* 1986; Schatz *et al.,* 1987). The electron hole is then transferred within some 40-280 ns from $P680^+$ to the D1 amino acid residue Y_Z (Brettel *et al.,* 1984; Meyer *et al.,* 1989) resulting in the formation of Y_Z^+ P680 Pheo Q_A^-. Finally the electron at Q_A^- is passed to Q_B^- site in 100-200 μs (Robinson & Crofts, 1983) and the Y_Z^+ is rereduced by the WOC with S-state dependent kinetics in the range 30-1300

μs (Babcock *et al.*, 1976; Razeghifard *et al.*, 1997). Blockage of the any of the forward reactions results in charge recombination with the possible formation of triplet states.

1.4 The Four Electron Water Oxidation Reaction

One of the key findings for the understanding of the water oxidation reaction mechanism was the observation that dark-adapted, PSII-containing samples release O_2 with a damped periodicity of four upon illumination with single turnover light flashes (Joliot, 1969). The phenomenological model to explain this observation was proposed by Kok and coworkers (Kok *et al.*, 1970) and invoked a cyclic reaction sequence through five intermediary states called the S-states. Beginning in S_0 and traversing to S_4, each S-state is advanced by a single quantum event. Upon reaching the S_4 state, O_2 is released (within 1-2 ms), S_0 is regenerated, and the cycle begins anew. The S-state cycle is illustrated below.

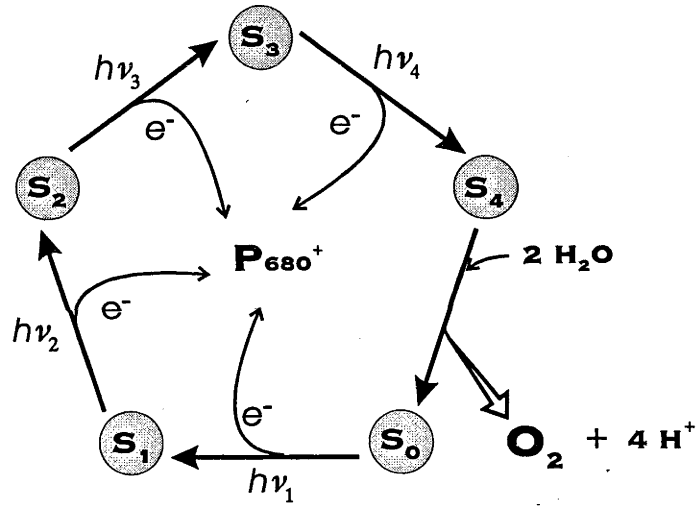

Figure 1-2 **Kok's S-state sequence.**

In the original Kok model the damping in the O_2 flash yield oscillations, or the effective desynchronisation of the S-state transitions, was accounted for by a miss parameter (α), representing the loss of the electron hole from the WOC or a failure of a trapping centre to complete the photochemistry, and a double hit parameter (β) representing a double excitation event (Forbush *et al.*, 1971). To explain the peak O_2 release on the third flash, the S_1 state was concluded to be dark stable.

The higher S-states (S_2, S_3) exhibit lifetimes from tens of seconds to several minutes, depending on the temperature, and effectively deactivate to the S_1 state (Forbrush *et al.*, 1971; Rutherford *et al.*, 1984; Messinger *et al.*, 1993). The S_0 state also exhibits a slow

relaxation to the S_1 state in tens of minutes (Vermaas *et al.*, 1984; Messinger *et al.*, 1993). This is a consequence of electron transfer to the tyrosine Y_D resulting in S_0Y_D becoming $S_1Y_D^{OX}$ (Styring & Rutherford, 1987). In addition there are proposed super-reduced S-states (S_{-1}, S_{-2}, S_{-3}) that are observable by addition of exogenous reductants such as hydroxylamine and hydrazine (Bouges, 1971; Kok & Velthuys, 1977; Beck & Brudvig, 1988; Messinger *et al.*, 1991; 1997b). Although these super-reduced states have as yet no demonstrated role in water oxidation, their discovery may place limitations on the oxidation states of the WOC.

1.5 Thermodynamic Issues

The photochemistry at the PSII reaction centre is driven by photons at 680 nm or shorter wavelength providing a maximum of 1.84 V for the excited state. The $P680^+$ midpoint potential Em is ~1.12 V (Klimov *et al.*, 1979) and the Q_A/Q_A^- Em is ~-0.08 V (Krieger *et al.*, 1995); thus, a 680 nm photon (1.84 V) is converted to a potential of ~1.2 V in the charge stabilised state which corresponds to a photochemical conversion efficiency of ~65%. If the same energetic comparison is made for the purple bacterial reaction centre, P870, a considerably lower efficiency of ~36% is found (Diner & Babcock, 1996). The apparent reason for the additional conversion efficiency in PSII is the considerably increased oxidation potential of $P680^+$ which is +0.5 V more oxidising than the bacterial $P870^+$. Recently, it has been demonstrated that the bacterial reaction centre midpoint potential can be fine tuned by the electrostatic interactions of neighbouring ligands (Artz *et al.*, 1997). Thus, the reason for the additional oxidising potential of $P680^+$ may also be related to stronger electrostatic interactions of the surrounding ligands in PSII reaction centre.

The overall efficiency of PSII is crucial for the photochemically driven oxidation of water. Depending on the water oxidation pathway there can be several different redox intermediates. Possible intermediates are shown in Figure 1.3 and the lower dotted line from the origin represents a theoretical minium value of 0.81 V per electron step for a concerted 4 step oxidation of water. As the oxidation potential of the WOC is < 1.1 V, some intermediates are unlikely to be attainable based on theoretical considerations. It is for this reason that the concerted path is favoured by many as the WOC would then essentially bypass all high energy (>1 V) intermediates.

Another mechanistic consideration is the storage of charge on PSII and the concept of electroneutrality. Accumulation of oxidation potential is energetically very costly in a

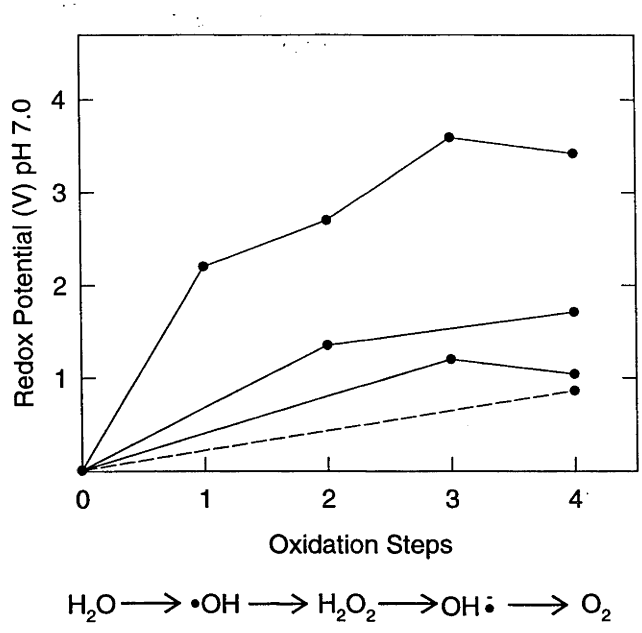

Figure 1-3 **A diagram of the redox potentials for various potential intermediates of water oxidation. The solid line represents oxidation via sequential oxidation events and the dotted line is the path of lowest potential via a concerted 4 electron oxidation pathway. The text indicates the molecular entities derived from the oxidation steps.**

low dielectric region of a protein (Rich, 1996). Recent models in PSII have invoked a mechanism whereby the WOC can accumulate oxidation potential without the net accumulation of charge through successive deprotonation events on the substrate water (Tommos & Babcock, 1998) thereby maintaining electroneutrality.

1.6 Molecular Organisation of the Mn_4 complex

Four Mn ions are bound in the WOC and serve as part of the catalytic site for water oxidation. The precise location of the Mn ions has not yet been determined although evidence from site-directed mutagenesis of cyanobacterial PSII suggests that a number of amino acid residues from the D1 and D2 polypeptides are involved (see Britt, 1996 and references therein). In particular, there is good evidence that at least one histidine residue provides a ligand (Tang *et al.*, 1994; but see also Preston & Seibert, 1991). However, a particular difficulty in assigning Mn ligands has been the overall inherent complexity of the PSII WOC system. Mutations resulting in apparent decreases in O_2 evolution activity may not necessarily reflect Mn binding but rather may represent Ca

binding, blockage of the photoassembly of the Mn cluster, disruption of electron transfer between $P680^+$ and Y_Z, or disruption in proton release pathways. Thus, although it is generally expected that the ligands to the Mn are derived only from the D1 and D2 polypeptides only a few candidates have been definitively identified. It is attractive then to suggest that other polypeptides may be involved in the ligation of the Mn_4 cluster. Indeed, studies with the neighbouring CP43 and CP47 have shown that their long lumenal domains are important in maintaining O_2 evolution activity and may be involved in Mn binding (Eaton-Rye & Vermaas 1991; Kuhn & Vermaas, 1993). There are in addition a number of low molecular weight polypeptides (*psb* I, *psb* L, *psb* W) which are closely associated with the reaction centre (Ikeuchi & Inoue, 1988; Ikeuchi *et al.,* 1989; Shi & Schroder, 1997) and remain functionally ill-defined.

An important finding for the understanding of Mn interactions within the WOC was the discovery of an electron paramagnetic resonance (EPR) signal arising from the S_2 state (Dismukes & Siderer, 1981). Centred at g ~2 with a width of ~1700 gauss and exhibiting at least 18 lines, the signal, commonly referred to as the multiline signal, is minimally derived from a mixed valence Mn dimer which incorporates additional magnetic interactions to enhance the linewidth. One explanation for this enhanced linewidth is that the complex is in fact a magnetically coupled tetranuclear cluster (Britt, 1996). However, an alternate explanation invokes a Mn dimer with special quadrupolar interactions (Åhrling & Pace 1995). A second S_2 EPR signal was also identified at g ~4.1 (Casey and Sauer, 1984, Zimmermann and Rutherford, 1984) and is consistent with a different structural state of the Mn complex. Both S_2 EPR signals are observable only at low temperatures (< 35°K). Subsequent EPR investigations have also identified Mn EPR signals from S_0 (Åhrling *et al.,* 1997; Messinger *et al.,* 1997a) and S_1 states (Dexhimer & Klein, 1992; Yamauchi *et al.,* 1997) which will provide important information about the organisation of the Mn_4 complex.

A second technique applied to elucidate the organisation of the Mn complex is X-ray absorption spectroscopy using synchrotron radiation. This technique can provide information about the ligand environment to the Mn as well as the oxidation states. The extended X-ray absorption edge fine structure (EXAFS) indicates that the Mn ions are in a homogenous structure with backscattering at ~1.9 Å from O/N ligands, ~2.7 Å from Mn-Mn and at ~3.3 Å from either Mn-Mn or Mn-Ca (Yachandra *et al.,* 1996; Penner-Hahn, 1998). Two Mn-Mn vectors are also observed at divergent vectors in oriented samples. The work of Yachandra *et al.,* (1996) indicates angles of ~ 55° and ~ 67° to the membrane

normal for the two 2.7 Å Mn and that of Schiller *et al.,* (1998) angles of ~80°. In addition, the inflection point of the X-ray absorption near edge structure (XANES) can provide information about the oxidation state of the Mn ions as a function of their S-state (Yachandra *et al.,* 1996; Penner-Hahn, 1998). Consensus on the earlier measurements suggests that the Mn oxidation increases on the S_0-S_1 and the S_1-S_2 transition. Interpretation, however, is divided as to whether there is a Mn oxidation increase on the S_2-S_3 transition (Ono *et al.,* 1992) or an ligand oxidation (Kusunoki *et al.,* 1993; Roelofs *et al.,* 1996). The Mn valence states as interpreted from X-ray absorption measurements suggest that the S_0 state contains either a Mn^{II}, Mn^{III}, Mn^{III}, Mn^{III} or a Mn^{II}, Mn^{III}, Mn^{IV}, Mn^{IV} configuration (Yachandra *et al.,* 1996; Penner-Hahn, 1998). Almost all models of the WOC invoke two Mn dimers separated by di μ-oxo bridges and typically include additional μ-carboxylo bridging ligands.

1.7 Extrinsic Proteins

A number of extrinsic proteins bind to PSII on the lumenal side of the thylakoid membrane and serve to optimise the oxygen evolution reaction. In higher plants three extrinsic proteins of 16, 23 and 33 kDa strongly influence the stability and activity of the WOC. Utilising selective techniques one or all of these extrinsic proteins can be removed (Debus, 1992; Seidler, 1996). Correlated with the loss of these proteins is a decrease in O_2 evolution activity and an apparent increase in generation of H_2O_2, as a water oxidation side product, as a consequence of compromised integrity of the WOC (Schröder & Åkerlund, 1986; Berg & Seibert, 1987; Hillier *et al.,* 1993) The extrinsic proteins do not appear to provide ligands to the Mn ions and higher plants (spinach) perform O_2 evolution in the complete absence of the 16, 23 and 33 kDa proteins with rates ~20% that of the control (Bricker, 1992). However, genetic deletion of the 33 kDa protein in the green algae *Chlamydomonas* indicates an essential requirement of the 33 kDa protein in this species (Mayfield *et al.,* 1987) Cyanobacterial PSII complexes have the 33 kDa extrinsic protein and appear to have analogous polypeptides to the 16 and 23 kDa proteins in the form of a 9 kDa and cyt c550 protein (Shen & Inoue, 1993). The cyanobacterium *Synechocystis* sp. PCC 6803 will grow photoautotrophically with the genetic deletion of the 33 kDa extrinsic protein (Burnap & Sherman, 1991; Mayes *et al.,* 1991; Philbrick *et al.,* 1991) but combined loss of the 33 kDa and the cyt c550 results in a photoheterotrophic strain (Shen *et al.,* 1995).

The extrinsic polypeptides therefore appear to stabilise the WOC cluster to varying degrees in different species. In higher plant (spinach) PSII, the absence of the 16, 23 and 33 kDa polypeptides results in a loss of 2 Mn ions from the WOC but the loss of the Mn is prevented by the presence of high (50-100 mM) Ca^{2+} and Cl^- ions in the suspending buffer media (Ono & Inoue, 1984; Kuwabara *et al.*, 1985). The function of the extrinsic proteins has been suggested to be involved in modulating of proposed cofactors Ca^{2+} and Cl^- to PSII (Seidler, 1996) but they also have a role in accessibility to the WOC as shown by the increased reactivity of exogenous reductants in the absence of the extrinsic polypeptides (Tamura *et al.*, 1990).

1.8 Ca, Cl, HCO_3 as Cofactors

Several ions have been suggested to be directly involved in the oxygen evolving reaction serving as catalytic cofactors. Ca^{2+} ions have been demonstrated to specificity restore O_2 evolving activity after various treatments which are believed to release bound functional Ca^{2+} ions from the WOC. Stiochiometrically 2 Ca^{2+} ions are bound to PSII samples; one of these Ca^{2+} ions is suggested to be located in the LHCII antenna while the second is believed to be associated directly with the WOC (Shen *et al.*, 1988; Ono & Inoue, 1988a). Treatment with either low pH (citrate, pH 3.0) or removal of 16 and 23 kDa proteins by 1-2M NaCl in conjunction with the ionophore A23187 and EGTA appears to release one Ca ion from PSII preparations (Ono & Inoue, 1988a; Cammarata & Cheniae, 1987) with a concurrent lowering in O_2 evolution activity. The loss in activity is then largely restored with the addition of high levels of exogenous Ca^{2+} ($\geq$ 10 mM). The binding of Ca^{2+} to PSII has been followed directly with $^{45}Ca^{2+}$ and supports the notion that these treatments do remove Ca^{2+} from a functional site resulting in a loss in the O_2 evolving activity (Ädelroth *et al.*, 1995). However, there are reports that Ca restorable activity can occur without release of Ca, suggesting there may be other Ca effects on O_2 activity (Shen & Katoh, 1991, although see Boussac & Rutherford, 1992a). Sr^{2+} ions have also been found to functionally replace Ca^{2+} ions in a partial restoration of total O_2 activity (Ghanotakis *et al.*, 1984). Samples that have been treated to deplete Ca appear to advance only to the S_2 state (Ono *et al.*, 1986) with consequent changes to the S_2 multiline EPR signal that is further modified upon Sr^{2+} reconstitution (Boussac & Rutherford, 1988; Boussac *et al.*, 1989). One EXAFS group has reported structural changes to the Mn_4 cluster upon Ca^{2+} depletion/Sr^{2+} reconstitution and interprets distance changes at 3.3Å as derived from both Mn-Mn and Mn-Ca interactions (Latimer *et al.*, 1995; 1998; Cinco *et al.*,

1998). Another group is unable to demonstrate any difference upon treatment and interprets only Mn-Mn inteactions at 3.3 Å (Riggs-Gelasco *et al.*, 1996). Therefor the precise functional role of the Ca^{2+} ion in the WOC remains unclear at the moment and although it does appear to be a prerequisite for the proper photoassembly of the Mn_4 complex (Chen *et al.*, 1995; Ananyev & Dismukes, 1997) it location is unclear.

Chloride has also been suggested to be a catalytic cofactor for the WOC based on treatments that reduce O_2 evolution activity and are subsequently restored upon addition of Cl^- ions. The reconstitution of activity, however, is not limited to Cl and can be replaced with other anions: $Cl^- > Br^- > I^- > NO_3^-$, in their decreasing order of effectiveness (Kelly & Izawa, 1978). The specific involvement of Cl^- in the catalytic reaction has been questioned in the literature (eg., Wydrzynski *et al.*, 1990; Pauly *et al.*, 1992). At present no conclusive evidence for direct Cl^- binding to the Mn cluster has been obtained using magnetic resonance or EXAFS measurements (Boussac, 1995; Yachandra et al 1996). In addition, quantitative binding measurements of Cl^- using radiolabelled $^{36}Cl^-$ shows a lack of direct correlation between the amount of halide and the extent of O_2 evolution activity (Lindberg *et al.*, 1990, 1993; Lindberg & Andréasson, 1996). Despite the $^{36}Cl^-$ findings, there is ample evidence to indicate that 'Cl depleted' samples are altered in terms of their PSII activity and spectroscopy. For example, the fast $P680^+$ rereduction kinetics clearly show that only two charges can be stably stored in the WOC after which increased charge recombination occurs in 'Cl depleted' samples (Ono *et al.*, 1986; Boussac *et al.*, 1992b; Lubbers *et al.*, 1993; Haumann *et al.*, 1996b). The EPR properties are also altered and it appears that 'Cl depleted' centres can be oxidised in the light to the S_2 state without giving rise to the characteristic multiline signal but which appears upon addition of Cl^- in the dark (Ono *et al.*, 1986). Thus, 'Cl depletion' appears to alter the redox potentials of the WOC but whether Cl^- is a direct prerequisite for the O_2 evolution reaction remains to be clarified.

It has also been proposed that bicarbonate is involved in the water oxidation reaction in photosystem II. The studies of effects of bicarbonate depletion were largely confined to the understanding of the electron transfer between Q_A and Q_B (Govindjee & Van Rensen, 1993) but more recent work has introduced the concept that the bicarbonate may well be a ligand to the Mn_4 complex in the WOC (Allakhverdiev *et al.*, 1997; Yruela *et al.*, 1998). Although this evidence is not yet unequivocal, bicarbonate as a ligand to the Mn could provide some of the yet to be accounted ligands to the Mn_4 cluster.

1.9 Substrate Water Measurements

In the original Kok model it could be inferred that the two substrate water molecules entered the reaction sequence during the last step, just prior to O_2 release (Kok *et al.*, 1970). Other models have also invoked this notion although more recent models predict substrate water binding to the WOC at the beginning of the S-state cycle (eg., Hoganson & Babcock, 1997; Tommos & Babcock, 1998; Witt, 1996; Pecoraro *et al.*, 1998; Limburg *et al.*, 1999). It is now generally favoured that a concerted four electron reaction during the S_4 to S_0 transition generates the O-O bond. Definitive experimental evidence on how and at which step the O-O bond is formed has, however, remained elusive but there have been three main experimental approaches to determine substrate water interactions at the catalytic site: proton release patterns, magnetic resonance of the Mn cluster, and oxygen isotope exchange by mass spectrometry.

1.9.1 Proton Release

The oxidation of two water molecules releases four protons and measurement of the extent and rate of proton release has provided a strong driving force into investigation of the mechanism of water oxidation. Initially a proton release pattern of 1:0:1:2 was supported by a number of other measurements (eg. electrochromism) but it became apparent that the proteins of PSII are able to modulate the release behaviour: PSII core samples, for example, exhibit a 1:1:1:1 pattern and thylakoids exhibit a strong pH dependence in the pattern (Lavergne & Junge, 1993). Measurements of proton release have also been performed in unstacked thylakoids to remove the kinetic limitations. These measurements revealed interestingly that the rate of H^+ release is on the same time scale as the oxidation of Y_Z (Haumann & Junge, 1994). This finding has been interpreted by some to indicate that proton release is derived from the oxidation of Y_Z directly (Hoganson *et al.*, 1995; Gilchrist *et al.*, 1995; Hoganson & Babcock, 1997). However, it is also argued that the proton release is not chemically derived from the deprotonation of Y_Z but is the result of electrostatically induced p*K* shifts of peripheral amino acids (Haumann & Junge, 1996; Ahlbrink *et al.*, 1988). The origin of the protons is currently hotly debated.

1.9.2 Magnetic Resonance

1.9.2.1 NMR Proton Relaxation

Paramagnetic relaxation of bulk water protons can be measured at room temperature by NMR techniques. The NMR-proton relaxation enhancement (NMR-PRE)

can then be used to investigate the interactions of solvent water with water bound in the coordination sphere of paramagnetic species such as Mn^{II} or Mn^{IV} ions. The NMR-PRE effects on PSII were first demonstrated by Wydrzynski *et al.,* (1976, 1978) and provide possibly the first direct evidence for Mn oxidation state changes during the S-state sequence. Subsequent NMR-PRE measurements were interpreted to invoke a Mn^{II} to Mn^{III} oxidation on the S_0 to S_1 transition, Mn^{III} to Mn^{IV} for the S_1-S_2 transition and no Mn oxidation on S_2-S_3 (Sharp, 1992). A key assumption in the interpretation of these results is that the PRE is directly governed by the rapid exchange between substrate water protons bound at the catalytic Mn site and the solvent protons. An important issue is how the surrounding protein matrix may influence the rate of proton exchange and in particular how various treatments may alter the rate of exchange. In particular, with respect to the effects of EDTA, one group (Sharp, 1992) has argued that the inclusion of EDTA is necessary to remove contributions of extraneous Mn ions, while the other group has suggested that EDTA alters the protein structure which changes the rate of proton exchange at the catalytic site (Wydrzynski & Renger, 1986). The issues of proton exchange and the involvement of EDTA have not yet been resolved and awaits further developments.

1.9.2.2 Continuous Wave EPR

Since the discovery of the S_2 state EPR Mn-multiline signal in PSII (Dismukes & Siderer, 1981) attempts have been made to try and identify interactions directly between the Mn_4 cluster and the substrate water. Several studies have utilised continuous wave (cw) -EPR measurements of PSII samples suspended in various isotopes of water to examine changes in hyperfine interactions through substrate water binding to the Mn. One of these studies (Hansson *et al.,* 1986) demonstrated a weak hyperfine broadening (< 0.5 mT) of the multiline signal in the presence of ^{17}O labelled water (spin, $I = 5/2$). However, because of the prolonged times used during sample preparation in this study, isotopic exchange at non-substrate-water oxygen ligands may have occurred. Other EPR studies were made of samples enriched with ^{2}H labelled water ($I = 1$); and again, in one case, a distinct hyperfine narrowing of the Mn multiline EPR signal was observed (Nugent, 1987). However, two other studies could not demonstrate the effect (Yachandra *et al.,* 1986; Haddy *et al.,* 1989). Thus, direct interactions between substrate water and the Mn using these cw techniques appears to be inconclusive at this point.

In another approach, it is known that water oxidation is inhibited by NH_3 and the multiline signal is modified. Two amine binding sites have been proposed in the WOC, one site that binds generic amines and is competitive with Cl^-, and a second (restricted) site that is non competitive with Cl^- and binds only NH_3 (Sandusky & Yocum, 1984; 1986). As NH_3 is isoelectronic with H_2O the second site is suggested to be a substrate H_2O binding site. Addition of NH_3 under conditions of high Cl concentration results in significant changes to the Mn multiline, with a narrowing of the hyperfine spacings that is interpreted to arise from the formation of a NH_2 imido bridges (Beck *et al.*, 1986; Beck & Brudvig, 1986; 1988; Brudvig & Beck, 1992). However, as the NH_3 - altered multiline signal undergoes period 4 oscillation, S-state cycling is not completely inhibited and the nature of the interaction has been questioned (Andréasson *et al.*, 1988; Boussac *et al.*, 1990).

1.9.2.3 Double Resonance and Pulsed EPR

In addition to the cw measurements, more sophisticated electron-nuclear double resonance (ENDOR) and electron spin echo envelope modulation (ESSEM) measurements have been undertaken to examine possible hyperfine interactions between water and water analogues and the EPR-detectable Mn. In one ENDOR study using cyanobacterial samples, no strong proton coupling could be observed as might be expected for a water ligand (Tang *et al.*, 1993). However, the authors considered that the signals may have been too broad and anisotropic and, due to limited sensitivity, could not therefore be resolved. In contrast, the results from two other ENDOR studies were interpreted to suggest that ^1H interactions do arise from water bound in the first coordination sphere of the Mn ions in the S_2 state (Kawamori *et al.*, 1989; Fiege *et al.*, 1996). In support of these observations are ESEEM studies utilising ^2H_2O and isotopically labelled (^{14}N, ^{15}N) ammonia as substrate analogues to the catalytic Mn (Britt *et al.*, 1989, 1990). In these cases the results also strongly suggested that substrate water does indeed bind to the catalytic Mn_4 cluster in the S_2 state and, via inference, in the S_1 state as well. The ammonia interactions were also interpreted as demonstrating a single NH_3-derived ligand consistent with an imido bridge. However, an earlier finding showed that the ^{17}O line broadening is superimposed on the ammonia modified EPR signal (Andréasson *et al.*, 1988) indicating that the *ammonia binding site* and the *^{17}O binding site* are separate. The most recent ESEEM report introduces more confusion to the understanding of the binding of the substrate water with the finding that there were no magnetic interactions between ^{17}O or ^2H enriched water and the EPR detected S_2 multiline signal (Turconi *et al.*, 1997). The authors

suggested that substrate water may interact at an S-state subsequent to S_2 or interact with non multiline Mn.

One general problem with the magnetic resonance approach to identify interactions between substrate water and the catalytic Mn is that it is difficult to unequivocally discriminate between the isotopic exchange by the substrate water and by other water, oxygen or proton ligands that may be in the first coordination sphere of the Mn cluster and also subject to exchange. A second problem is there is not yet complete agreement in the literature as to the origin of the S_2 state EPR signals, i.e. whether they arise from magnetic interactions between a di- or a tetra-nuclear Mn complex (Britt , 1996; Åhrling & Styring, 1999). If the EPR signals arise from only part of the functional Mn, then perhaps only part of the Mn-water interactions is observable. A third problem with the magnetic resonance approach is that line-broadening effects through quadrupole effects by ^{17}O nuclei may obscure other magnetic interactions.

1.9.3 Mass Spectrometry

In an alternative approach to studying the interactions between the substrate water and the catalytic site, isotopic exchange measurements of labelled water can be made of photogenerated O_2 using mass spectrometric techniques. This technique deals only with exchange of the substrate water but is open to interpretation regarding the nature of the binding site. The experimental protocol essentially involves rapid transfer of PSII samples from ^{16}O labelled water to ^{18}O labelled water (or vice versa) and then measurement of the photogenerated ^{18}O labelled oxygen products. The first measurements of this type were made by Radmer and Ollinger (1980). They found that following the addition of $H_2{}^{18}O$ the same isotopic composition was evolved in the photogenerated O_2. From this finding their interpretations favoured the idea that there was no bound substrate water in the S_1 state as they expected water to be strongly bound and exchanging slowly at a higher oxidation state Mn ion. A follow up study on the S_2 and S_3 states also revealed "no nonexchangeable water" in S_2 or S_3 states (Radmer & Ollinger, 1986). The authors again favoured the idea that there was no bound H_2O intermediates and suggested that the substrate water entered only during the final S_3-S_4-S_0 transition. The Radmer and Ollinger series of experiments were, however, restricted to a kinetic resolution of no better than ~30 s due to sampling and stabilisation times for their measuring system. Thus, being kinetically limited, they left open the possibility that more rapid exchange of substrate water could occur but considered it as unlikely. Interest in this area was sustained at the

time with further measurements on the S_3 state (Bader *et al.,* 1987). In this work the S_3 state was also found to undergo rapid exchange and by inference suggested not to contain O_2 precursors or bound water derivatives. However, as all mass spectrometric measurements up to this point were limited to a kinetic resolution of > 20-30 sec, others were careful not to exclude the faster exchange of bound substrate water as a possibility (eg., Rutherford, 1989; Debus, 1992) particularly in light of the concurrent findings of μ-oxo exchange in Mn^{III} dimers (Sheats *et al.,* 1987).

Improvement to the time response was of obvious importance in order to exclude the possibility that bound substrate water undergoes rapid exchange. As the earlier measurements were limited largely due to the *stabilisation time,* i.e. the time following introduction of ^{16}O or ^{18}O labelled water and the measurement, this was a key aspect of the experimental setup that needed improvement. This problem was greatly reduced by Messinger *et al.,* (1995) with the use of a closed-chamber system and steps to reduce the O_2 background in the labelled water by addition of by oxygen scavenging enzymes (glucose oxidase). In this work the minimum stabilisation time was reduced to ~30 ms, a considerable improvement on the earlier measurements. The findings with the improved kinetic resolution were quite markedly different to the earlier work. The S_3 state was found to have two phases of isotopic exchange, a slow phase with a rate constant of 2.2 s^{-1} (10°C) and an unresolved fast phase (Messinger *et al.,* 1995). This result thus established that the two water binding sites exist in the S_3 state and were different in nature; but as to how different remained an issue. Without resolution of the fast phase of exchange it was impossible to determine whether the second substrate water underwent a faster exchange or entered into the reaction sequence during the final S_3-S_4-S_0 transition.

1.10 Thesis Goals

My research goals were to improve upon the work of Messinger *et al.,* (1995) by reducing the injection response time to enable faster kinetic resolution of the exchange reactions in the S_3 state. Further detailed characterisation of the S_3 state could then be undertaken. There was also a very important need to address the questions of the ^{18}O exchange in the earlier S-states.

The hardware requirements for these objectives were met in two parts. The first part involved improving the injection response by reducing the volume of the sample chamber. I managed to reduce the chamber volume to 160 μl which meant the isotopic enrichment could be met with a smaller injection of $H_2{}^{18}O$ and more rapid mixing. A

solenoid assisted injection system was also trialed. The result was that the injection could be completed with a $t_{½}$ of ~4 ms. The second part of the hardware requirements involved accessing the earlier S-states. This was achieved by the use of three separate flash lamps coupled with a 3-1 fibre optic for sample illumination. The use of 3 separate flash lamps avoided the 50 ms recharging time that was imposed with a single flash lamp. Flashes could thus be spaced with less than 1 ms for the rapid turnover of the sample. To minimise light attenuation in the fibre optic, large numerical aperture fibres were used and the length kept to a minimum. Thus, ^{18}O exchange kinetics that were slower than the time required to give the multiple flashes could be measured, i.e. 3 ms for the S_2 state.

The results of my work is divided essentially into three sections in Chapter 3. The first section outlines the measurements, the normalisation problems associated with multiple flashes, the underlying double hitting probability, injection limitations and the associated injection correction. The second section presents the results for the ^{18}O exchange kinetics and temperature dependence for the S_0, S_1, S_2 and S_3 states. The third section then outlines extensive characterisation of the S_3 state to provide information on the nature of the substrate binding sites at the final 'stable' S-state from which the formation and release of the O_2 product takes place.

Discussion of the data and implications of the findings in terms of the possible water binding sites are then outlined in the final Chapter.

CHAPTER 2

2. INSTRUMENTATION AND METHODOLOGY

2.1 Mass Spectrometry: An Outline

Mass spectrometry is a molecular analysis technique that provides selectivity in mass. The essential principle of this technique is based on an ion optics source that generates a beam of charged sample molecules which exhibit a range of kinetic energies. When the ion beam is placed in a magnetic field, separation by mass will occur. Mathematically, this can be represented as a molecule of mass M and charge Z which, when accelerated across a potential V, will experience a force and move in a circular path of radius R when placed within a magnetic field B i.e.

$$M / Z = B^2R^2 / 2V$$

Thus, heavier ions will be deflected the least and produce a beam with a large radii, whereas the lightest ions are deflected the most and have a beam with the shortest radii. The detection of different mass species is then spatially dependent.

The measurements performed for these studies utilised a relatively simple mass spectrometer offering resolution of molecules less than ~100 mass units and uses a hot filament for molecular ionisation. The instrumentation can be divided into three main sections: 1) the source which provides molecular ionisation, beam formation and acceleration; 2) the flight tube which intercepts the poles of a magnetic field inducing deflection; and 3) the collector for detection of the incoming ions.

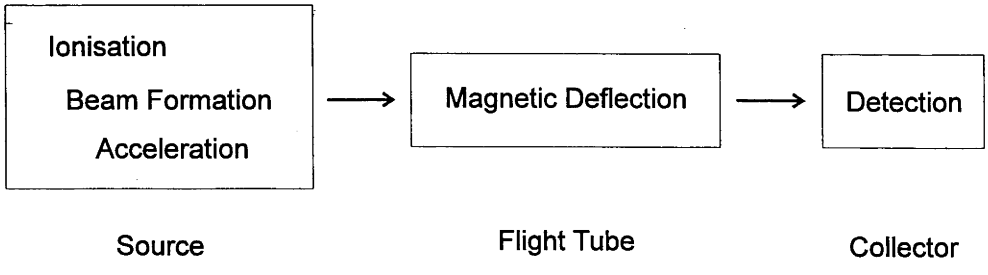

In the VG Micromass (Winsford, UK) instrument used in my studies, the sample gas mixture enters the source through an inlet directly onto a hot filament where emitted electrons ionise the gas molecules through close approach or collision. Positively charged ions are then magnetically focused into a beam and accelerated out through a slit. The acceleration process occurs due to repulsion incurred by a positive potential (1-2 kV) in the

ionisation chamber. These positive ions leave the source through a (source) slit and accelerate to a second defining (alpha) slit at zero potential. The ion beam leaving the source then enters the semicircular flight tube placed between the poles of a magnet where a magnetic field separates the beam of differing mass into differing radii. At the end of the flight tube is another (resolving) slit and a faraday cup as a collector for the ions. The current at the cup is proportional to the number of incident ions and hence the partial pressure of the corresponding isotopic molecular species in the sample gas. Mass spectrometers operate at high vacuum to minimise beam divergence from intramolecular collisions and to minimise background contamination of the measured species

Mass spectrometry is highly suited for measurements of gas molecules. Incorporation of stable isotopes of oxygen and carbon has allowed many experiments to determine the fluxes for a metabolic process (eg., Hoch & Kok, 1963; Radmer & Kok, 1976). For measurements in the liquid phase, a silicone rubber or a teflon membrane permeable to gasses (eg., O_2 and CO_2) is used. When combined with a stirrer, rapid equilibration between the liquid phase and the gas phase is possible.

2.2 Sample Preparations

2.2.1 Thylakoid Membranes

Thylakoid membranes were prepared from hydroponically grown spinach by grinding the leaves in 30 mM MES (pH 6.5), 350 mM sorbitol, 15 mM NaCl, 5 mM $MgCl_2$ in a Waring blender for 10 s. The homogenate was then filtered through two layers of gauze and two layers of nylon cloth (20 μm mesh size) and centrifuged for 5 min at 5,000 rpm in a Sorval GSA rotor. The pellet containing thylakoid membranes was resuspended in a medium containing 30 mM HEPES (pH 6.8), 400 mM sucrose, 15 mM NaCl, 5 mM $MgCl_2$ and washed once before being frozen as small beads in liquid N_2 and stored at -80°C. All sample buffers used during the various measurements were pH calibrated at the appropriate temperature.

2.2.2 PSII Membrane Fragments

PSII membrane fragments were prepared according to the method of Berthold *et al.*, (1981) with minor modifications. Fresh thylakoid membranes were resuspended in a buffer medium containing 30 mM Mes-NaOH (pH 6.5), 400 mM sucrose, 15 mM NaCl and 5 mM $MgCl_2$ at 2.5 mg Chl ml^{-1}. The total volume (**V**) of the thylakoid suspension was then diluted with a **V**/4 volume of a 25% (v/v) Triton X-100 solution which was added

slowly to the thylakoid suspension to solubilise the stromal thylakoid membranes. The 25% Triton X-100 solution was made up in 30 mM MES (pH 6.5), 15 mM NaCl and 5 mM $MgCl_2$. The final detergent concentration for membrane solubilisation was 5% Triton X-100 at a concentration of 2 mg Chl ml^{-1}. The thylakoid/Triton X-100 solution was stirred in the dark for 20 min before centrifugation for 4 min at 9,000 rpm in a Sorval SS-34 rotor to remove starch contamination and non-solubilised material. The resulting supernatant was then centrifuged for 20 min at 20,000 rpm (SS-34). The pellet containing the PSII membrane fragments was washed twice more to remove residual detergent and then finally resuspended in 30 mM HEPES (pH 6.8), 400 mM sucrose, 15 mM NaCl, 5 mM $MgCl_2$ before being stored as frozen beads at -80°C

2.2.3 PSII Core Samples

Core PSII samples were prepared from PSII membrane fragments using procedure of van Leeuwen *et al.,* (1991) which was modified for use with POROS® fast flow media. Frozen PSII membrane fragments were thawed, centrifuged for 10 min at 20,000 rpm (SS-34) 2°C and resuspended in BTS400 buffer medium containing 20 mM Bis-Tris (pH 6.5), 20 mM $MgCl_2$, 5 mM $CaCl_2$, 10 mM $MgSO_4$, 400 mM sucrose and 0.03% (w/v) n-dodecyl-β-D-maltoside (Boehringer Mannheim), to a concentration of 2 mg Chl ml^{-1}. The total volume (V) of the suspension was then diluted with a V/7 volume of a 10% (w/v) n-dodecyl-β-D-maltoside solution (final concentrations: 1.25% detergent and 1.75 mg Chl ml^{-1}). The solution was gently stirred in the dark at room temperature and then given a 20 min centrifugation at 20,000 rpm (SS-34) 20°C to remove non-solubilised material. The resulting supernatant was then prefiltered through a 0.2 μm Millipore RC filter and then loaded onto the POROS HQ 20 column. The column was first equilibrated with BTS400, after which the sample was loaded and washed at 5 ml min^{-1} until A_{440} was reduced to <0.1. The PSII core preparation was eluted from the column by a 2 min linear gradient of 0-100 mM $MgSO_4$ and the eluted fraction was then concentrated with an Amicon concentration cell (YM-100 membrane) before being stored at -80°C.

2.2.4 Depletion of Extrinsic Proteins

Depletion of the 16 and 23 kDa extrinsic proteins was performed by 1 M NaCl washing (Åkerlund *et al.,* 1982; Kuwabara & Murata 1983). For this procedure, the PSII sample was centrifuged and resuspended in 1 M NaCl at 1 mg Chl ml^{-1} and incubated on ice in the dark. At 10 min intervals the sample was passed twice through a teflon

homogeniser. After a 30 min treatment the sample was centrifuged and resuspended for a second 30 min 1 M NaCl treatment with 10 min intervals between gentle homogenisation. The sample was then finally centrifuged and washed twice in 30 mM HEPES (pH 6.8), 400 mM sucrose, 15 mM NaCl, 5 mM $MgCl_2$ before storage at -80°C.

Depletion of the 16, 23 and 33 kDa extrinsic proteins was performed by 1 M $CaCl_2$ ...ng (Ono & Inoue, 1983). For this procedure, the PSII sample was centrifuged and resuspended in 1 M $CaCl_2$ at 1 mg Chl ml^{-1} and incubated on ice in the dark. At 10 min intervals the sample was passed twice through a teflon homogeniser. After a 30 min treatment the sample was centrifuged and resuspended for a second 30 min 1 M $CaCl_2$ treatment with 10 min intervals between gentle homogenisations. The sample was then finally centrifuged and washed twice in 30 mM HEPES (pH 6.8), 400 mM sucrose, 15 mM NaCl, 5 mM $MgCl_2$ before storage at -80°C.

2.2.5 Ca^{2+} Depletion

Samples were prepared according to Ono & Inoue (1988a) using the protocol of Latimer *et al.*, (1995). PSII membranes were first washed twice in 0.25 mM MES pH 6.5, 400 mM sucrose, 15 mM NaCl and resuspended to 6 mg Chl ml^{-1}. The sample was then diluted to 2 mg Chl ml^{-1} with 20 mM citrate (pH 3.0), 400 mM sucrose, 15 mM NaCl and kept on ice for 5 min. The sample was further diluted with 50 mM MES (pH 6.5), 400 mM sucrose, 15 mM NaCl, 100 μM EGTA, washed once and then washed again in 30 mM HEPES (pH 6.8), 400 mM sucrose, 15 mM NaCl, 5 mM $MgCl_2$, 100 μM EGTA before being stored frozen. Chelex 100 (BioRad, biotechnology grade) was used to remove residual Ca^{2+} ions in all of the buffer solutions before use. Reconstituted samples (>1 hr incubation on ice) were prepared with 50 mM $SrCl_2$ or 50 mM $CaCl_2$.

2.2.6 Cl^- Depletion

Samples were washed three times in low chloride medium containing 20 mM MES (pH 6.5), 400 mM sucrose (Lindberg *et al.*, 1993) and then dialysed for 20 hours in the same low chloride medium. Solutions were made with high purity MILLI-Q water (Millipore), MES (Sigma Ultra; Cl- < 0.005%), sucrose (BDH Aristar; Cl^- < 0.5 ppm), $K_3(FeCN)_6$ (Fluka, Cl^- < 0.005%) and NaBr (Fluka; Cl^- < 0.1%).

2.2.7 Ammonia Treatment

Thylakoid samples were centrifuged and resuspended in 30 mM HEPES (pH 6.8), 400 mM sucrose, 15 mM NaCl, 5 mM $MgCl_2$ containing 100 mM NH_4Cl (Britt *et al.*, 1989; Dau *et al.*, 1995). The resultant free base concentration of NH_3 was 2 mM.

2.3 O_2 Evolution Measurements

2.3.1 Clark Electrode

Oxygen evolution was measured with a Hansatech O_2 electrode at 25°C using saturating light (>5000 μmol m^{-2} s^{-1}). Measurements were performed with 10-20 μg Chl in 1 ml of standard buffer media (30 mM HEPES (pH 6.8), 400 mM sucrose, 15 mM NaCl, 5 mM $MgCl_2$) with 400 μM of recrystallised *p*-phenyl-benzoquinone (PPBQ) and 500 μM $K_3Fe(CN)_6$ as artificial electron acceptors

2.3.2 Joliot Electrode

Flash induced O_2 signals were measured using an unmodulated Ag/Pt electrode (Messinger *et al.*, 1997b). Saturating light flashes were provided from a xenon lamp (FX-193 lamp, 1 μF, 1 kV capacitor; EG & G, Salem MA) and the amperometric signal was recorded on a computer after being uncoupled from the background noise with an isolation transformer. The electrode chamber was regulated to a constant temperature with a water bath. Each sample was loaded onto the Pt electrode in the dark, the -750 mV polarisation voltage was then applied and after a 2 min stabilisation time the sample was excited with 16 flashes at 2 Hz repetition frequency.

2.3.3 Mass Spectrometry

Samples for mass spectrometic measurements were thawed in the dark. For measurements at pH values different to the standard medium (pH 6.8), the samples were centrifuged and washed twice at the desired pH (5-9) or D_2O (pL 6.8). Before each measurement sample aliquots were given a single preflash and then given a dark period (10 min 25°C or 30 min 0°C) to enrich the S_1 population.

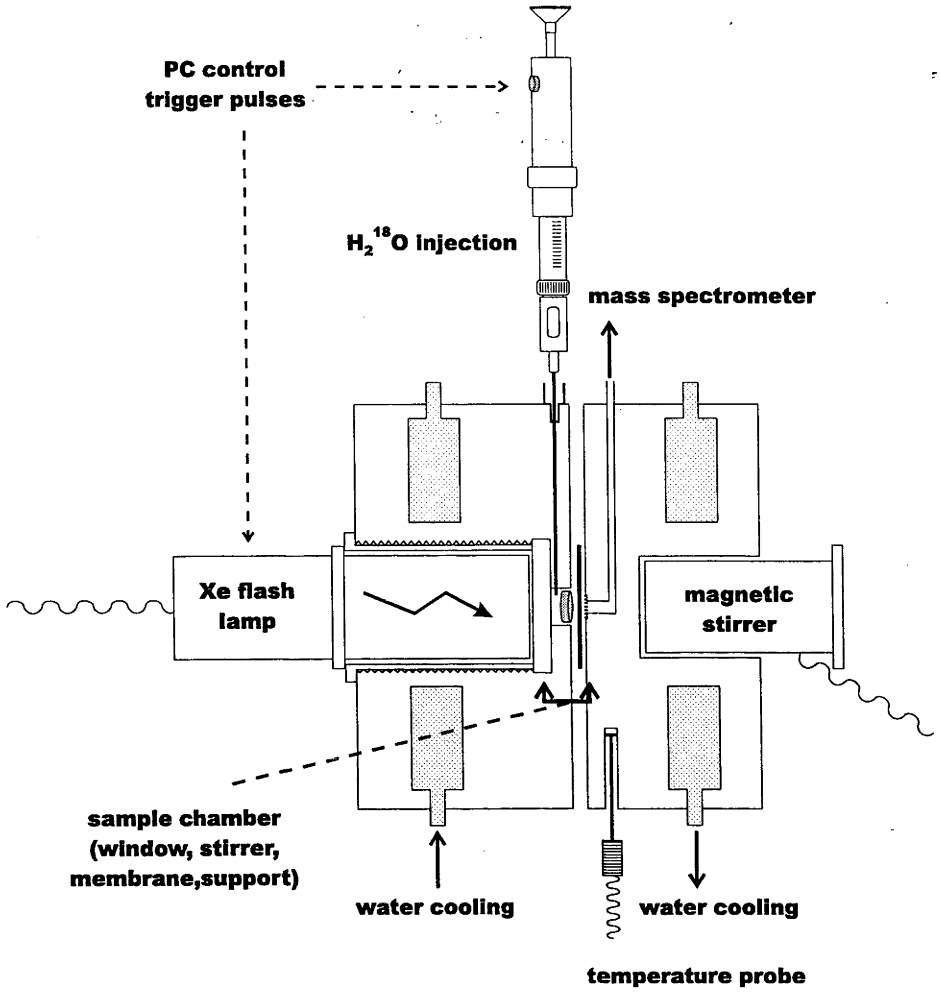

Figure 2-1 **The experimental sample cuvette used for the mass spectrometric measurements of ^{18}O exchange. The internal volume of the chamber was 160 µl. Further details are in the text.**

Flash induced O_2 production by the sample was measured at m/e = 32, 34 or 36 with an in-line mass spectrometer (Vacuum Generation MM6, Winsford, UK) for the unlabelled, single and double labelled ^{18}O-molecular oxygen, respectively. A custom built stirred stainless steel cuvette shown in Figure 2.1 was connected to the mass spectrometer via a dry ice/ethanol water vapour trap. A silicon membrane (Mempro MEM 213, 25 µm thick) was used to separate the liquid phase from the mass spectrometer inlet allowing the passage of gasses. Rapid injection of $H_2{}^{18}O$ was achieved with a Hamilton CR-200 syringe that was triggered with a computer-actuated solenoid. Samples were illuminated by a series of saturating light flashes from a xenon lamp (FX-193 lamp, 1-4 µF, 1 kV capacitor; EG & G, Salem MA) which was positioned directly in front of the sample chamber window. For rapid flash sequences, a bank of 3 flash lamps were used coupled via a short 3 to 1 fibre optic. A chlorophyll concentration of 0.5 or 0.8 mg ml^{-1} was used for optimal S/N. The

flash and injection sequence was controlled via a visual basic computer program and accurate timing intervals were established with a digital oscilloscope. Temperature control of the chamber was achieved via a water circulator and set within ±0.2 °C of the desired temperature according to an internal probe.

The isotopic exchange rates were measured for the S_0, S_1, S_2 and S_3 states at various temperatures between 0 and 25°C. For these measurements the thylakoids were loaded in the dark and the cuvette degassed for 12 min. Signals from the mass spectrometer were recorded on an x-t plotter. The slow response of the instrument due to the gas diffusion pathlength meant that the O_2 yield per flash had to be determined by extrapolating to the time of flash excitation (see Figure 3.1).

The O_2 background caused by the injection of labelled water (Y_{inj}) was subtracted from the photogenerated O_2 by performing a separate injection of the labelled water under the same conditions but without flashing. To reduce the size of the Y_{inj}, small quantities of glucose, glucose oxidase and catalase were added to the labelled water prior to injection. This caused a reproducible reduction in Y_{inj} without interfering with the photogenerated O_2. Typically the Y_{inj} was reduced to <3% of the $^{34}Y_3$ (t=∞); however, it was ~30% $^{36}Y_3$ (t=∞) due to a background of ^{36}Ar.

2.3.3.1 Injection response

To profile the kinetics of the injection and mixing response, fluorescein dye was injected into the chamber and its fluorescence yield was measured with a PAM 101 modulated fluorimeter (Heinz Waltz, Effeltrich, Germany) at 100 kHz and recorded on a digital oscilloscope. The fluorescence was excited by a LL-450 LED source and detected by an ED-101US/D photodiode (Waltz) with the respective addition of LS-450 and LL-500 (Corion) cut-off filters.

2.3.3.2 ^{18}O Enrichment

The exact ^{18}O isotopic enrichment in the sample chamber was determined from the ratio of isotopically labelled CO_2 peaks at m/e = 44, 46 and 48, i.e.

$$44 : 46 : 48 = (1-\varepsilon)^2 : 2\varepsilon(1-\varepsilon) : \varepsilon^2 = 100\% \qquad \textbf{Equation 2-1}$$

where ε is the ^{18}O% concentration. Typical ^{18}O enrichment values were highly reproducible eg. for a 25 µl injection ε = 12.0 ± 0.5 %. The rapid ^{18}O isotopic equilibration with CO_2 is a consequence of the thylakoid carbonic anhydrase catalysed and the non catalysed hydration/dehydration reactions of CO_2. Experimentally the low natural

abundance of ^{18}O in water (0.2%) did not interfere with the photogenerated labelled $^{18}O_2$ derived from the injection.

2.3.4 Kok Analysis

Deconvolution of the O_2 flash yield patterns was performed according to the Kok type of analysis to obtain the miss probability (α), the double hit probability (β) and the $[S_1]$ concentration. The oscillations were based on the formula:

$$Yn = (1-\alpha)[S_3]_{n-1} + \beta[S_2]_{n-1} \qquad \text{Equation 2-2}$$

where the yield of O_2 at a given flash (Yn) is the result of a S_3 population undergoing a single turnover and a population of S_2 undergoing a double hit. The entire S-state distribution can then be represented as a matrix vector with the population distribution after (S_n) and before (S_{n-1}) a flash. K is then defined as the *turnover matrix* incorporating the α and β parameters.

$$S_n = \mathbf{K}\, S_{n-1} \qquad \text{Equation 2-3}$$

where

$$[S]_n = \begin{bmatrix} S_0 \\ S_1 \\ S_2 \\ S_3 \end{bmatrix} \quad \text{and} \quad \mathbf{K} = \begin{bmatrix} \alpha & 0 & \beta & 1-\alpha \\ 1-\alpha-\beta & \alpha & 0 & 0 \\ \beta & 1-\alpha-\beta & \alpha & 0 \\ 0 & \beta & 1-\alpha-\beta & \alpha \end{bmatrix}$$

The analysis is similar to that outlined in Messinger *et al.*, (1991) although in this work no double turnovers during the S_3 transition were incorporated. A PC based Excel (solver) routine was applied for minimisation to derive the turnover matrix parameters.

The error analysis presented throughout this thesis is the standard error (±SE). This is an measure of the uncertainty in the estimates of the regression coefficients. The data that has been fit to exponential components and the linear regression analysis are therefore all expressed as standard errors.

CHAPTER 3

3. RESULTS

3.1 Determination of ^{18}O Exchange

3.1.1 Oxygen Measurements by Mass Spectrometry

Mass spectrometry was used to measure the O_2 yield as a function of light flashes. However, mass spectrometers have an inherently slow instrumental response time caused by O_2 diffusion through the membrane and then into the source. To overcome this problem and determine the O_2 yield per flash, the flash spacing was increased to several seconds, i.e. typically 20 sec. Also, due to the continual draw down of gases in the sample, the O_2 yield was determined by extrapolation of the signal back to the time point of the flash. To minimise deactivation of the S-states during the flash spacings, reduced temperatures were used (typically 10°C). Figure 3.1A shows the flash induced patterns of the $^{16,16}O_2$ product at m/e = 32, the $^{16,18}O_2$ product at m/e = 34 and the $^{18,18}O_2$ product at m/e = 36 after the injection of 25 µl of $H_2{}^{18}O$. At each mass the extrapolated yield for Y_3 is quantified and the amount of O_2 produced is given in brackets in fmol. The O_2 yields on Y_3 derive an equilibrium enrichment of ε = 11.5% from Equation 2.1.

Figure 3.1B shows the extrapolated O_2 yields for the m/e = 32 data as a function of each light flash to produce an oscillation pattern. Plotted together with this data is the theoretical fit based on the minimised Kok parameters: $[S_1]$ = 100%, α = 10.0% and β = 2.3%. In Figure 3.1C, a Joliot measurement of the same sample and under the same conditions is shown. The Joliot measurement and the mass spectrometric measurement produce very similar patterns despite the differences in chlorophyll concentration and inherent time constants. One point where there is a divergence is in the slightly higher amplitude of Y_3 in the mass spectrometric measurements. This result is likely to be a consequence of a partial deactivation of the higher S-states, particularly manifested in the flashes beyond Y_4. The partial deactivation results in a lower value for the S-state normalisation parameter ($\Sigma(Y_4$-$Y_7)/4$) leading to an overestimation of Y_3 on a relative scale. However, despite the slightly higher value for Y_3, there will be a constant relative change in the amplitude under different experimental conditions that will normalise out.

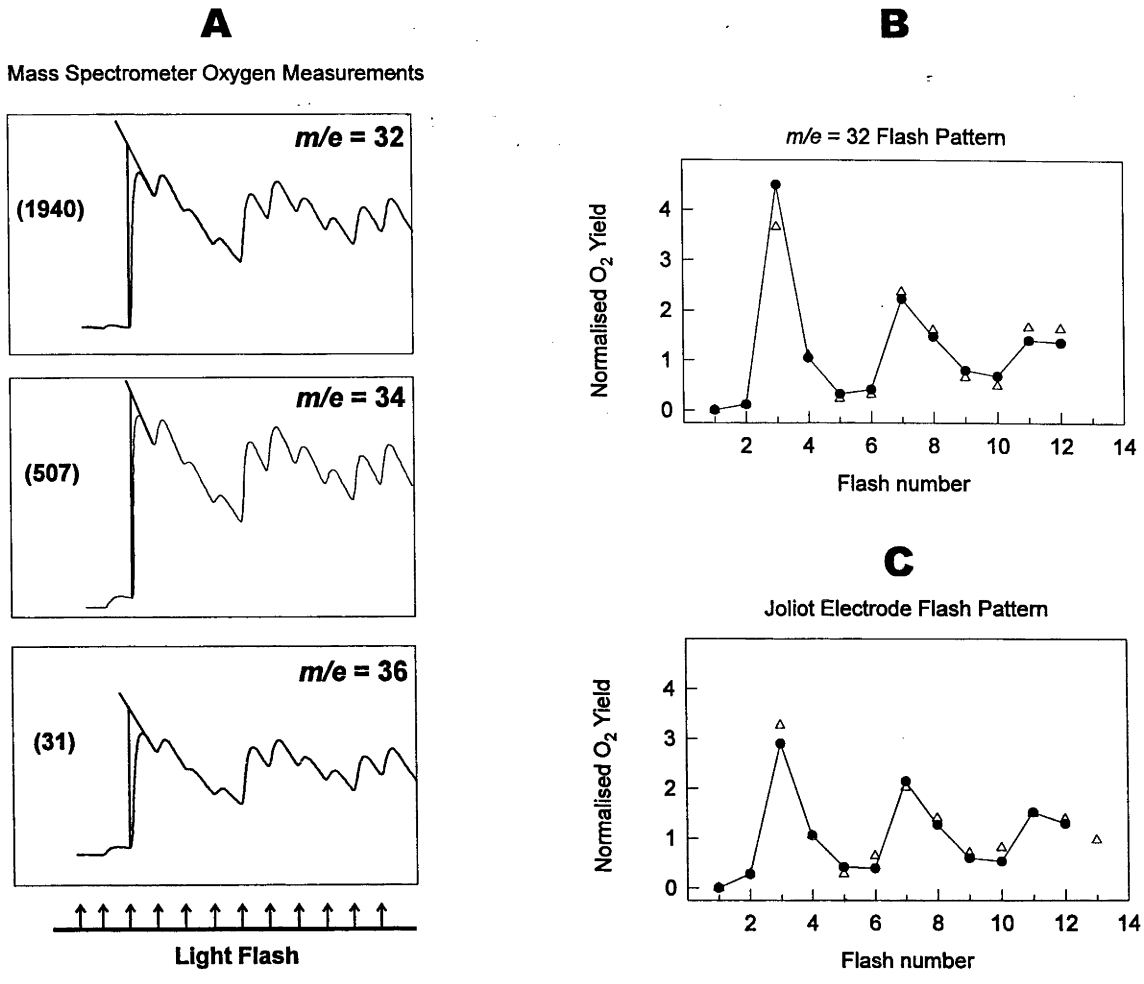

Figure 3-1 **(A) Mass spectrometric measurements of flash induced O_2 evolution of different oxygen isotopic masses from spinach thylakoid samples. O_2 yields in fmol (in parenthesis) are extrapolated from the Y_3 value as indicated. (B) The O_2 yield plotted as a function of flash number for the *m/e* = 32 data (•) with the fitted values (Δ) derived from the Kok parameters α = 10.0%, β = 2.3%, $[S_1]$ = 100%. (C) Joliot electrode measurements of O_2 yield per flash (•) with fitted values (Δ) based on α = 10.9, β = 6.2%, $[S_1]$ = 100%. Flash patterns were normalised to the sum $(Y_4\text{-}Y_7)/4$.**

3.1.2 ^{18}O Exchange Measurements

The complete isotopic exchange for substrate water in the WOC can not be determined from a single (sample) measurement. Thus, in order to measure the exchange kinetics, ^{18}O labelled water is added to a sample in a particular S-state that is followed by a defined time period after which the centres are flash-advanced through to the S_3-S_4-S_0 transition and the ^{18}O labelled oxygen products are released. This measurement is then performed over a series of exchange times in order to determine the exchange kinetics. The ^{18}O exchange rates can then be calculated from plots of the $^{18}O_2$ yield as a function of the discrete exchange-time points.

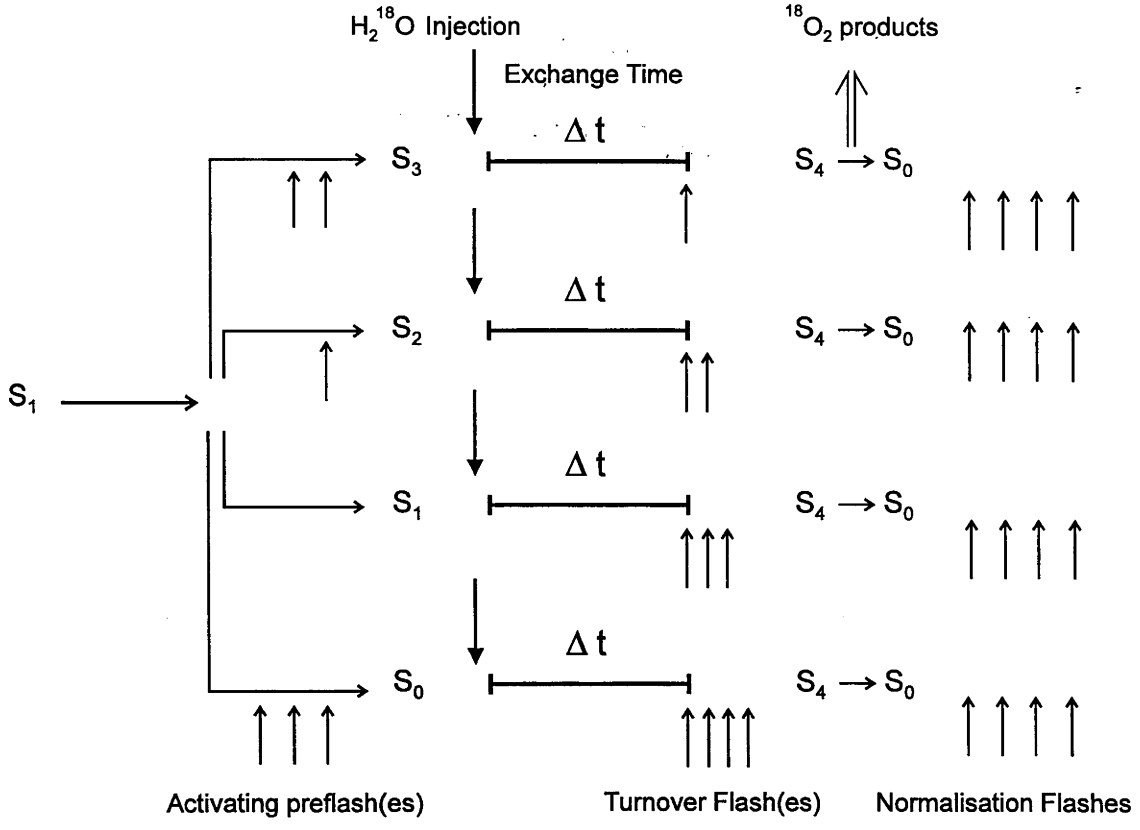

Figure 3-2 **Injection and flash spacings for the ^{18}O exchange measurements. S_1 enriched samples were prepared by giving a sample a preflash and dark incubation period. A series of *activating preflashes* is then given to generate the desired S-state whereupon an $H_2{}^{18}O$ injection is made. Following an *exchange time* to allow for ^{18}O exchange to occur, a series of *turnover flash(es)* is given to photogenerate ^{18}O labelled molecular oxygen products. A series of *normalisation flashes* is then given for standardisation purposes.**

To measure ^{18}O exchange for the different S-states the flash sequences as depicted in Fig 3.2 were used. S_1 enriched samples are given a sequence of *activating preflashes,* then, at a given S-state, ^{18}O labelled H_2O is injected and an *exchange time,* Δt, is provided for the bound water to exchange with ^{18}O labelled water. After the *exchange time,* a series of *turnover flashes* are applied to advance the sample through to the S_4 state whereupon the photogenerated $^{18}O_2$ is determined. Following this, a series of *normalisation flashes* are applied to generate a oscillation pattern for subsequent analysis. During a particular measurement, the injection/flash protocol is adjusted to maintain a constant deactivation time between the *turnover flash(es)* sequence and the preceding *activating flash(es).* The deactivation period was typically 10 seconds (eg. 5 s injection delay + 5 s exchange time) although for slower exchange kinetics longer deactivation times were used. Note that Δt is the length of time given in a particular S-state for $H_2{}^{18}O$ to exchange with bound water and

does not include the turnover flash period. Following the *exchange time* there needs to be rapid advancement of the sample to the S_3-S_4-S_0 transition where the incorporated ^{18}O label can be measured in the oxygen products. However, the measurement of the exchange following a series of turnover flashes is complicated by two features inherent to S-state cycling.

One problem originates in the kinetics of S-state turnover. Rapid advancement is essential for the resolution of fast exchange in the S_0, S_1 and S_2 states. To ensure rapid advancement special consideration for the flash lamps was made and experimentally three flash lamps were optically coupled to the sample chamber with a 3→1 fibre optic for sample illumination. However, in terms of the sample turnover, the use of closely spaced flashes (ms separation) results in only a partial turnover of S-states which is effectively manifested as a decreased yield of the S_3-S_4-S_0 transition. Kinetic limitations of S-state turnover have been examined earlier (Kok *et al.,* 1970; Bouges-Bocquet, 1973; Diner, 1975). The explanation is that a state S_n after photoexcitation immediately converts to an activated state Sn' which then subsequently relaxes in the dark to the S_{n+1} state i.e.

$$Sn \rightarrow S_n' \rightarrow S_{n+1}.$$

The turnover kinetics are generally interpreted as being limited by the reoxidation of the acceptor pool (Diner, 1975). One may therefore expect that under a very rapid flash regime, the S-state turnover to be arrested due to charge recombination reactions.

The S-state turnover for spinach thylakoids used in this study was determined using mass spectrometry (at both m/e = 32 and m/e = 34). Figure 3.3 shows the turnover kinetics for the $S_2 \rightarrow S_3$ transition as measured at m/e = 34. The kinetics appear biphasic with a $t_{½}$ ~10 ms at 10°C; a fit to two exponentials gives a fast phase k_f = 335 s^{-1} and a slow phase k_s = 16 s^{-1}. These kinetics are considerably slower than those reported earlier ($t_{½}$ ~0.4 ms) (Kok *et al.,* 1970; Bouges-Bocquet, 1973; Diner, 1975); however, the combination of reduced temperature (10°C) and extreme anaerobic conditions in the mass spectrometer sample chamber are likely to explain the difference (Diner, 1974).

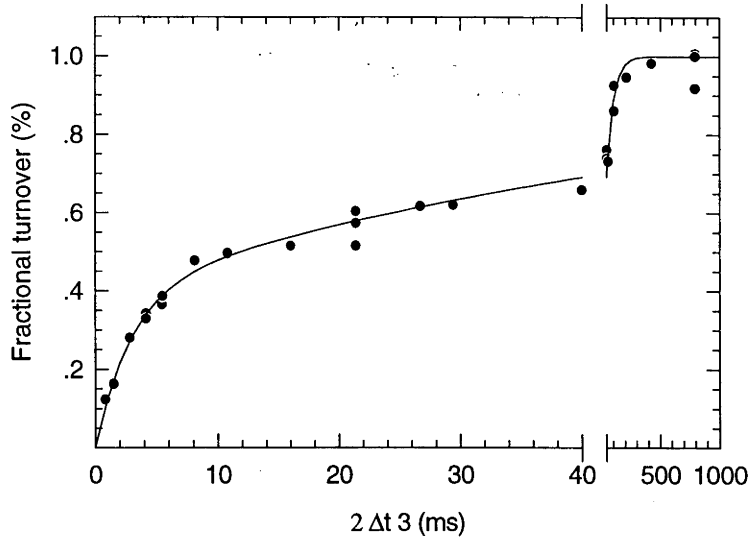

Figure 3-3 **S_2-S_3 turnover kinetics measured by varying the flash interval between the second and third flashes. The yield of O_2 was measured at m/e = 32 from spinach thylakoid membranes at 10°C. The solid line is a fit to the sum of two exponentials k_f = 335 ± 58 s^{-1} (49%) and k_s = 16 ± 2 s^{-1} (61%).**

The triple flash used in the S_1 measurements offer an even more drastic effect on the turnover efficiency as three closely spaced flashes are required. Figure 3.4 depicts the oscillation patterns following various *turnover flash* spacings derived from mass spectrometric measurements at m/e = 34. Figure 3.4A depicts what is essentially a control sample with a 1000 ms spacing but Figure 3.4B depicts a double flash 2 Δt 3 sequence with

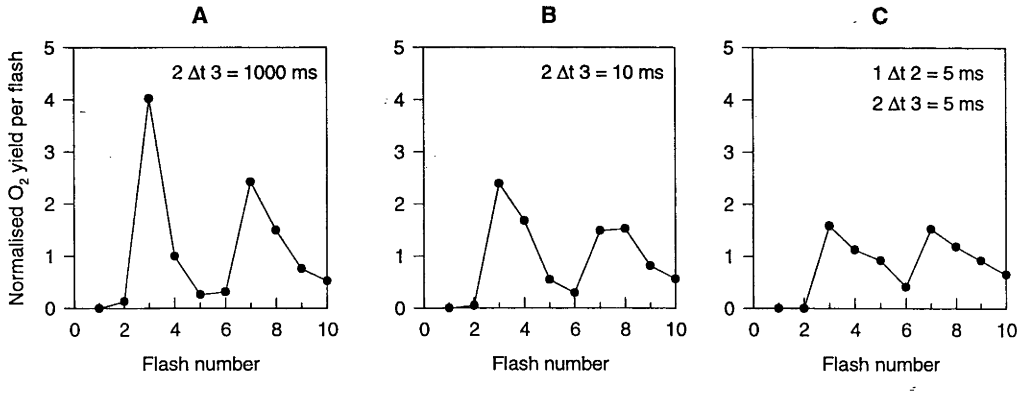

Figure 3-4 **S-state turnover measured at m/e = 34 following injection of ^{18}O labelled water. A) S_2 double flash spacing 2 Δt 3 of 1000 ms, B) S_2 double flash spacing 2 Δt 3 of 10 ms and C) S_1 triple flash spacings 1 Δt 2 Δt 3 of 10 ms. Separate experiments were performed to derive the underlying Y_2 and Y_1 contributions in the double and triple flash experiments as the time response of the mass spectrometer was insufficient to separate them discretely (see text for details).**

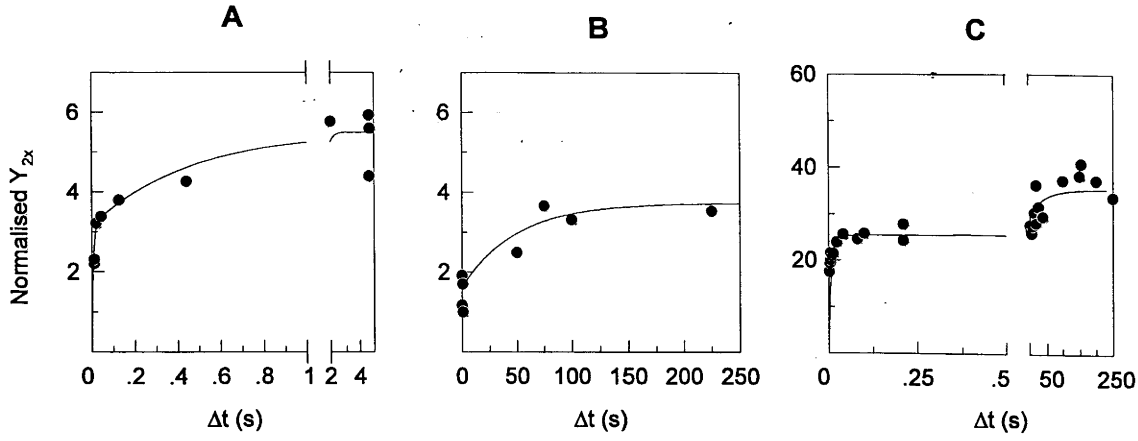

Figure 3-5 Extent of double hits on the O_2 yield (Y_{2x}) as a function of exchange time for the (A) S_2, (B) S_1 and (C) S_0 experiments (see Figure 3.2). Measurements were made at m/e = 34 as a function of the exchange time, Δt, between the injection of $H_2{}^{18}O$ and the turnover flash(es). Solid lines derive the theoretical applied double hit concentration used to correct the experiments.

a 10 ms spacing and the signal is more damped in comparison to the control. Figure 3.4C demonstrates a triple flash sequence 1 Δt 2 Δt 3 with 5 ms spacings and this too is even further damped in comparison to the control sample. For the S_0 measurements the 1 Δt 2 Δt 3 Δt 4 flash sequence was 10 ms separation with the first lamp firing twice. It should be noted that the damping due to incomplete turnover is constant and therefore no correction is needed for the normalised ^{18}O exchange experiment.

A second complication is due to the double hit factor. In a multiple flash experiment (i.e. measurements of S_0, S_1 or S_2) there is a finite probability that the turnover flashes following the $H_2{}^{18}O$ injection will result in some double hitting of the centres. Thus, the final turnover flash to advance S_3-S_4-S_0 will be contaminated by a small concentration of centres that have undergone double hits from the earlier S_0, S_1 or S_2 states (defined here as Y_{2x}). Because of the slow response of the mass spectrometer, the O_2 yield on these earlier flashes can not be resolved from the final turnover flash (Y_Σ). The underlying double hit oxygen yield (Y_{2x}) can, however, be compensated for by simply performing an ^{18}O exchange measurement of the centres undergoing double hitting. In other words, the Y_{2x} arises from the first turnover flash in the S_2 state experiment, the first and second turnover flashes in the S_1 experiment and the first three turnover flashes in the S_0 state measurement, as illustrated in Figure 3.2. If experiments are performed with ^{18}O injection and flashes up to the final flash which advances the bulk population of centres through S_3-S_4-S_0, the double hit O_2 (Y_{2x}) can be determined. The Y_{2x} component is also influenced by the exchange time so the double hit contribution must to be determined at

each exchange time (Δt) used. It should be noted that there is no Y_{2x} arising from the S_3 experiment as the ^{18}O labelled water is added before a final turnover flash for the S_3-S_4-S_0 transition. Figure 3.5 shows the Y_{2x} contributions to the signal for the S_2 state (A), the S_1 state (B) and the S_0 state (C). For the S_2 experiment the initial yield of Y_{2x} is about 6% of the total signal but as the exchange time, Δt, is shortened Y_{2x} is decreased slowly to about 3% and then rapidly to 0%. The biphasic behaviour in Y_{2x} is a property of the ^{18}O exchange behaviour for the two substrate water molecules. The solid lines represent the corrections applied to the data to remove the contributions of Y_{2x}. For the S_1 and S_2 experiments the Y_{2x} contributions to the $m/e = 36$ data were so small as to be effectively ignored (data not shown); however, the additional mixing of the S-states in the S_0 experiment required that the $m/e = 36$ data set to be corrected and similar corrections were used (data not shown).

Based on the above two considerations, it is apparent that the S_3 experiment is the easiest measurement to perform because no complications arise from Y_{2x} or from in the turnover efficiently due to closely spaced flashes.

3.1.3 Y_3 Normalisation

In order to determine the true O_2 yield on the designated turnover flash ($Y_{\Sigma(M)}$), the underlying double hit contributions (Y_{2x}) must be removed. These underlying values can be accurately determined as described in the preceding section. In addition, the presence of an O_2 contribution due to injection of ^{18}O labelled water (Y_{inj}) must also be corrected for. This can be done precisely by performing separate injection blanks in to the sample. As outlined in the instrumentation and methodology section (2.2.6.3), Y_{inj} could be greatly reduced by the addition of small quantities of glucose, glucose oxidase and catalase which, in a highly reproducible manner, lowered the O_2 content in the $H_2{}^{18}O$ injection without effecting the photogenerated O_2 levels. The important factor was to control accurately the absolute amounts of the enzyme and the substrate glucose levels in order not to interfere with the sample O_2 evolution amounts.

Finally, to make allowance for small variations in the sample concentration and changes in the membrane permeability between measurements, the $Y_{\Sigma(M)}$ values were normalised to a steady-state value derived from the sum of the four *normalisation flashes* as illustrated in Figure 3.2 (i.e., Y_4 to Y_7. for the S_1 S_2 and S_3 measurements and Y_8 to Y_{11} for the S_0 measurement). Thus, the normalised $Y_{\Sigma(N)}$ can be derived as follows:

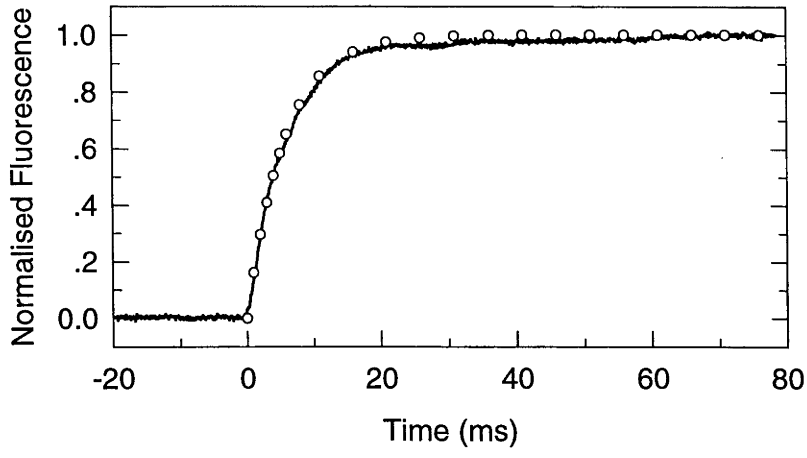

Figure 3-6 **Injection profile of the sample chamber as monitored by fluorescence. The sample chamber contained 160 µl of standard buffer medium into which 30 µl of a 9% fluorescein solution was injected. The observed fluorescence (solid line) rises to a steady state level which can be fit to a single exponential with k_{inj} = 175 s^{-1} (open circles).**

$$Y_{\Sigma(N)} = (Y_{\Sigma(M)} - Y_{inj} - Y_{2x}) / \Sigma_{(normalisation\ flashes)} \qquad \textbf{Equation 3-1}$$

For comparative purposes, the $Y_{\Sigma(N)}$ values were then normalised to one by placing the points at long exchange times (i.e. $\Delta t \gg 10$ sec) equal to one.

3.1.4 Injection Limitations.

In order to determine the overall kinetic limitations of the experimental setup the injection response of the sample chamber was measured. Figure 3.6 shows the injection and mixing response of the sample chamber system as profiled by the fluorescence yield changes upon the injection of fluorescein dye at 10°C. The fluorescence trace will fit to a first-order exponential with k_{inj} = 175 s^{-1} as determined by non-linear curve fitting. There were no significant variations in the fluorescence response due to injection volume over the range 20-40 µl or to changes in the solution viscosity at different temperatures (data not shown). For these reasons we assume that the mixing in the chamber is instantaneous and that it is due to the force of the injection itself.

3.1.5 Corrections for Injection

As the kinetics of the ^{18}O exchange approach that of the injection response, corrections need to be performed to derive the true ^{18}O exchange behaviour. The corrections compensate for two influencing effects: 1) the changing (increasing) level of ^{18}O enrichment, and 2) the changing (decreasing) sample concentration brought about by the injection. Both of these effects can be incorporated into a term to correct the measured O_2 yields as a function of the injection response into the sample chamber, i.e.

$$Y_{\Sigma(C)}(t) = Y_{\Sigma(N)}(t) \frac{\varepsilon}{\varepsilon(1-\exp(-175\ t)\ (1+(\Delta chl \times \exp(-175\ t)))}$$

$$\text{where } \Delta chl = ([chl]_{(t=0)} - [chl]_{(t=\infty)}) / [chl]_{(t=\infty)} \qquad \textbf{Equation 3-2}$$

where $Y_{\Sigma(C)}(t)$ is the corrected value for the normalised O_2 yield $Y_{\Sigma(N)}$ at a given value of Δt.

In principle, a further correction for the non-linear dependence of the $^{16,18}O_2$ yield from the $H_2{}^{18}O$ enrichment according to Equation 2.1 would apply. This correction, however, is too small under our conditions to affect the data and was ignored.

Figure 3.7 compares the effect of the injection corrections on a simulated kinetic of

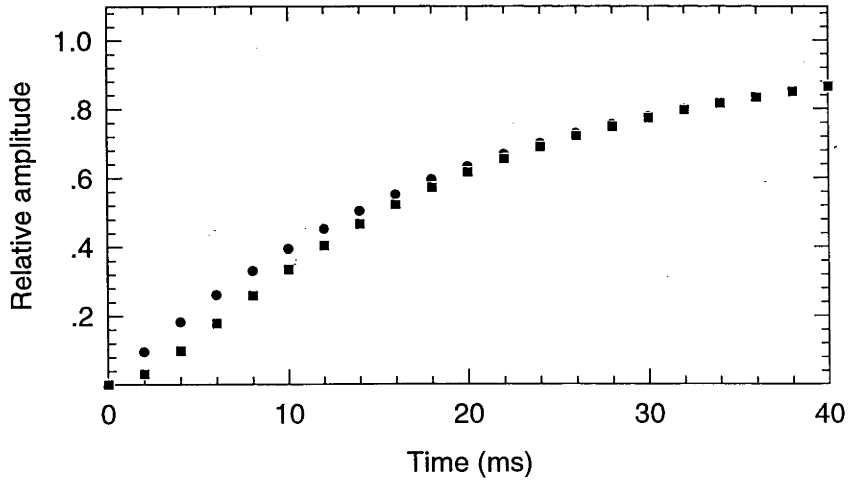

Figure 3-7 **Relative influence of the injection response (■) to a model data set exhibiting a single exponential with k = 50 s^{-1} (●). This illustration is effectively the inverse of the measured data, which after correction is converted to an apparent first order reaction. The nonlinearity in the injection response (■) is brought about by the isotopic enrichment and sample concentration. Note that corrections for injection response are only of concern with Δt values up to about 20 ms.**

50 s^{-1}. The corrections have the overall effect of increasing the observed values but, as can be seen, their influence is only apparent for data points at short Δt intervals of ≤ 20 ms. The injection corrections were made to all ^{18}O exchange measurements exhibiting fast exchange kinetics, i.e. m/e = 34 data in the S_3 state, but was not performed with the slower exchange data.

3.2 S-state Dependence of ^{18}O Exchange

3.2.1 ^{18}O Exchange in the S_3 State

The ^{18}O exchange for the S_3 state is the most straightforward measurement to perform. The ^{18}O exchange behaviour for the S_3 state of thylakoid samples at 10°C is shown in Figure 3.8 where the normalised O_2 yields of the third flash ($Y_{3(C)}$) are plotted as a function of Δt for the mixed labelled $^{16,18}O_2$ species at m/e = 34 (left) and for the double labelled $^{18,18}O_2$ species at m/e = 36 (right). The plot of the m/e = 36 data for the S_3 state exhibits only a single kinetic phase which is fit with a single first-order exponential function:

$$^{36}Y_{3(C)} = (1-\exp(-^{36}k\, t)) \qquad \textbf{Equation 3-3}$$

The fit for the m/e = 36 data is shown by the solid line in Figure 3.8B and yields a rate constant from non-linear curve fitting of 2.1 ± 0.1 s^{-1}.

In contrast to the m/e = 36 data, a plot of the m/e = 34 data reveals two distinct kinetic phases: a fast component and a slow component, as shown in Figure 3.8A. The inset in Figure 3.8A show an expanded time ordinate to reveal the fast component. The two phases, however, are unequal in magnitude, with the fast phase constituting slightly more than half of the total signal. The basis for this difference in amplitude is well explained by the enrichment phenomenon which is based on the difference in the exchange rates for the two phases. As the apparent kinetics for the two phases differ by a factor of about 10, the fast phase is virtually complete before the slow phase begins. Thus, at short Δt, only one substrate water molecule exchanges per PSII. This means with an ^{18}O enrichment of ε = 12%, the m/e = 32: 34: 36 distribution of O_2 isotopes will be 88:12:0. On the other hand, at longer Δt when the second substrate molecule is also exchanging, the equilibrium O_2 isotopic distribution will be 77.44:21.12:1.44 (Equation 2.1). Therefore, the relative contributions of the fast and slow phases will be unequal, with the fast component representing ~57% (i.e. 12/21.12) of the total amplitude and the slow component ~43%.

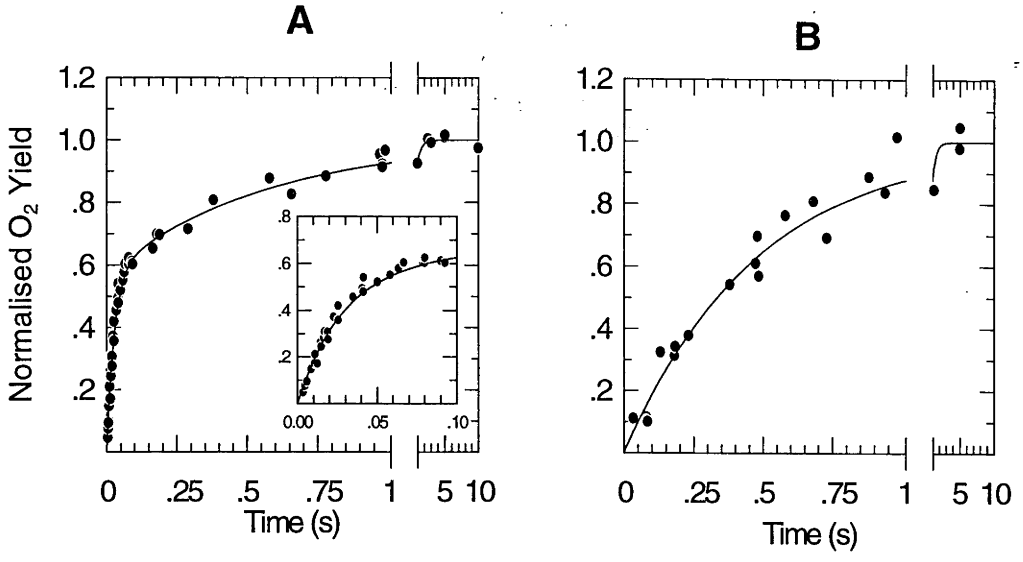

Figure 3-8 **^{18}O exchange measurements for the S_3 state of spinach thylakoid samples. Measurements were made at (A) m/e = 34 and (B) m/e = 36 as a function of the exchange time Δt at 10°C. Solid lines are a kinetic fit of the normalised O_2 yield data on the third flash. The measurements were performed in 30 mM Hepes (pH 6.8), 400 mM sucrose, 15 mM NaCl and 5 mM $MgCl_2$.**

The 0.57:0.43 distribution between the two phases is found consistently in the m/e = 34 data. Thus, the exchange kinetics for the m/e = 34 data can be fit exactly by the sum of two first-order exponentials functions as follows:

$$^{34}Y_{\Sigma(C)} = 0.43(1-\exp(-{}^{34}k_1\, t)) + 0.57(1-\exp(-{}^{34}k_2\, t)) \qquad \textbf{Equation 3-4}$$

The fit for the m/e = 34 data is shown by the solid line in Figure 3.8A and the rate constants are summarised in Table 3.1. It is important to note that the rate constant for the m/e = 36 data (^{36}k) is virtually identical to the rate constant for the slow phase in the m/e = 34 data ($^{34}k_1$). The obvious explanation for this is that the water molecule in slow exchange is the rate limiting step in the formation of the $^{18,18}O_2$ double labelled species.

Table 3-1 **Rate constants for ^{18}O exchange in the S_3 state at 10°C.**

	^{36}k (s^{-1})	$^{34}k_1$ (s^{-1})	$^{34}k_2$ (s^{-1})
S_3 State	2.1 ± 0.2	1.9 ± 0.2	36.8 ± 1.9

3.2.2 ^{18}O Exchange as a Function of S-state

The complete S-state dependence of the ^{18}O exchange is shown in Figure 3.9, measured for $m/e = 34$ and $m/e = 36$ oxygen products. The data from Figure 3.8 for the S_3 state are reproduced at the top of Figure 3.9 along with the data for the S_2, S_1 and S_0 states. The solid lines in Figure 3.9 are a fit of the exchange behaviour based on Equations 3.3 and 3.4 for the respective $m/e = 34$ and $m/e = 36$ data. The corresponding rate constants are listed in Table 3.2. There are several striking features in the data. One feature is that for each S-state there is a measurable slow phase of exchange. Another observation is that two phases of exchange are resolved only in the S_3 state. In the S_0, S_1 and S_2 states the fast phase is equal to or faster than the injection response of 175 s^{-1} of the current measuring system.

The limited kinetic resolution of the experimental setup is sufficient to show that the $^{34}k_2$ exchange rate on the S_2-S_3 transition slows down by at least a factor of ~5. It is interesting to note, however, that on this transition there is no change to the $^{34}k_1$ exchange rate. In contrast, on S_1-S_2 there a speeding up of $^{34}k_1$ by a factor of ~100, and on S_0-S_1 the data indicates there is a slowing by a factor of ~500. The results indicate that the substrate water binding site which gives rise to the slow phase of exchange undergoes changes as the S-state cycle advances. It should also be noted that the exchange data closely fit the expected amplitude distribution for the fast and slow phases i.e., 0.57:0.43.

Table 3-2 **Rate constants for ^{18}O exchange as a function of S-state at 10°C**

S-State	^{36}k (s^{-1})	$^{34}k_1$ (s^{-1})	$^{34}k_2$ (s^{-1})
S_3	2.1 ± 0.2	1.9 ± 0.2	36.8 ± 1.9
S_2	2.2 ± 0.1	1.9 ± 0.3	>175
S_1	0.022 ± 0.002	0.021 ± 0.002	>100
S_0	18 ± 3	8 ± 2	>100

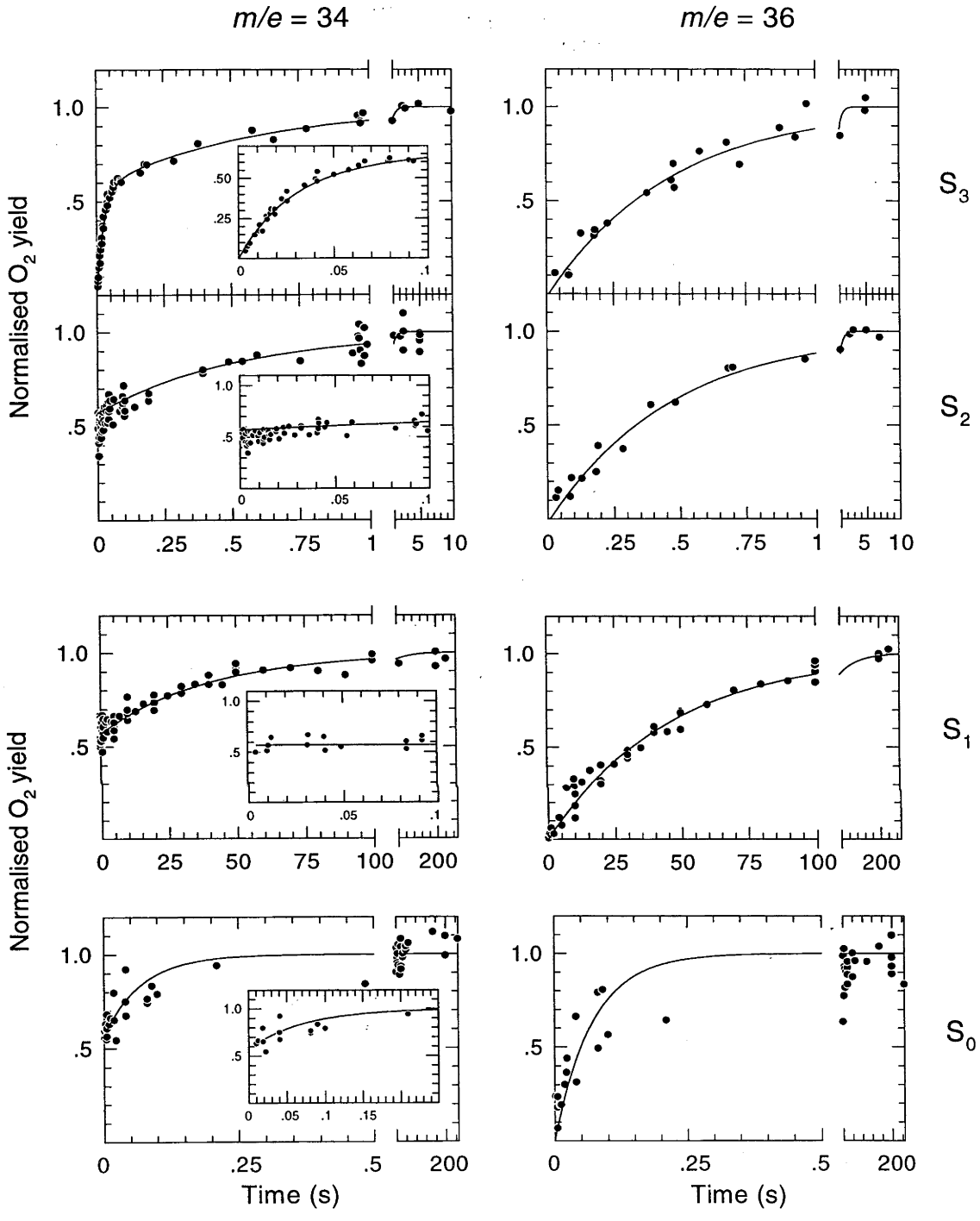

Figure 3-9 S-state dependence of the ^{18}O exchange kinetics for spinach thylakoid samples at 10°C. Measurements were performed at m/e = 34 (data on the left) and at m/e = 36 (data on the right). Note the differing time axis that are set according to the kinetics. The solid lines are a kinetic fit to the data.

3.2.3 Temperature Dependence

Each of the resolved exchange kinetics in the S_0, S_1, S_2 and S_3 states exhibit a temperature-dependent behaviour. Table 3.3 lists the calculated rate constants for the observable fast and slow phases of exchange as a function of S-state over a 0 to 20 °C temperature range. Within each data set the exchange rates decrease as the temperature decreases. The slowing down in the exchange processes, however, was not sufficient to resolve the fast phase of exchange in the S_0, S_1 or S_2 states at 0°C. The data show that the slower exchange process ($^{34}k_1$ and ^{36}k) decreases by about an order of magnitude as the temperature is reduced from 20°C to 0°C for the S_1, S_2 and S_3 states and that the faster exchange process ($^{34}k_1$) in the S_3 state decreases by a factor ~3. The data clearly demonstrate that exchange processes for the two substrate water molecules in the S_3 state have notably different temperature dependencies.

Table 3-3 Rate constants for ^{18}O exchange as a function of temperature in the S_0, S_1, S_2 & S_3 states

S-State	Temperature °C	^{36}k (s^{-1})	$^{34}k_1$ (s^{-1})	$^{34}k_2$ (s^{-1})
S_3	20	4.9 ± 0.5	4.9 ± 1.0	55.2 ± 7.1
	15	2.8 ± 0.2	3.0 ± 0.4	54.0 ± 4.4
	10	2.1 ± 0.2	1.9 ± 0.2	36.8 ± 1.9
	5	1.2 ± 0.1	1.3 ± 0.3	24.3 ± 3.5
	0	0.41 ± 0.08	0.37 ± 0.08	18.5 ± 1.1
S_2	20	4.2 ± 0.5	4.4 ± 1.2	>175
	10	2.2 ± 0.1	1.9 ± 0.3	>175
	0	--	0.52 ± 0.14	>175
S_1	20	0.060 ± 0.016	0.060 ± 0.005	>100
	10	0.022 ± 0.002	0.021 ± 0.002	>100
	0	0.0061 ± 0.0005	0.0033 ± 0.0015	>100
S_0	10	18 ± 3	8 ± 2	>100

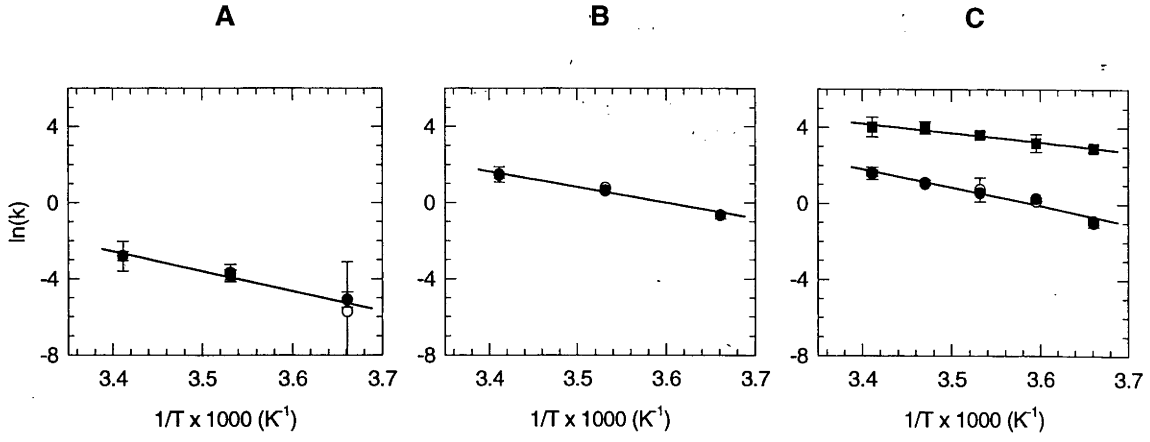

Figure 3-10 **Arrhenius plots of the rate constants listed in Table 3.3 for the;(A) S_1, (B) S_2 and (C) S_3 states. The exchange rates, when resolved, were plotted with solid symbols for the *m/e* = 34 data and open symbols for the *m/e* = 36 data. Often the *m/e* = 36 data are not clearly seen as the *m/e* = 34 data is overlayed directly. The derived activation energies and preexponentials are listed in Table 3.4.**

The temperature dependence of the exchange rates was then examined according to Arrhenius behaviour defined by the equation;

$$k = A_O \exp(-Ea / RT) \qquad \textbf{Equation 3-5}$$

where k is the reaction rate; A_O the pre-exponential or frequency factor; Ea the activation energy; T the absolute temperature and R the gas constant. Arrhenius plots of ${}^{36}k$, ${}^{34}k_1$ and ${}^{34}k_2$ for S_1, S_2 and S_3 are shown in Figure 3.10 for temperatures between 0-20°C. The overall linearity in the Arrhenius plots indicates that a single rate determining step is responsible for the ^{18}O exchange processes in this temperature region. A close inspection of the S_3 data may also hint at a possible temperature break point in the fast phase ${}^{36}k$ and ${}^{34}k_1$ data at ~5°C but this requires additional points to validate. Due to the possible effects of cryoprotectant on the exchange kinetics (see Section 3.3.6), temperatures <0°C require detailed analysis although preliminary data suggests that for the S_3 state at least, Arrhenius plots are non linear below 0°C (data not shown).

The Arrhenius parameters are listed in Table 3.4 and reveal some interesting features. The analysis reveals that the fast and slow phases of exchange in the S_3 state exhibit differing activation energies and preexponential constants, suggesting the exchange processes arrises from separate sites. The slow phase of exchange (k_1) exhibits on average considerably greater activation energies on all S-state (~80 kJ mol^{-1}) than the fast phase of exchange (k_2) in the S_3 state. The slow phase of exchange additionally exhibits

considerably greater preexponential values with a magnitude not inconsistent with that of a unimolecular process.

Table 3-4 Arrhenius parameters for the ^{18}O exchange processes in the S_1, S_2 and S_3 states.

	k_1		k_2	
S-State	E_a^1 (kJ mol^{-1})	A_O^1 (s^{-1})	E_a^2 (kJ mol^{-1})	A_O^2 (s^{-1})
S_3	79 ± 6	6.4×10^{14}	39 ± 5	8.1×10^{8}
S_2	68 ± 7	6.2×10^{12}	--	--
S_1	86 ± 10	1.6×10^{14}	--	--

3.3 S_3 State Investigations: The Final Step Before O_2 Release.

The S_3 state is the final 'stable' S-state generated before the final S_3-S_4-S_0 transition and O_2 release. For this reason the S_3 state is crucial for understanding the overall mechanism of O-O bond formation.

3.3.1 ^{18}O Exchange for Different Types of PSII Samples

PSII containing samples of decreasing complexity were investigated at level of the S_3 state in order to address the possibility that the organisation of the thylakoid membrane itself might impose a kinetic limitation on the ^{18}O exchange process. The samples measured were PSII membrane fragments, which no longer have vesicular continuity, and PSII core particles, which are discreet non-membranous particles. Figure 3.11 shows the O_2 flash yield patterns for the PSII fragments and core particles while the fitted Kok parameters are listed in Table 3.6, along with the steady-state O_2 evolution activities. Both of these samples were measured in the presence of 0.5 mM FeCN as electron acceptor which was needed to facilitate the O_2 flash oscillations (thylakoids, with their inherently larger acceptor pool, did not necessitate the addition of FeCN). Addition of FeCN did not affect the ^{18}O exchange kinetics directly (data not shown) but the inclusion of FeCN was found to substantially lengthen the S-state deactivation times. This resulted in deeper O_2 oscillation patterns which was particularly important in the Kok analysis of the PSII core samples. The addition of FeCN also increases the double hits on the first flash by oxidising Q_{400}, the PSII non-heme iron associated with the plastoquinone acceptors (Petrouleas & Diner, 1986).

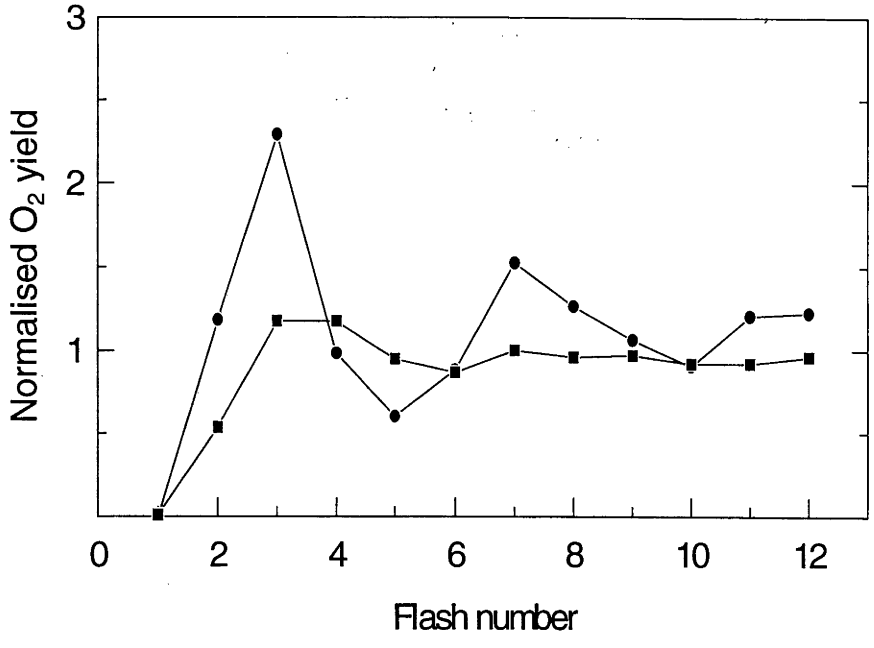

Figure 3-11 Oxygen flash yield measurements for spinach PSII membrane fragments(●) and PSII core particles (■) measured at m/e = 34 following injection of ^{18}O labelled water.

The maximum steady-state rates of O_2 evolution for these samples were quite high, indicative of good sample integrity. The PSII membrane fragments had rates of ~670 μmol (mg of Chl)$^{-1}$ hr^{-1} and the PSII core sample exhibited rates consistent with the 1200 μmol (mg of Chl)$^{-1}$ hr^{-1} rates reported by van Leeuwen *et al.*, (1991)

Figure 3.12 shows the ^{18}O exchange for the PSII membrane fragments and the PSII core preparation measured at m/e = 34. The ^{18}O exchange rates are listed in Table 3.5 and compared with the rates for the thylakoid membranes from Table 3.1. It is immediately apparent that there is only small difference between the ^{18}O exchange data for thylakoid and PSII membrane fragments i.e., $^{34}k_1$ is 2.0 ± 0.2 vs 2.3 ± 0.4 and $^{34}k_2$ is 37.2 ± 2.1 vs 42.3 ± 5.7 s^{-1}, respectively. Thus, water transport across the thylakoid membrane is unlikely to be influencing the ^{18}O exchange process. The spinach PSII core sample, however, does exhibit a slight slowing down in both phases of exchange (by a factor of ~2) compared to thylakoids. The slowing down of *both* phases is possibly indicative of an overall effect of PSII structure on the exchange process. In particular, this effect may be related to the extrinsic 16 and 23 kDa polypeptides which are absent in this type of PSII core preparation. It also may be related to the use of the non-ionic detergent n-dodecyl-β-D-maltoside which is used for the solubilisation of the PSII complex from the lipid membrane. The effect of detergent, however, is not apparent with Triton X-100 prepared

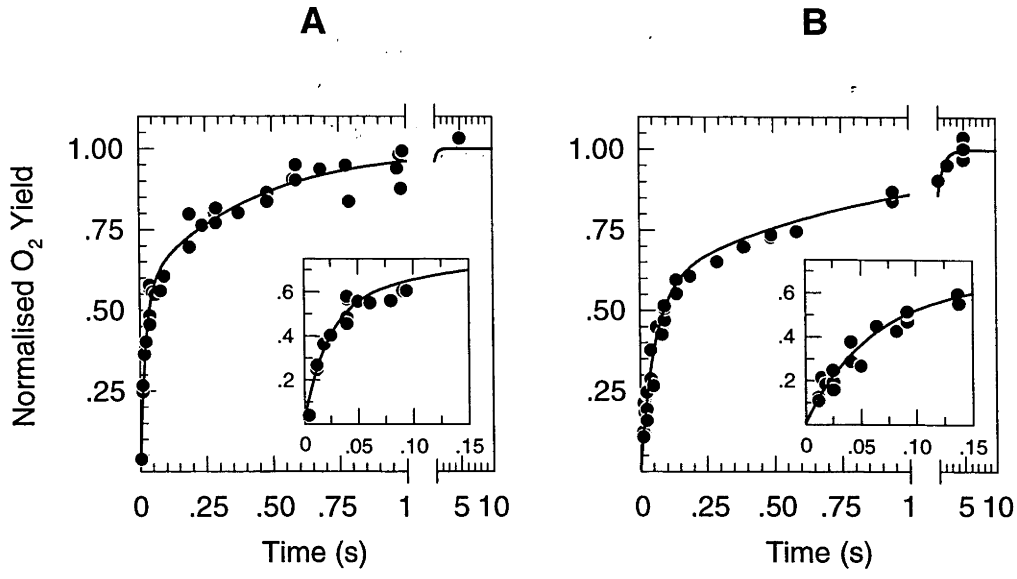

Figure 3-12 ^{18}O exchange measurements for the S_3 state of (A) spinach PSII membrane fragments and (B) PSII core samples. Measurements were performed at $m/e = 34$ as a function of the exchange time Δt at 10°C. Solid lines are kinetic fits to the normalised O_2 yield on the third flash.

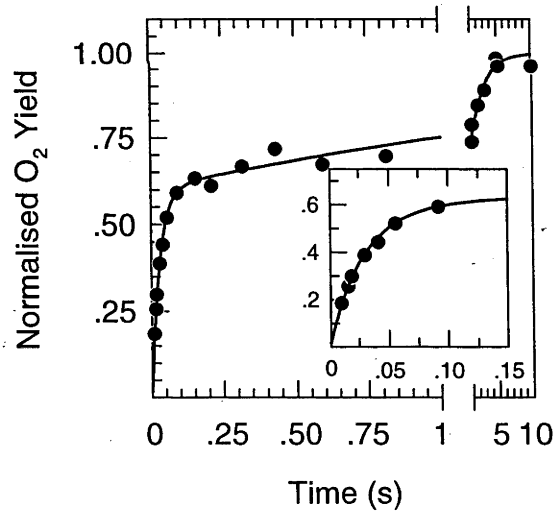

Figure 3-13 ^{18}O exchange measurements of the S_3 state of PSII core particles from the cyanobacterium *Synechococcus elongatus*. Measurement were preformed at $m/e = 34$ as a function of the exchange time Δt at 10°C. This sample was kindly provided by Dr. A. Zouni & Prof. H Witt, Technical University, Berlin.

PSII membrane fragments. A cyanobacterial PSII core sample prepared by the Witt laboratory in Berlin is shown in Figure 3.13.. In this case, the slow exchange process in the S_3 state is also affected (by a factor of ~4) but there is no apparent difference in the fast phase of exchange compared with the spinach thylakoids..

Table 3-5 Rate constants for ^{18}O exchange in the S_3 state of different PSII samples at 10°C

Sample	$^{34}k_1$ (s^{-1})	$^{34}k_2$ (s^{-1})
Thylakoid membranes (spinach)	1.8 ± 0.2	36.8 ± 1.9
PSII Membrane fragments (spinach)	2.3 ± 0.4	42.3 ± 5.7
PSII core particles (spinach)	1.1 ± 0.4	18.0 ± 3.9
PSII core particles (cyanobacteria)	0.5 ± 0.1	34.6 ± 2.3

Table 3-6 Steady-state rates of O_2 evolution and the Kok parameters for variously treated PSII-containing samples from spinach

Sample	Rate, O_2 evolution μmol (mg Chl)$^{-1}$ hr^{-1}	Percentage of control	Miss α (%)	Double hit β (%)
Thylakoids	238[1]	100	10.1	2.8
+ 100 mM NH_4Cl	109[1]	46	25.6	12.0
+ 30% EG	245[1]	103	13.7	1.7
in D_2O (pL 6.8)	---	---	10.2	3.8
PSII membrane fragments	672[1]	100	15.7	18.4
1 M NaCl washed	174[1]	26	19.8	26.7
1 M $CaCl_2$ washed	57[2]	8	58.7	13.5
Ca depleted	30[3]	4	---	---
+ 50 mM $SrCl_2$	135[3]	20	16.7	13.0
+ 50 mM $CaCl_2$	342[3]	51	19.6	10.2
Cl depleted	349[4]	52	16.6	18.1
+ 50 mM NaBr	460[4]	68	15.2	19.0
+ 50 mM NaCl	519[4]	77	---	---
PSII Cores	1185[2]	---	42.2	15.1

Buffers: (1) 30 mM HEPES (pH 6.8), 400 mM sucrose, 15 mM NaCl, 5 mM $MgCl_2$; (2) 30 mM HEPES (pH 6.8), 400 mM sucrose, 15 mM NaCl, 5 mM $MgCl_2$, 100 mM $CaCl_2$; (3) 50 mM MES (pH 6.5), 400 mM sucrose, 15 mM NaCl, 100 μM EGTA; (4) 20 mM MES (pH 6.5), 400 mM sucrose.

3.3.2 The Effect of Extrinsic Proteins Depletion

The extrinsic polypeptides of PSII function in general to provide an accessibility barrier to stabilise the WOC (Seidler, 1996). An interesting possibility thus arises that the extrinsic polypeptides may influence the ^{18}O exchange kinetics by regulating the accessibility of the substrate water during the water oxidation reaction (Wydrzynski *et al.*, 1996). To explore this possibility, treatments which remove the extrinsic proteins by high ionic strength were employed: a 1M NaCl wash was used to deplete the 16 and 23 kDa and a 1M $CaCl_2$ wash to deplete the 16, 23 and 33 kDa polypeptides. These two treatments result in a consequential decrease in O_2 evolution activity. The NaCl washed samples were reduced to 26% of the control activity and the $CaCl_2$ washed samples to 8%. This is

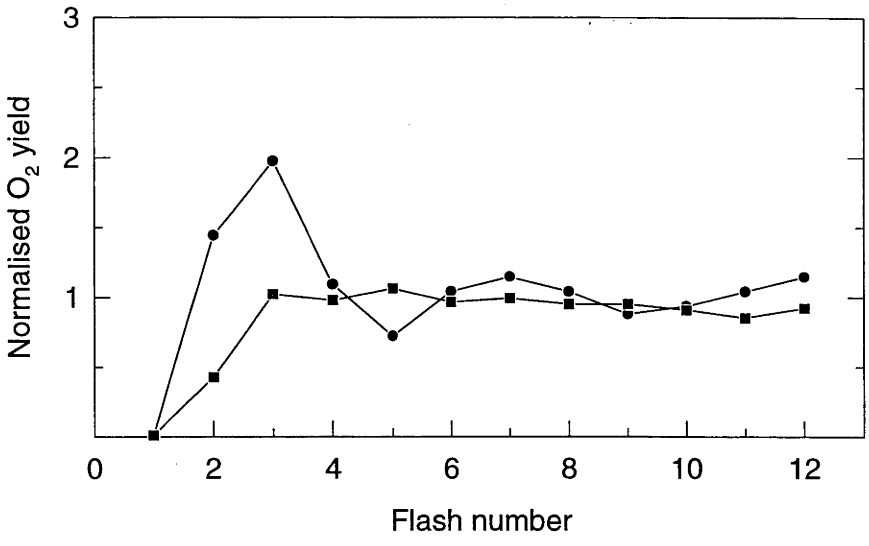

Figure 3-14 Oxygen flash yield measured at m/e = 34 for PSII membrane fragments that were washed with 1M NaCl (●)and 1M $CaCl_2$ (■) following injection of ^{18}O labelled water.

shown in Table 3.6. The losses in activity are greater than has been typically reported (eg., Ono & Inoue, 1984; Bricker, 1992) but are likely due to the double wash treatments and gentle homogenisations that were used to prepare the samples in this study. The O_2 flash patterns for the corresponding samples are shown in Figure 3.14. In both cases the samples exhibit very strongly damped oscillations but nevertheless have a peak O_2 yield on the third flash. The derived Kok parameters are given in Table 3.6.

The salt-washed samples represents the most severely disturbed samples that were used for the ^{18}O exchange measurements. Despite the low activity, ^{18}O exchange data could be measured with sufficient S/N. Figure 3.15 depicts the m/e = 34 mixed labelled exchange behaviour for the NaCl and $CaCl_2$ treated samples. The data still reveals two exchange phases in the S_3 state. The kinetic fit to these data are presented in Table 3.7. From the fit it is clear that the extrinsic polypeptides are in some way involved in the ^{18}O exchange processes as their removal causes a slowing in both phases of the exchange in the S_3 state. The NaCl-washed sample exhibits a decrease in the slow exchange from 2.3 s^{-1} to 1.7 s^{-1}, or a factor of ~1.4, whereas the fast exchange is decreased from 43 s^{-1} to 23 s^{-1}, or factor of ~1.9. The $CaCl_2$-washed samples reveal an even greater decrease in the exchange rates with the slow phase being reduced to 1.5 s^{-1}, or a factor of ~1.5, and the fast phase to 9.5 s^{-1}, or a factor of ~4.5.

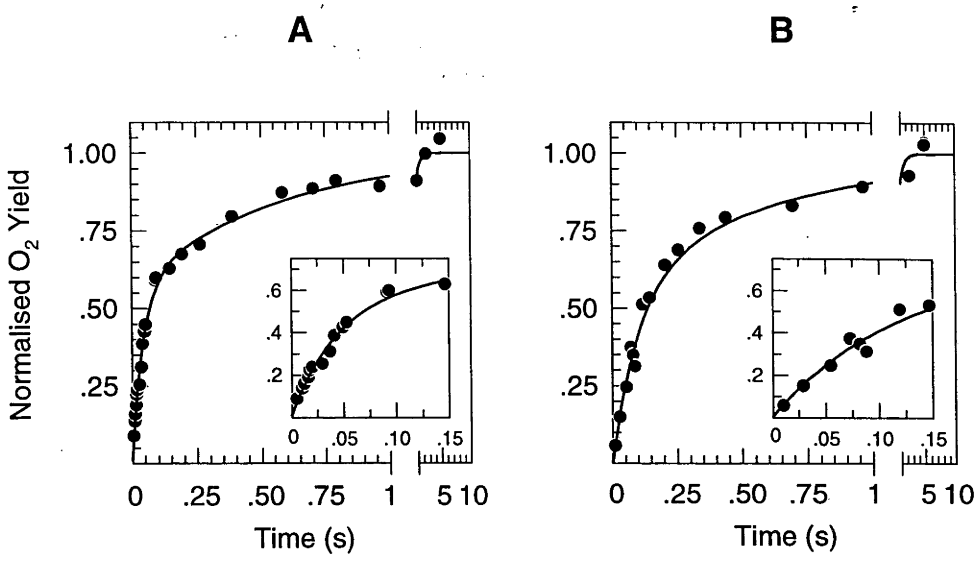

Figure 3-15 **^{18}O exchange measurements for the S_3 state of spinach PSII membrane fragments washed in (A) 1 M NaCl and (B) 1 M $CaCl_2$. Measurements were made at m/e = 34 as a function of the exchange time Δt at 10°C. Solid lines are a kinetic fit of the normalised O_2 yield on the third flash.**

Table 3-7 **Rates constants for ^{18}O exchange in the S_3 state of salt-washed PSII membrane fragments at 10°C**

Sample	$^{34}k_1$ (s^{-1})	$^{34}k_2$ (s^{-1})
PSII Membrane fragments	2.3 ± 0.4	42.3 ± 5.7
PSII; 1M NaCl washed	1.7 ± 0.3	22.5 ± 2.0
PSII; 1M $CaCl_2$ washed	1.5 ± 0.7	9.5 ± 2.4

The effect of the removal of the extrinsic polypeptides thus appears to be a general slowing in the ^{18}O exchange process. This finding would then seem to exclude the possibility that the extrinsic polypeptides are imposing an overall kinetic barrier to the substrate water exchange as an opposite effect would be expected. Instead there may be long range structural interactions effects on the catalytic site caused by the loss of these proteins. Such long range interactions apparently result in stronger binding of the in substrate water.

3.3.3 Calcium Depletion Experiments

A number of reports have indicated that Ca ions are essential for both assembly and the functioning of the WOC (Debus, 1992; Boussac & Rutherford, 1994). A Ca depleted sample was prepared by the low pH (citrate) treatment (Ono & Inoue, 1988a) and gave steady-state rates of O_2 evolving activity that were practically zero (4% of the control) as shown in Table 3.6. The data in Table 3.6 also shows that the addition of 50 mM $CaCl_2$ restores activity to 51% of the control and the addition of 50 mM $SrCl_2$ restores the activity to about 20%. The reconstituted activities are somewhat lower than previously reported, where the restored activities were 76% and 28% of the control, respectively (Ono & Inoue, 1988a). A possible reason for the lower reconstitution in activity may be due to the shorter incubation time used in this work (2 min at 25°C) than in the earlier work (10 min at 0°C).

The PSII membrane samples treated with citrate/pH 3 were of insufficient activity to measure with the mass spectrometer until reconstituted with 50 mM $CaCl_2$ or $SrCl_2$. It should be noted that reconstitution of the sample in these measurements was for > 1 hr to ensure maximal recovery of the activity. Both the $CaCl_2$ and $SrCl_2$ reconstituted samples exhibit oscillations in O_2 flash yield measurements as shown in Figure 3.16. The derived Kok parameters are given in Table 3.6 and these are surprisingly similar to the control PSII membrane fragments. At this point it is worth considering that Sr reconstituted centres

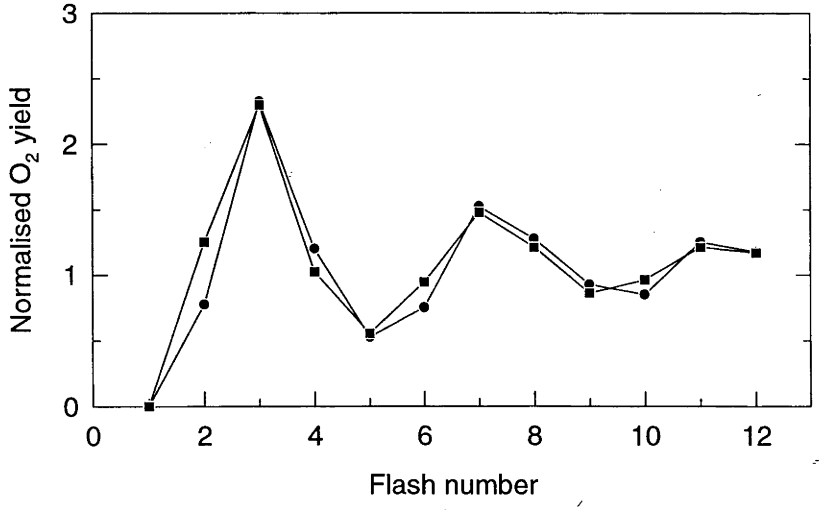

Figure 3-16 O_2 flash yield measurements for Ca-depleted PSII membrane fragments reconstituted with 50 mM $CaCl_2$ (●) and 50 mM $SrCl_2$ (■). Measurements were made at m/e = 34 following injection of ^{18}O labelled water.

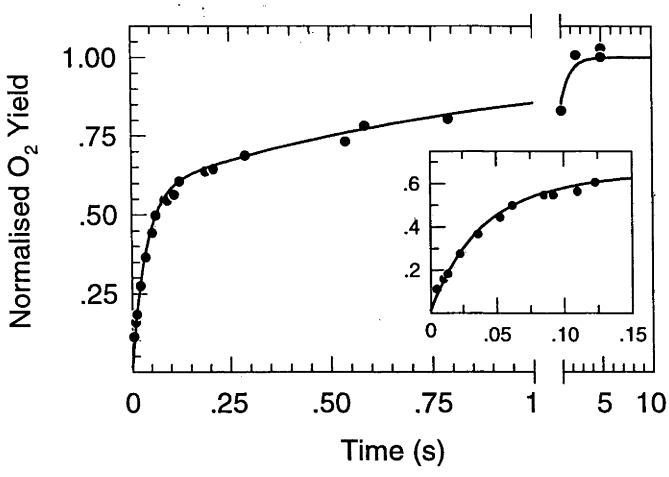

Figure 3-17 **^{18}O exchange measurements for the S_3 state of Ca^{2+} depleted spinach PSII membrane fragments reconstituted in (A) 50 mM $CaCl_2$. Measurements were made at m/e = 34 as a function of the exchange time, Δt at 10°C. Solid lines are a kinetic fit of the normalised O_2 yield on the third flash.**

exhibit slowed S-state advancement (Westphal & Babcock *personal communication*; see also Boussac *et al.*, 1992b). Such kinetic limitations, however, are not observed here presumably because of the low flash frequency (0.05 Hz) used for the mass spectrometric measurements.

The S_3 state ^{18}O exchange kinetics for the $CaCl_2$ reconstituted PSII sample is shown in Figure 3.17. This sample shows clear biphasic kinetics with a slow phase of exchange of 1.1 s^{-1} and a fast phase of 28.1 s^{-1} (Table 3.8). The two phases are well described by the 57%:43% ratio for the fast/slow kinetic phases as seen in untreated PSII samples (Figure 3.12) although the two exchange rates are decreased by 30-50%. The $SrCl_2$ reconstituted sample is shown in Figure 3.18 and it is interesting to note that the two distinct phases of exchange are no longer apparent. Measurement at m/e = 36 was undertaken to independently resolve the exchange rate for the slow component k_1. By cross-correlating the m/e = 34 and m/e = 36 data (i.e. when $^{34}k_1 = k_1$) the two phases of exchange could be determined to be $^{34}k_1 = 5.9 \pm 0.7$ for the slow phase and $^{34}k_2 = 14.7 \pm 7.2$ for the fast phase (Table 3.8). Based on these observations, it is clear that both exchange processes are affected by the Sr reconstitution. The data indicate that there is a specific increase in the slow phase of exchange, representing one of the few conditions where this happens.

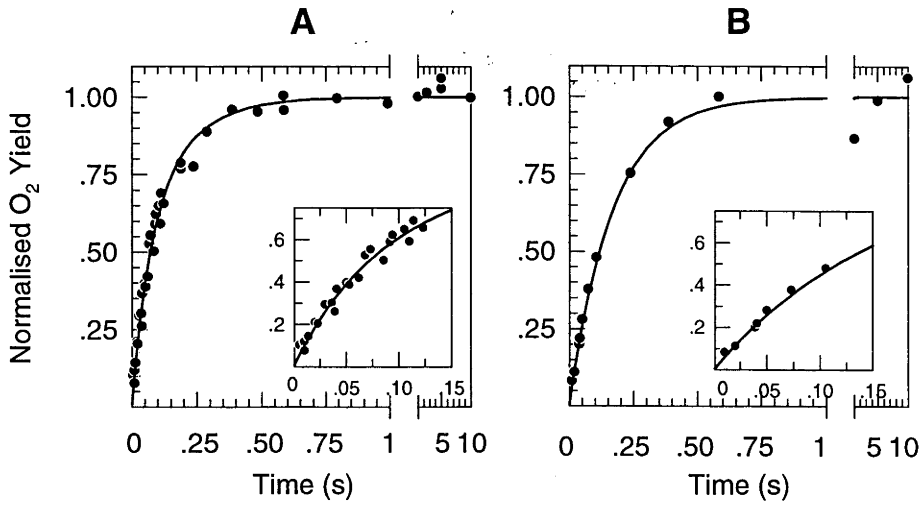

Figure 3-18 **^{18}O exchange measurement for the S_3 state of Ca^{2+} depleted spinach PSII membrane fragments reconstituted in 50 mM $SrCl_2$. Measurements were made at (A) m/e = 34 and (B) m/e = 36 as a function of the exchange time Δt at 10°C. Solid lines are a kinetic fit of the normalised O_2 yield on the third flash.**

Table 3-8 **Rates constants for ^{18}O exchange in the S_3 state of Ca-depleted PSII membrane fragments reconstituted with 50 mM $CaCl_2$ or $SrCl_2$ at 10°C**

Ca-depleted sample	$^{34}k_1$ (s^{-1})	$^{34}k_2$ (s^{-1})
+ 50 mM $CaCl_2$	1.1 ± 0.1	28.1 ± 1.8
+ 50 mM $SrCl_2$	5.9 ± 0.7†	14.7 ± 7.2

† Cross-correlated value where $^{34}k_1 = {}^{36}k$

3.3.4 Chloride Depletion Experiments

Chloride ions have also been suggested to be directly involved in the water oxidation reaction (Boussac & Rutherford, 1994). It has been shown quantitatively that there is ~1 Cl^- ion tightly bound per intact PSII centre. This Cl^- will undergo slow exchange under conditions of low [Cl^-] (Lindberg *et al.*, 1993; Lindberg & Andréasson, 1996). In contrast, the conventional protocols for 'Cl^- depletion' using SO_4^- treatment or alkaline pH 10 exposure, result in the dissociation of the 16 & 23 kDa polypeptides (Homann, 1988; Wincencjusz *et al.*, 1997). Based on the observations in Section 3.3.2 in which the removal of the extrinsic proteins alters the ^{18}O exchange, these latter protocols

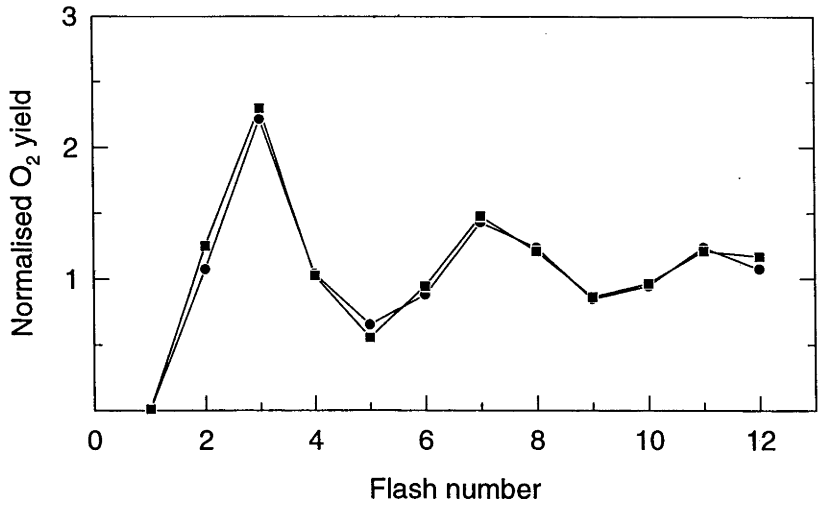

Figure 3-19 **O_2 flash yield patterns for PSII membrane fragments 'Cl⁻ depleted' (●)and then reconstituted with 50 mM NaBr (■). Measurements were made at *m/e* = 34 as a function of the exchange time, Δt at 10°C. Solid lines are a kinetic fit of the normalised O_2 yield on the third flash. Depletion of Cl⁻ was performed by washing the sample ×3 in low [Cl⁻] buffer followed by a 18hr dialysis, see materials section for details.**

were not used for investigating the Cl⁻ effects. Instead the low [Cl⁻] treatment of Lindberg *et al.*, was used. In this case the rates of O_2 evolution following 'Cl⁻ depletion' (the samples were washed 3 times in Cl⁻ free media and then dialysed for 18 hr) was reduced to 52% of the control activity. Addition of 50 mM NaCl increased the O_2 evolution activity to 77% of the untreated control after a 2 min incubation at 25°C while the addition of 50 mM NaBr increased the activity to 68%. These results are shown in Table 3.6. Greater effects may have been observed if longer incubation/reconstitution periods were used.

The O_2 flash yield patterns for the Cl⁻ depleted sample and the sample reconstituted with 50 mM NaBr are shown in Figure 3.19. The flash patterns indicate that there is no major effect on the S-state transitions by the Cl⁻ depletion protocol used. The α and β parameters are not greatly different, as shown in Table 3.6, and the oscillation patterns are practically superimposable to the control PSII membranes shown in Figure 3.12. This was a surprising result in view of the significant increases in O_2 evolution activity following CaCl or NaBr addition. The results in this work are quite contrary to the results of SO_4^- or pH 10 treatments (i.e. Ono *et al.*, 1986; Boussac *et al.*, 1992b; Hundelt *et al.*, 1997) for Cl⁻

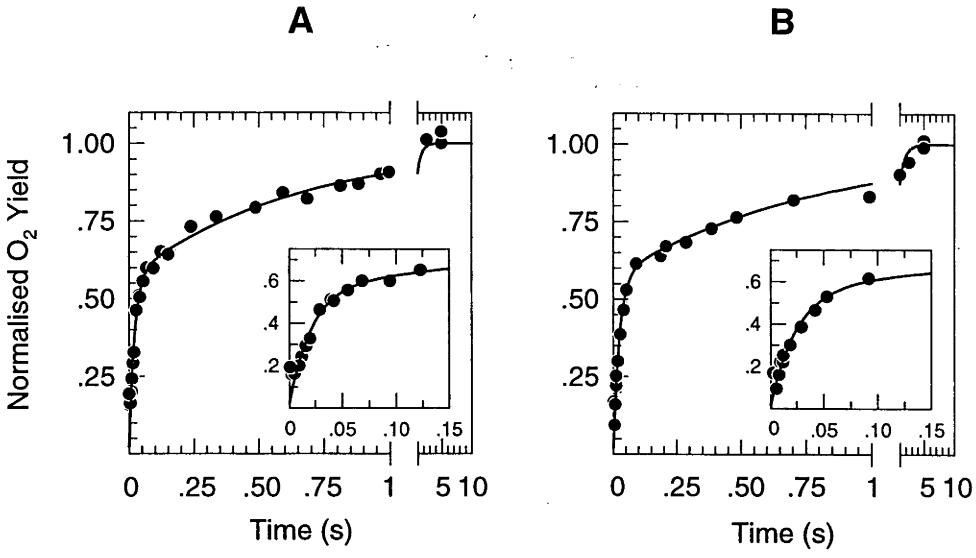

Figure 3-20 **$H_2{}^{18}O$ exchange measurement in the S_3 state of (A) Cl^- depleted spinach PSII membrane fragments or (B) Cl^- depleted samples reconstituted with 50 mM NaBr. Measurements were made at m/e = 34 as a function of the exchange time Δt at 10°C. Solid lines are a kinetic fit of the normalised O_2 yield on the third flash ^{18}O exchange.**

depletion which have been interpreted as causing specific blocks to the S-state transitions. The difference in results may be explained by the manner (or severity) by which the Cl^- is depleted. As analogous to the Sr^{2+} reconstitution measurements (Section 3.3.3), kinetic limitation by the low flash frequencies (0.02 Hz) used here may obscure the Cl^- effects.

The ^{18}O exchange behaviour for the 'Cl^- depleted' and NaBr reconstituted PSII membrane fragments are shown in Figure 3.20 and the calculated rate constants are listed in Table 3.9. Under these conditions, the two phases of exchange are still apparent. In comparison to the control PSII membrane fragments (Table 3.5), the Cl^- depleted samples exhibit a some what decreased rate of exchange for the slow phase ($^{34}k_1$) with a relative slowing down of ~1.5. Addition of 50 mM NaBr results in a similar exchange behaviour but with a further decrease in the slow phase to 1.2 s^{-1}. In both cases the fast phase of ^{18}O exchange ($^{34}k_2$) remained unchanged, within the error of the measurement.

Table 3-9 **Rates constants for ^{18}O exchange in the S_3 state of Cl^- depleted PSII membrane fragments at 10°C**

PSII sample	$^{34}k_1$ (s^{-1})	$^{34}k_2$ (s^{-1})
Cl^--depleted	1.5 ± 0.3	46.4 ± 5.2
+ 50 mM NaBr	1.2 ± 0.2	40.1 ± 3.8

The reports of Cl^- depletion by using low [Cl^-] indicate that O_2 evolution activity can be reduced to 30-35% of the control activity and the chloride bound was <0.02 Cl^-/PSII (Lindberg *et al.*, 1993; Lindberg & Andréasson, 1996). For the work presented here, $^{36}Cl^-$ radiolabel was not used to quantify bound Cl^-. Instead a protocol using a $AgNO_3$ assay was used to measure [Cl^-] (Lindberg *et al.*, 1993). Using this assay the 'Cl^- free buffer' used in the experiments was found to contain 2.6 ± 0.1 μM Cl^-. Based on the Cl^- dependent recovery of O_2 evolution activity in the 'Cl^- depleted' PSII membrane fragments (Lindberg & Andréasson, 1996) the addition of 2.6 μM would result in ~10% recovery in O_2 evolution activity (Andréasson *personal communication*). Thus, the difference in residual activities for Cl^- depletion samples used in the present work can be accounted for.

3.3.5 Ammonia Substitution Experiments

Ammonia is a likely substrate analogue because it is isoelectronic with water. Two NH_3 binding sites in the WOC have been proposed: one site competitive with Cl^- that binds amines in general (NH_3, CH_3NH_3 etc); and a second site that does not bind Cl^- and is specific for NH_3. The second site is suggested to be a substrate water binding site (Debus, 1992). It is the NH_3 binding to the second site that results in alterations to the Mn multiline signal (Beck & Brudvig, 1986; Beck *et al.*, 1986).

. The interaction of ammonia with the WOC was investigated by addition of 100 mM NH_4Cl to a sample of spinach thylakoid membranes. The use of 100 mM NH_4Cl is considered to block amine binding to the first site through competitive Cl^- binding and allow NH_3 binding to the second site (Sandusky & Yocum, 1984; 1986). The steady-state rates of O_2 evolution for a thylakoid sample measured in the presence of 100 mM NH_4Cl (pH 7.5) were 46% of the control activity as shown in Table 3.6. This extent of inhibition is very similar to that reported previously (Andréasson *et al.*, 1988; Boussac *et al.*, 1990). Early studies using thermoluminescence measurements suggested that high concentrations of NH_3 blocks the S-state cycling beyond S_3 (Ono & Inoue, 1988b) but it has been

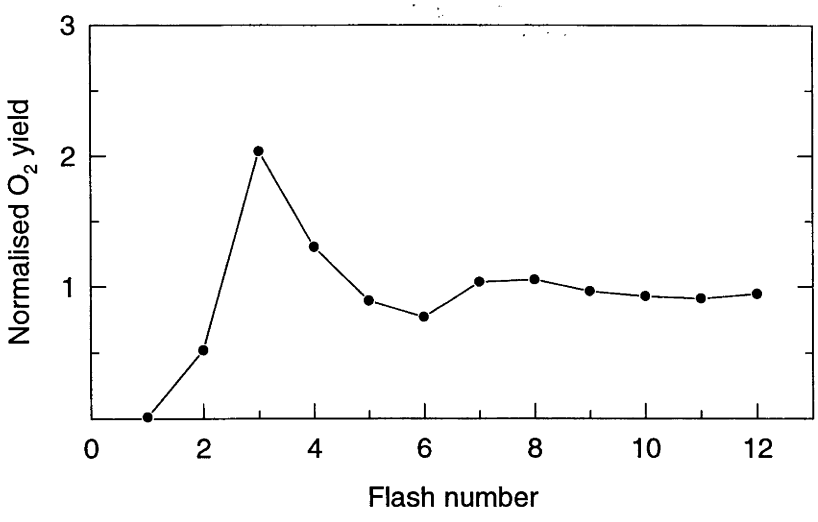

Figure 3-21 **O_2 flash yield measurements for thylakoid membranes in the presence of 100 mM NH_4Cl measured at m/e = 34 following injection of ^{18}O labelled water.**

demonstrated that S-state cycling will proceed in the presence of 100 mM NH_4Cl although with a damped oscillation (Delrieu, 1976). The effect of 100 mM NH_4Cl on the O_2 oscillation pattern in thylakoid membranes is shown in Figure 3.21. The Kok parameters for this sample are listed in Table 3.6 and indicate that NH_3 results in a considerable increase in the miss and double hit parameters as compared to the control. This result is consistent with the current interpretations in which the S-state advancement is slowed down by the binding of NH_3 (Boussac *et al.*, 1990).

The ^{18}O exchange kinetics are also influenced by the presence of 100 mM NH_4Cl and this is shown in Figure 3.22 for the S_3 state. The rate constants from the kinetic fit to this data are given in Table 3.10. The results show that the two phases of exchange slow down compared to the control thylakoid samples, with the extent of the slowing down ~1.8% and ~2.5%, for the fast and slow phases respectively. These data would then suggest that the interaction of NH_3 (at the Cl^- insensitive site) affects both substrate water molecules in the S_3 state.

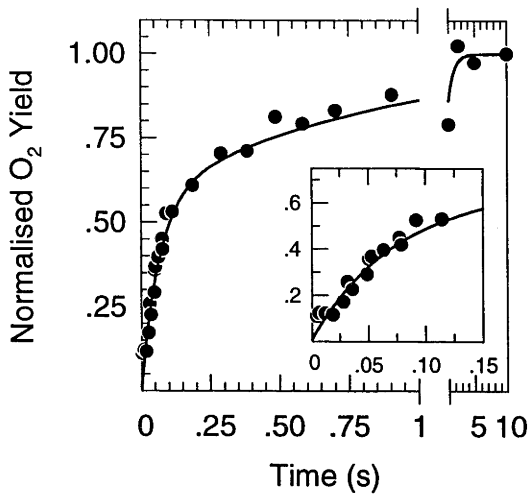

Figure 3-22 **^{18}O exchange measurements for the S_3 state of spinach PSII membrane fragments in the presence of 100 mM NH_4Cl. Measurements were made at m/e = 34 as a function of the exchange time Δt at 10°C. Solid lines are a kinetic fit of the normalised O_2 yield on the third flash.**

Table 3-10 **Rate constants for ^{18}O exchange in the S_3 state of NH_4Cl treated thylakoid membranes at 10°C**

Thylakoid sample	$^{34}k_1$ (s^{-1})	$^{34}k_2$ (s^{-1})
Thylakoid membranes	1.8 ± 0.2	36.8 ± 1.9
+ 100 mM NH_4Cl	1.1 ± 0.3	14.9 ± 2.1

3.3.6 Solvent Effects by Ethylene Glycol

Ethylene glycol (EG) is commonly employed as a cryoprotectant for PSII samples (Farkas & Malkin, 1979). There are indications that EG interacts directly with the Mn in the WOC: ENDOR measurements suggest that EG is accessible to the pocket around the Mn ions associated with the multiline signal (Kawamori *et al.*, 1989), and there is a form of the g ~4.1 EPR signal that appears only in the presence of EG (Smith & Pace, 1996). It is interesting to note, however, that at EG concentrations below 50% there is no effect on the net O_2 evolution activity in PSII fragments (Hillier *et al.*, 1997). As shown in Table 3.6, the present study shows this is also the case with thylakoid samples in 30% EG.

The O_2 flash oscillation pattern for spinach thylakoids in 30% EG is shown in Figure 3.23 and reveals that this sample maintains the deep oscillation behaviour. Kok analysis gives values of α = 13.7% and β = 1.7% for the EG treated samples (Table 3.6) which are only slightly different from the control. Interestingly, the double hit parameter is the lowest measured for any sample used in the present study.

The ^{18}O exchange rates in the S_3 state at 10°C is shown in Figure 3.24. The two phases of exchange are apparent in the data and a kinetic fit gives the rate constants listed

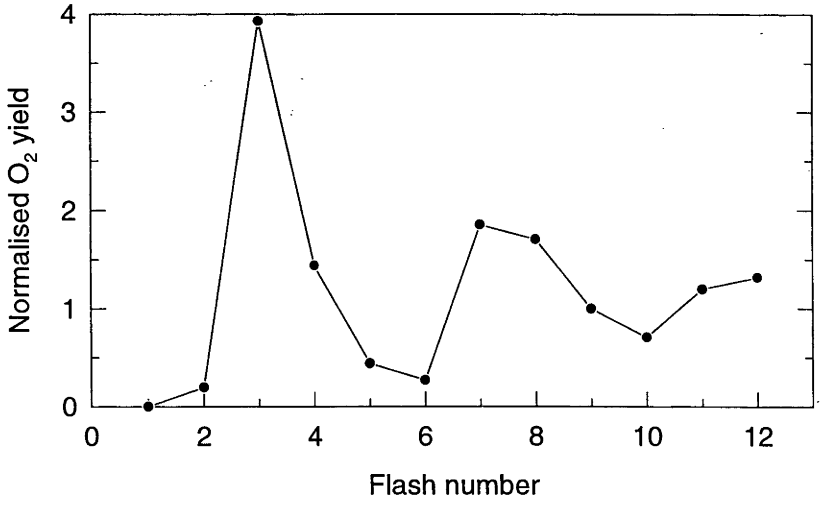

Figure 3-23 **O_2 flash yield patterns for spinach thylakoid membranes in the presence of 30% ethylene glycol measured at *m/e* = 34 following injection of ^{18}O labelled water.**

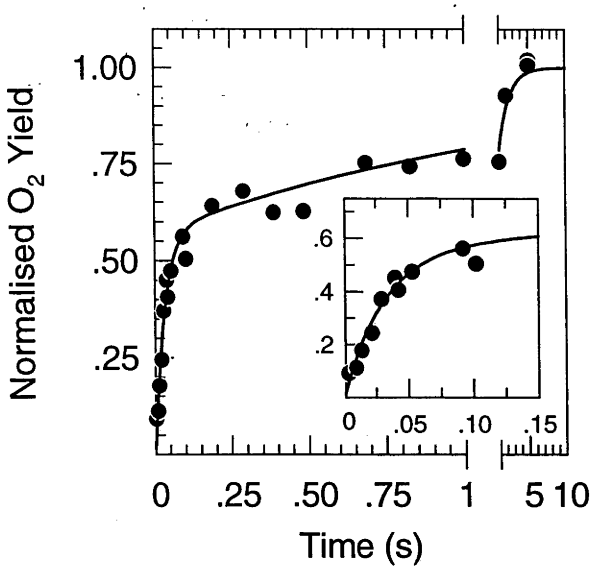

Figure 3-24 **^{18}O exchange measurements for the S_3 state of spinach PSII membrane fragments in the presence of 30% ethylene glycol. Measurements were made at m/e = 34 as a function of the exchange time Δt at 10°C. Solid lines are a kinetic fit of the normalised O_2 yield on the third flash.**

in Table 3.11. The results indicate that the slower kinetic component ($^{34}k_1$) is decreased relative to the control sample by a factor of ~2.6 while the faster component ($^{34}k_2$) is decreased by a factor of ~1.2. Clearly one of the substrate water binding sites is much more affected by the presence of ethylene glycol.

Table 3-11 Rates constants for ^{18}O Exchange in the S_3 state of thylakoid membranes in the presence of 30% Ethylene Glycol at 10°C

S_3 state at 10°C	$^{34}k_1$ (s^{-1})	$^{34}k_2$ (s^{-1})
Thylakoid membranes	1.8 ± 0.2	36.8 ± 1.9
+ 30% Ethylene glycol	0.7 ± 0.2	31.4 ± 3.8

3.3.7 pH Dependence

Investigation into the pH dependence of the exchange rates was undertaken to provide insight into the exchange mechanisms. It may be anticipated that water exchange at a metal site is strongly pH dependent. For example it has been reported that the oxo ligand in horseradish peroxidase (HRP) readily exchanges with the bulk solvent water at neutral pH but not at alkaline pH (Hashimoto *et al.*, 1986a).

The ^{18}O exchange rates in the S_3 state for spinach thylakoids were examined over the pH range from 5 to 9. To perform this analysis several buffers were selected and their pH values set accordingly at 10°C. Figure 3.25 depicts the influence of pH on the peak oxygen yield after the third flash. At the standard pH 6.8 used for the majority of the measurements in this study, the O_2 yield is essentially a maximum. Under either more acidic or more alkaline conditions activity declines with the strongest effects over the pH 8 to pH 9 range.

Figure 3.26 shows the effect of pH on the ^{18}O exchange in the S_3 state at 10°C: part (A) gives the data for the slow phase of exchange ($^{34}k_1$) and part (B) gives the data for the fast phase ($^{34}k_2$). In both sets of data, the exchange rates are fairly constant over pH 5-8,

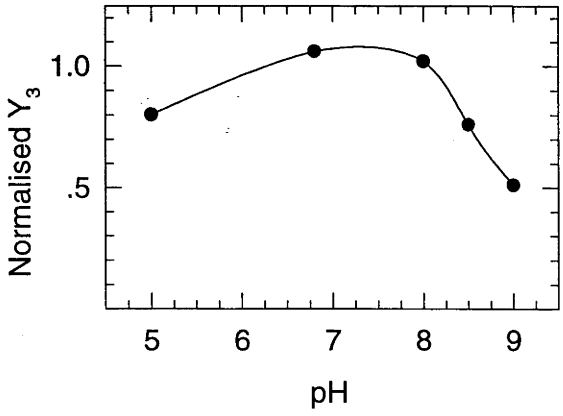

Figure 3-25 **Mass spectrometric measurements of the peak O_2 yield on the third flash (Y_3) as a function of pH in thylakoid samples. All measurements were made at 10°C in calibrated buffer media. The following acids and organic buffers were used: 5 = Succinate; 6.8 = Hepes; 8-8.5 = Tricine; and 9 = Ches.**

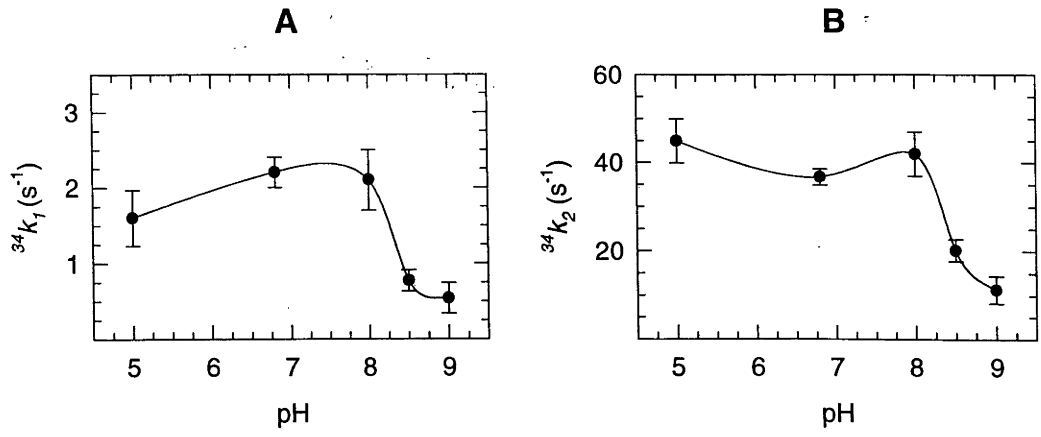

Figure 3-26 The effect of pH measured on (A) the $^{34}k_1$ slow phase of ^{18}O exchange and (B) the $^{34}k_2$ fast phase of ^{18}O exchange at 10°C. All measurements were using 10°C calibrated buffer.

although there may be a slight increase in $^{34}k_2$ at pH 5. The behaviour of the ^{18}O exchange rates correlates quite well with the pH dependence of the peak O_2 yield measurements shown in Figure 3.25.

At more alkaline conditions, above pH 8, Figure 3.26 shows that both phases of exchange ($^{34}k_1$ and $^{34}k_2$) undergo a notable slowing down. The decrease in the two rate constants parallels the loss in the peak O_2 yields shown in Figure 3.25. This result may indicate that the overall sample activity is lost through a decrease in substrate exchangeability at the WOC. The decrease in substrate exchangeability could be interpreted in a number of ways: a loss of the extrinsic polypeptides; a shift in the pK of the Mn_4 complex leading to a deprotonation of a substrate water molecule itself; or a deprotonation of an adjacent group that affects the exchange reaction. There is also an indication that the exchange reaches a plateau region above pH 9 as the exchange rates at pH 8.5 and pH 9.0 are nearly the same. This observation is probably inconsistent with a formal substrate water deprotonation because the exchange rates differ only by less than an order of magnitude over the pH range. It may, however, be related to a changes of a nearby base that either manifests a subtle structural change to the Mn_4 complex itself or to changes in the mechanism of exchange at the metal site.

3.3.8 Deuterium Isotope Effects

Information on the role of hydrogen bonding to the substrate water molecules can be obtained by measuring the effects of deuteration on the ^{18}O isotope exchange. Thylakoid membranes were resuspended and washed twice in 98% D_2O 'standard buffer

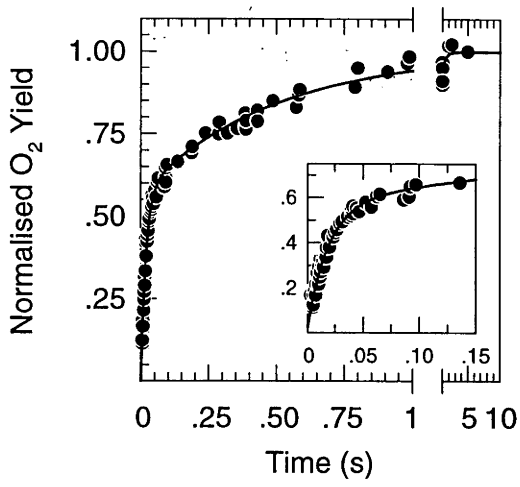

Figure 3-27 **^{18}O exchange measurements for the S_3 state of spinach thylakoid membranes in D_2O buffered media. Measurement were made at *m/e* = 34 as a function of the exchange time Δ t at 10°C. Solid lines are a kinetic fit of the normalised O_2 yield on the third flash.**

medium. Due to the increased ionisation constant of D_2O and its influence on a glass electrode (Glasoe & Long, 1960; Covington *et al.*, 1966) the pH value is increased by 0.4 units relative to the electrode to give an equivalent pL 6.8 reading for deuterated solvent (where L is a *lyonium* ion: H or D). The samples were loaded into the sample chamber and the ^{18}O exchange kinetics were determined after injection of $H_2{}^{18}O$. As the injection was nondeuterated there will be dilution of [D_2O] by the added $H_2{}^{18}O$ to ~85%. This value is accurate to within ± 0.5% as it is derived from the same effective dilution as the ^{18}O enrichment.

The effect of deuteration on the O_2 oscillation pattern was negligible (data not shown). Based on the Kok analysis of the deuterated and the control (H_2O suspended) thylakoid samples, there were no significant differences in the miss and double hit parameters as shown in Table 3.6.

In contrast, the ^{18}O exchange is altered by the presence of deuterated solvent. Figure 3.27 shows the ^{18}O exchange data in the S_3 state for the thylakoid membranes in D_2O buffered media. A kinetic fit to the data is shown and the derived rate constants are listed in Table 3.12. The kinetic components in deuterated solvent are indicated with the subscript 'D'. The exchange rates in deuterated buffer media are $^{34}k_{1(D)} = 2.0 \pm 0.2$ s^{-1} and $^{34}k_{2(D)} = 53.3 \pm 2.1$ s^{-1} for the slow and fast phases, respectively. Relative to the control rates ($^{34}k_1 = 1.8 \pm 0.2$ s^{-1} and $^{34}k_2 = 36.7 \pm 1.9$ s^{-1}, respectively) there appears to be no

effect of deuteration on the slow phase but there is a significant increase in the fast phase. The experiment was repeated several times to ensure confidence in the result and $^{34}k_{2(D)}$ was consistently observed to increase relative to the H_2O sample. The effect of deuteration is thus one of the few treatments that manifests an effect on only one phase of ^{18}O exchange (the other is ethylene glycol, see Section 3.3.6).

Solvent isotope effects on acids and bases result in a shift in pK of ~0.4 units in D_2O (Schowen & Schowen, 1982). The earlier experiments for the pH dependence of ^{18}O exchange in the S_3 state (Section 3.3.7) indicate the exchange rate $^{34}k_{2(D)}$ is outside the $^{34}k_2$ boundaries in the pH 6-8 region. This suggests that an event larger pK shift is unlikely to explain the increase in the fast exchange rate. The specific increase in the fast phase therefore indicates a solvent isotope effect. The value is inverted (less than unity) with $^{34}k_{2(H)}/^{34}k_{2(D)} = 0.68$. If one presumes a linear dependence with $[D_2O]$ then the k_H/k_D in 100% deuterated solvent, may decrease to ~0.58.

Based on the H/D ratio in exchange rate for the fast phase, the reaction is likely to involve a secondary isotope effect attributable to isotopic (H vs D) substitution where no oxygen bonds to H/D are made or broken during the rate limiting step of the exchange reaction. According to Cleland (1995) a primary isotope effects will always be greater than unity but a secondary isotope effect can be less than unity, indicating that the isotopic atom is bonded more strongly in the transition state. Based on the magnitude and the inverted nature of the deuterium effect, it is attractive to suggest that during the fast phase of ^{18}O exchange there is the involvement of H-bonding. This comes as no surprise as H-bond networks are widely postulated to exist in the WOC (i.e., Berthomieu *et al.*, 1998; Hays *et al.*, 1998). If this is indeed the case, then the D-bonded transition state during the fast ^{18}O exchange is of higher energy (ΔG) than the H-bonded transition state. This again is not unreasonable to expect with the potential for stronger D-bonds vs H-bonds (Scheiner & Cuma, 1996).

The data on the deuterium effect may therefore be taken as a good indication that the substrate water molecule in fast exchange in the S_3 state is H-bonded to a nearby base (B) either via O-H...B or via O...H-B mechanism while the other substrate water molecule in slow exchange is not. Measurements of the deuterium isotope effects in PSII (Bögershausen *et al.*, 1996; Haumann *et al.*, 1997; Karge *et al.*, 1997) and in cytochrome c oxidase (Hallén & Nilsson, 1992) have also shown a secondary isotope effects but these are normal (greater than unity) yet exhibit similar relative magnitude (ie. k_H/k_D ~1.4) and are

interpreted in terms of the involvement of H-bonding during the electron transfer reactions.

Table 3-12 **Rate constants for ^{18}O exchange in the S_3 state of thylakoid membranes suspended in D_2O buffered media at pL 6.8 and 10°C**

Sample	$^{34}k_{1(D)}$ (s^{-1})	$^{34}k_{2(D)}$ (s^{-1})
Deuterated solvent	2.0 ± 0.2	53.3 ± 2.1

CHAPTER 4

4. DISCUSSION

The present investigation was undertaken to provide information on the general question of *how and when during the photosynthetic water oxidation reaction does the substrate water bind to photosystem II.* Indeed, the whole basis for understanding the photosynthetic water oxidation reaction requires this knowledge. It is, however, not a straightforward problem to address due to the difficulty in separating the substrate water from the solvent water, and the inability to lower the substrate concentration much below 55 M. To circumvent this problem, kinetic measurements of ^{18}O isotopic exchange from labelled water can be used to unequivocally identify the involvement of the substrate water and then to probe the substrate binding sites. The basis of this study was the development of a time-resolved mass spectrometric technique to perform such isotope exchange measurements. The results have resolved several important issues for the reaction mechanism of water oxidation. They can be summarised in 4 points.

1) Substrate water exchange at the catalytic site exhibit S-state dependence strongly supporting the idea that the Mn forms the substrate binding sites.
2) The magnitude of the exchange rates under all conditions are remarkably fast, where the exchange is typically completed in less than one second. The slowest exchange measured ($t_{½}$~50 s) occurs for one of the substrate water molecules in the S_1 state. Exchange rates of these magnitudes indicate relatively labile binding for the substrate water molecules.
3) In the S_3 state two exchange rates can be resolved, indicating that both substrate molecules are bound separately in the S_3 state. At least one substrate molecule is bound from the initial S_0 state.
4) Only small changes in the substrate water exchange rates in the S_3 state occur as a result from a variety of physical and biochemical treatments, indicating that the substrate binding sites are sensitive to subtle structural changes.

4.1 Substrate Binding During the S-states

Perhaps the most important question to determine is at what step in the S-state cycle does the substrate water bind. Based on the time resolution of current mass spectrometric technique, a measurable exchange kinetic will conclusively show the existence of a substrate water in a particular S-state. The justification for this is that the O_2

release upon the S_3-S_4-S_0 transition takes ~2 ms (Jursinic & Dennenberg, 1990; Lavorel 1992; Razeghifard & Pace, 1998). Based on the Y_Z^{OX} re-reduction kinetics (Babcock *et al.*, 1976; Razeghifard *et al.*, 1997) the S-state advancement from S_0 to S_3 will take perhaps another 1 ms. Thus one complete turnover of the S-state advancement is about ~3 ms and any ^{18}O exchange that is slower would mean that the substrate water has insufficient time to enter the catalytic site. Therefore, from the exchange data (Table 3.2) we can clearly show that at least one substrate water molecule is bound throughout the entire S-state reaction sequence from S_0 to S_3 (i.e. exchanging species with $^{34}k_1$ and ^{36}k) while the second substrate water molecule (i.e. the exchanging species with $^{34}k_2$) is present at least in the S_3 state. These results are summarised in Table 4.1.

Table 4-1 Summary of substrate water binding at each of the formal S-states based on the ^{18}O exchange data.

S-state	Substrate water binding site #1	Substrate water binding site #2
S_0	Present	?
S_1	Present	?
S_2	Present	?
S_3	Present	Present

It would seem likely that the two water molecules are bound from the beginning of the reaction sequence but it is also possible that the S_0, S_1 or S_2 states have only one substrate water molecule bound and that the second substrate binding site is created in the S_3 state, on the S_2-S_3 transition. In this case, the kinetic constraint would be that the k_{ON} for binding is faster than the $^{34}k_2$ equilibrium exchange in the S_3 state. At present the kinetic resolution of the current equipment is insufficient to unequivocally decide between these two possibilities.

4.2 Possible Mechanisms to Explain ^{18}O Exchange

Injection of $H_2{}^{18}O$ into a preset S-state and then the appearance of ^{18}O in the photogenerated O_2 reflects an isotopic exchange process between the bulk solvent water and the substrate water bound within the WOC. The exchange kinetics that have been resolved in this work over the S_0 - S_3 states all reside within the range ~10^2-10^{-2} s^{-1} and can be interpreted in terms of two overall mechanisms: a) exchange of water bound to a metal

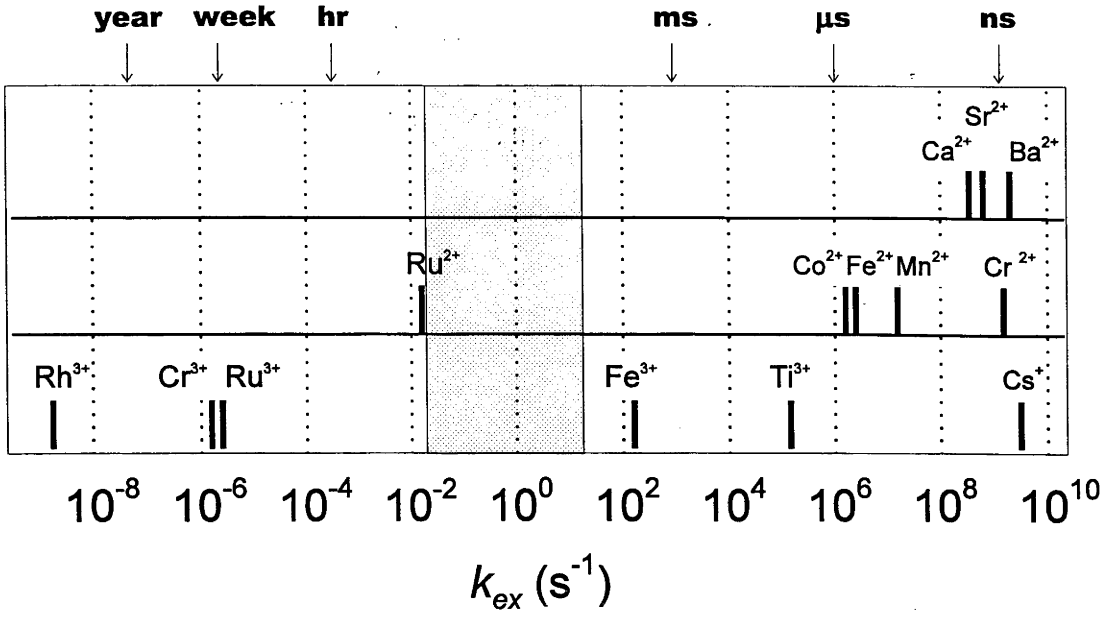

Figure 4-1 Pictorial representation of water ligand exchange rates for various hexaaqua metal ions. The central grey region indicates the resolvable exchange kinetics determined for the substrate water exchange during photosynthetic water oxidation.

site (Mn or Ca), or b) diffusional or isotopic equilibration processes where free water must be translocated to the binding site through the protein matrix.

4.2.1 Water Exchange at a Metal Site

Rates of whole water exchange at a metal site span a tremendous range, at least 18 orders of magnitude. Figure 4.1 presents in graphical form the water exchange for a selected number of hexaaqua metal ions in various oxidation states. The water exchange rates that have been measured in this work for the S_0, S_1, S_2 and S_3 states all reside within the region ~10^{2}-10^{-2} s^{-1} which is essentially mid range for the metal ions as shown in Figure 4.1. For water exchange at a metal site, probably the most significant factors are the charge and ionic radius of the ion and any electronic occupancy of *d* orbitals (Lincoln & Merbach, 1995). As a general rule, the exchange rates will decrease as the metal is oxidised and the ionic radius of the metal centre (M) decreases, i.e. $k_{ex}(M^{II}\text{-}OH_2) > k_{ex}(M^{III}\text{-}OH_2) > k_{ex}(M^{IV}\text{-}OH_2)$. A decrease in ^{18}O isotopic exchange is thus consistent with the oxidation of a metal centre.

Figure 4.1 illustrates that the rapid H_2O exchange rate for hexaaqua Mn^{II} is 2×10^{7} s^{-1} as measured by Ducommun *et al.*, (1980). Notably absent from Figure 4.1 are the water ligand exchange rates for Mn^{III} and Mn^{IV} ions. Indeed, due to the nature of the oxidising potential of these ions they do not readily exist in aqueous solution and the water exchange for these ions are currently unknown. However, based on a comparison with different

Table 4-2 **Water ligand exchange rates for various di- and tri- valent metal ions.**

Metal Ion	Exchange Rate (s^{-1})	Reference
Divalent		
$[Mn(H_2O)_6]^{2+}$	2×10^7	Ducommun *et al.*, 1980
$[Fe(H_2O)_6]^{2+}$	4×10^6	Ducommun *et al.*, 1980
$[Ru(H_2O)_6]^{2+}$	2×10^{-2}	Rapaport *et al.*, 1988
$[Ca(H_2O)_6]^{2+}$	3×10^8	Eigen *et al.*, 1963
Trivalent		
$[Fe(H_2O)_6]^{3+}$	2×10^2	Grant *et al.*, 1981
$Fe(H_2O)_5OH]^{2+}$	1×10^5	
$[Ru(H_2O)_6]^{3+}$	4×10^{-6}	Rapaport *et al.*, 1988
$[Ru(H_2O)_5OH]^{2+}$	6×10^{-4}	

oxidation states of Fe or Ru ions (Figure 4.1 or Table 4.2), the metal ligand exchange rates for Mn ions may be expected to slow down by ~10^4 s^{-1} for each formal oxidation state increase. Similarly, comparison with Cr^{III} (Table 4.3) provides an estimate for Mn^{IV} as the two ions are isoelectronic with a stable d^3 configuration. Thus, in general, the exchange of water ligands may be expected to lie in the range of ~ 10^3-10^1 s^{-1} for Mn^{III} and ~ 10^{-4}-10^{-6} s^{-1} for Mn^{IV}. Calculations currently underway at present (Kuzak & Pace, *personal communication*) appear to support these boundaries for water ligand exchange. The resolved exchange rates for the S_0, S_1, S_2 and S_3 states are thus consistent with water binding to either Mn^{III} or Mn^{IV} ions. The unresolved faster exchange rates in the S_0 S_1 and S_2 states could be consistent with Mn^{II} ions. There are, however, other important factors to consider.

A very important factor for water ligand exchange at a metal site is the protonation state of the water ligand. In the general case, it may be expected that the exchange decreases with a decrease of protonation, i.e. $k_{ex}(M\text{-}OH_2) > k_{ex}(M\text{-}OH)$, at a given oxidation state of the metal centre. The protonation state in turn will depend on the pK of the complex which is a function of both the oxidation state of the metal centre and the character of its ligation. As it turns out, Mn^{IV} ions are poor Lewis bases and the high oxidation potential will tend to polarise bound water favouring oxo ligands. The pK's for various Mn complexes have been listed earlier (Tommos & Babcock, 1998) and the following trends were noted: 1) the pK increases as the net charge of the Mn cluster increases; and 2) the increase in oxidation state appears to be less important that the

Table 4-3 **Water ligand exchange rates for fully protonated and monodeprotonated forms of monomeric and divalent transition metal ions.**

Metal ion	Exchange Rate (s^{-1})	Reference
Monomeric		Xu *et al.*, 1980
$[Cr^{III}(H_2O)_6]^{3+}$	2×10^{-6}	
$[Cr^{III}(H_2O)_5OH]^{2+}$	2×10^{-4}	
Dimeric		Crimp *et al.*, 1994
$[Cr^{III}(\mu\text{-}OH)_2Cr^{III}]^{4+}$		
H_2O trans μ-OH	4×10^{-4}	
H_2O cis μ-OH	7×10^{-5}	
$[Cr^{III}(\mu\text{-}OH)_2Cr^{III}OH]^{3+}$		
H_2O trans μ-OH	1×10^{-2}	
H_2O cis μ-OH	5×10^{-3}	

increase in net charge. The pH dependence for the substrate water exchange in the S_3 state (Figure 3.26) indicate that the p*K*'s for the substrate binding sites reside outside the pH 5-8 range. Based on the relatively fast substrate water exchange, it is attractive to suggest that the two substrate water molecules are bound in a protonated form with p*K* values above pH 8.

It should also be noted that protonation of the surrounding ligands also has a significant effect on water ligand exchange. The data in Table 4.2 and Table 4.3 include several examples of trivalent metal ions that are 6-coordinate. Deprotonation of one of the water ligands leads to a significant labilisation in the primary coordination sphere of the metal ion resulting in faster ligand exchange and lower net charge. The water exchange rates at metal ions with a single -OH ligand, for example, increase typically by ~10^2. Thus, deprotonation of neighbouring ligands can have a considerable effect on water ligand exchange. In summary, the deprotonation of the substrate water itself will slow the substrate exchange rate but the deprotonation of a neighbouring ligand may well result in the opposite effect, with an increase in the substrate exchange rate.

A further consideration is the structure of the complex as a whole. As the Mn_4 cluster is widely considered to be organised as a pair of Mn dimers with connecting μ-oxo bridges, it is relevant to consider the water exchange rates for the Cr^{III} di-hydroxo bridged dimer. Table 4.3 lists the water exchange rates for the monomeric Cr^{III} (Xu *et al.*, 195) and di-hydroxo bridged Cr^{III} complexes (Crimp *et al.*, 1994). As discussed above, the

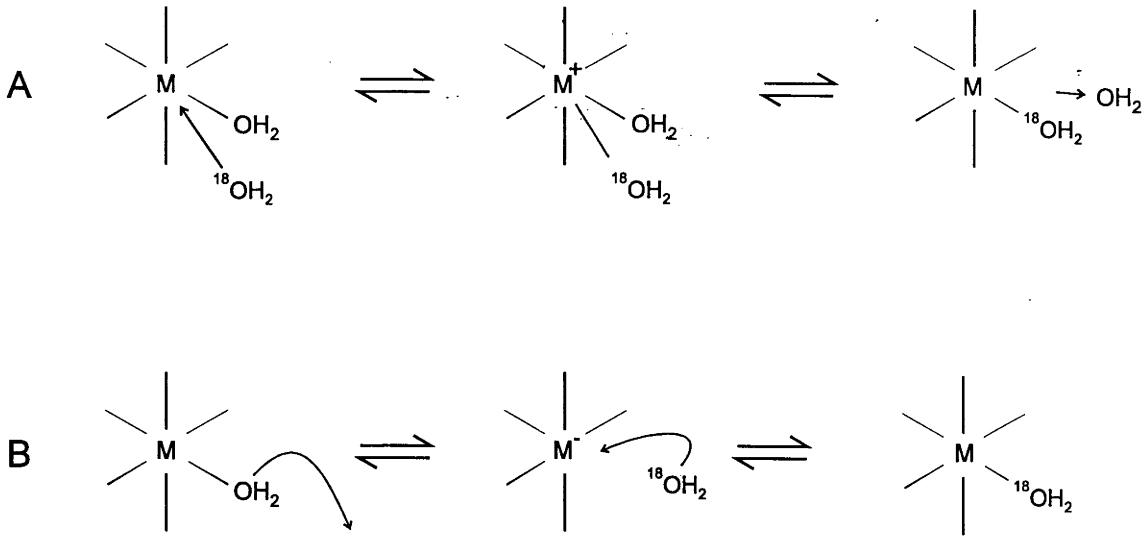

Scheme 4-1 Water ligand exchange on a metal ion via (A) associative exchange or (B) dissociative exchange mechanisms. See text for details.

deprotonation of a ligands in a monomeric ion results in a labilisation of the primary coordination sphere and a increase in water exchange rates. The di μ-oxo bridged Cr^{III} also undergoes an increase in exchange rates upon mono-deprotonation of a ligand. The effect of deprotonation in both the monomeric and dimeric Cr^{III} species is an increase in exchange rate of $\sim 10^2$ s^{-1}. It is also important to note that the water ligand exchange rates also increase upon the addition of a di-hydroxo bridge, by at least an order of magnitude. The overall protonation behaviour is also observed in monomeric Rh^{III} (Laurenczy *et al.*, 1991) and the di-hydroxo bridged Rh^{III} complexes (Drljaca *et al.*, 1996; 1998). The effect of deprotonation is argued to be cumulative (Crimp *et al.*, 1994). Thus, a Mn^{IV} species which would ordinarily be expected to have a slow terminal ligand exchange, could have substantially increased exchange through μ-oxo bridge formation and ligand deprotonation. Consequently, these arguments can be used to interpret the measured exchange rates in terms of Mn^{IV} intermediates.

Other important factors that may influence the water ligand exchange rates at a metal site are the coordination geometry (axial vs equatorial) and spin state of the metal centre (high spin vs low spin). Mn^{III} ions, for example, are in d^4 configuration and, if in 6 coordinate octahedral geometry, may exhibit *Jahn-Teller* distortions due to degeneracy in the e_g orbital. These distortions result in a lengthening of the axial bonds. The water exchange from such a longer axial bond is anticipated to be considerably faster. Conversely, the equatorial ligand bonds are shorter and will result in a slower water ligand exchange. The structure of the Mn_4 cluster in the WOC is yet to be defined but the Mn is believed to be

mainly coordinated to carboxyl ligands (Yachandra *et al.*, 1996; Dittmer & Dau, 1998) which would tend to promote high spin clusters.

The formal mechanisms of water ligand exchange on a metal site are quite diverse. Two principle exchange pathways exist: associative and dissociative exchange, although there is a continuum of intermediate pathways. The two pathways are illustrated in Scheme 4.1. Associative exchange proceeds via an intermediate of increased coordination number where the exchange is controlled by the access of the entering ligand water (i.e. the ability to generate an additional ligation site) and the k_{ON} rate. Conversely, dissociative exchange proceeds via the expulsion of a water molecule and the k_{OFF} rate is the determining factor.

4.2.2 Other Oxygen Ligand Exchange at a Metal Site

There may be a number of possible intermediates in the water oxidation pathway and it is important to appreciate that the ^{18}O exchange kinetics reflect an exchange reaction between the bulk solvent water and bound water intermediates within the WOC. Thus, the exchange measurements could reflect not only whole water exchange but also the exchange of μ-oxo (-O-), peroxo (-O-O-) or oxo (=O) species. Indeed, various models for photosynthetic water oxidation have invoked such μ-oxo, peroxo and oxo intermediates in the S_3 state. The critical implication for these models is how the O-O bond is generated.

4.2.2.1 μ-Oxo Bridges

The Mn_4 cluster is generally agreed to be arranged as two di-μ-oxo bridged Mn dimers based on numerous spectroscopic measurements. Some proposals have suggested that the μ-oxo bridges of the Mn dimers act as intermediates in the water oxidation reaction (Yachandra *et al.*, 1996) by condensing via a μ-η^2:η^2 peroxo intermediate to generate O_2, as proposed for some binuclear Cu systems (Tolman, 1997). This model is cleverly integrated with the oxidation states and distance changes associated with the EXAFS measurements during the S-state cycling. Others have invoked the condensation of the μ-oxo bridges from one of the Mn dimers to form a peroxo intermediate which is then oxidised by the second Mn dimer to produce O_2 (Pecoraro, 1994). The key question for these mechanisms is can a μ-oxo bridge exchange occur in less than a second?

It has been demonstrated that the μ-oxo oxygen bridge can exchange with solvent water in binuclear model Mn^{III} μ-oxo dimers (Sheats *et al.*, 1987) though the relevant exchange rates are not known. Typically, however, the μ-oxo exchange is a slow process. Table 4.4 provides a list of some oxo bridges that undergo ^{18}O exchange. The defining

influence on the μ-oxo exchange rate appears to be the pathway for exchange. Thus, the $[Mo^{V}O_3]^{4+}$ species proceeds via an intramolecular pathway (Thompson *et al.*, 1993) and the $Cr^{III}(\mu\text{-}OH)_2Cr^{III}$ proceeds via a ring opening mechanism (Crimp *et al.*, 1994). In contrast, the $Rh^{III}(\mu\text{-}OH)_2Rh^{III}$ complex is inert to μ-oxo exchange (Drljaca *et al.*, 1998).

Table 4-4 Oxygen exchange rates for μ-oxo bridges in various metal complexes

Metal complex	Exchange rate (s^{-1})	Reference
$(Fe^{III})_2$ μ-oxo in *Ribonucleotide reductase*	8×10^{-4} [a]	Sjöberg *et al.*, 1983
$Cr^{III}(\mu\text{-}OH)_2Cr^{III}$	1×10^{-5}	Crimp *et al.*, 1994
$Rh^{III}(\mu\text{-}OH)_2Rh^{III}$	substitution inert	Drljaca *et al.*, 1998
$Ru^{III}\text{-}O\text{-}Ru^{III}$	6×10^{-6} [b]	Hurst *et al.*, 1992
$[Mo^{IV}_3O_4(H_2O)_9]^{4+}$	$t_{½} > 10$ years	Richens *et al.*, 1989
$[Mo^{V}O_3]^{4+}$	$\sim 10^{-6}$ [b]	Thompson *et al.*, 1993

Conditions: (a) 4 °C; (b) 40°C; or otherwise ambient room temperature.

The μ-oxo exchange in the Cr^{III} dimer proceeds via a ring opening step with a ΔH of ~100 kJ mol^{-1} (Crimp *et al.*, 1994). The exchange rates for the slow phase in the WOC, particularly in the S_1 state, exhibit similar high activation energies and the magnitude of the rates approach the value of the Cr dimer (Table 4.4). As discussed earlier, deprotonation of the complex significantly affects the exchange rates of terminal species and similarly can also affect the exchange of μ-oxo bridges. The monodeprotonated $Cr^{III}(\mu\text{-oxo})Cr^{II}OH$ species has a bridge exchange rate of 2×10^{-3} s^{-1}, which is notably faster than the protonated form of 1×10^{-5} s^{-1} of the complex (Table 4.3). Furthermore, deprotonation events are likely to be cumulative (Crimp *et al.*, 1994). It is therefore attractive to consider the possibility that the slow phase of exchange in the WOC is from a μ-oxo bridge between two Mn^{III} centres. However, it would seem that the current proposal for Mn oxidation buildup, i.e. advancement of Mn^{II} to Mn^{III} to Mn^{IV} on the $S_0 \rightarrow S_1 \rightarrow S_2$ transition, is inconsistent with the S-state dependent behaviour in exchange rates. In summary, at this stage, and until definitive exchange rates for Mn di μ-oxo model compounds are measured, a labile μ-oxo bridging structure for a Mn complex in the WOC cannot be excluded conclusively.

4.2.2.2 Peroxo Intermediates

A concerted 4 electron pathway for water oxidation is generally considered to be more difficult thermodynamically than a two 2 electron oxidation pathway involving a stable peroxo intermediate (Krishtalik, 1990). As such peroxo intermediates have been proposed to be produced early in the water oxidation reaction sequence, prior to the S_4 state (Renger, 1993; Karge *et al.*, 1997). Various assays for PSII light induced H_2O_2 generation have produced signals that are interpreted to arise from a S_2 state bound peroxide intermediate (Ananyev & Klimov, 1989; Klimov *et al.*, 1993). Peroxo intermediates have been proposed in Mn model compounds, some of which can perform water oxidation (Armstrong, 1992; Aurangzeb *et al.*, 1994; Debé *et al.*, 1998). However, the initial finding of one fast and one slow exchange kinetic for the substrate water in the S_3 state by Messinger *et al.*, (1995) does not support the existence of a long-lived symmetrical peroxide intermediate. Rather the peroxide that is observed is considered to arise from a side reaction (Wydrzynski *et al.*, 1996)

Further refinements to the peroxide intermediate hypothesis (Karge *et al.*, 1997) have suggested that the terminal water ligands in the S_3 state are in rapid (~1 ms) redox isomerisation with a peroxidic state i.e.

$$Mn^{IV}\,O(H)_u \;\; Mn^{IV}\,O(H)_v \quad \Leftrightarrow \quad Mn^{III}\text{-}(H)_xO\text{—}O(H)_y\text{-}Mn^{III}$$

where u, v, x and y refer to the number of protons bound to the substrate oxygen. This mechanism would appear consistent with the ^{18}O exchange data for the S_3 state. However, the model does not address the following questions: 1) in what direction does the equilibrium lie as isomerisation times < 1 ms imply a very dynamic and rapid mechanism; 2) the consequent rapid proton release/uptake pathways should imply very different k_H/k_D ratios for the peroxidic and non-peroxidic states; and 3) can such a mechanism account for the appearance on the S_2-S_3 transition of a resolvable phase of exchange (Table 3.3). It seems that the current proposed peroxo-intermediate model would have considerable difficulty in accounting for the S-state dependence of the ^{18}O exchange measurements (Table 3.2).

4.2.2.3 Terminal Oxo Ligands

Involvement of oxo ligands on Mn^{IV} ions is an attractive possibility for the formation of the dioxygen bond (Hoganson *et al.*, 1995; Messinger *et al.*, 1995). A limited number of oxo ligand exchange rates are known but unfortunately none for a Mn^{IV}=O.

Table 4.5 lists examples of Ti, V and Mo complexes and, generally speaking, the oxygen exchange rates are quite slow. The important issue for oxo exchange with solvent water is that the oxo species must first be protonated. The Ti=O species listed in Table 4.5 is an example where the oxo oxygen is believed to be easily protonated to account for its unexpectedly fast exchange when compared to that of V (Comba & Merbach, 1987). However, exchange of the oxo ligand on the Ti, V and Mo ions also involve complex intermolecular reactions, so these examples should be considered with caution when making comparisons with PSII.

Table 4-5 Oxo exchange rates for various metal complexes

Metal Complex	Rate of exchange	Ref
$Ti^{IV}=O$	2×10^{4}	Comba & Merbach, 1987
$V^{IV}=O$	2×10^{-5}	Johnson & Murmann, 1983
$[Mo^{V}O_3]^{4+}$	4×10^{-3} [a]	Thompson *et al.*, 1993

Conditions: (a) 0 °C; otherwise ambient room temperature.

There are some biological examples of oxo exchange involving Fe and Mn porphyrin systems. Both horseradish peroxidase (HRP) compound II and the cytochrome c peroxidase (CCP) undergo $Fe^{IV}=O$ exchange with bulk water, but only when H-bonding is present to the oxo ligand (Hashimoto *et al.*, 1986a; Hashimoto *et al.*, 1986b). Similarly without H-bonding there is no oxo exchange in model $Fe^{IV}=O$ porphyrins (Hashimoto *et al.*, 1987). The HRP enzyme can also undergo Mn substitution, and although catalytically active (Yonetani & Asakura, 1969), does not undergo ^{18}O exchange with solvent water (Nick *et al.*, 1991). To account for the absence of exchange it was suggested that the weaker $Mn^{IV}=O$ bond in the HRP enzyme and the enhanced basicity alters the H-bond donor group (Makino *et al.*, 1986; Nick *et al.*, 1991). This interpretation appears to be supported by studies of model $Mn^{IV}=O$ porphyrin (Czernuszewicz *et al.*, 1988; Groves & Stern, 1988) which do exhibit a more weakened $Mn^{IV}=O$ bond than in Fe^{IV} or Cr^{IV} complexes and is attributed to the half filled t_{2g} d-orbitals of Mn^{IV}. Taken together these findings suggest that the oxo exchange for a Mn^{IV} complex necessitates at least the involvement of a strongly basic group in close proximity to impose a H-bond. An alternate mechanism may exist involving the generation of a cation on the metal centre and relocation of electron density (Kramarz & Norton, 1994), analogous to organic carbonyls.

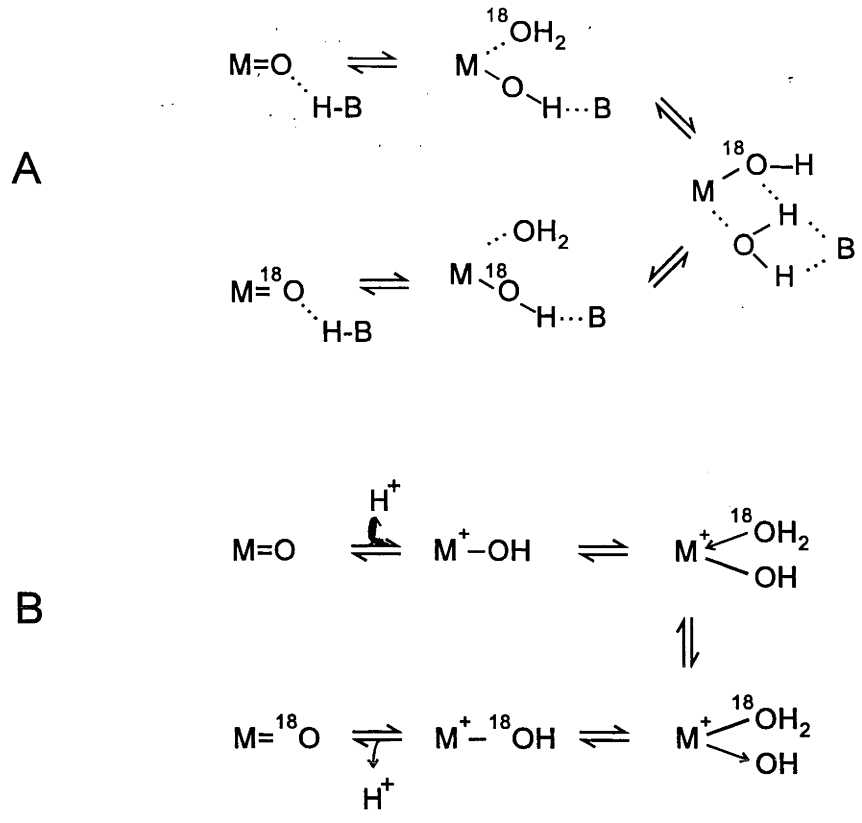

Scheme 4-2 Exchange of a terminal oxo ligand with bulk solvent water involving protonation through either A) the formation of H-bonding between an adjacent bases or B) the formation of a cation analogous to the mechanism in organic carbonyls. See text for details.

The two reaction schemes depicting oxo exchange pathways with bulk solvent water are illustrates in Scheme 4.2.

There are a number of other high valence metal ions with oxo ligands, largely derived from the porphyrin field, which are able to undergo oxygen exchange with the bulk solvent water. These exchange processes have often been considered to be relatively fast due to the incorporation of ^{18}O label from solvent into oxygenated products. However, this view has been challenged recently (Nam & Valentine, 1993) and the fast rates of oxo exchange need to be also considered in terms of redox tautomerism mechanisms (Bernadou *et al.*, 1994). To date no Mn^{IV}=O exchange has been demonstrated with solvent water in a non-porphyrin system. One of the kinetic constraints with Mn^{IV} is the d^3 configuration and the half filled t_{2g} orbitals: d_{xy}, d_{yz} and d_{xz}. Such electronic configurations tend to make inherently stable complexes as the electron distribution repels incoming ligands. An example of this situation is the high spin Cr^{III} ion which exhibits a very slow water exchange (Table 4.2). Conversely, a 5 coordinate Mn^{IV} may exhibit a very different ligand field splittings which would change the filling of the d orbitals. Although the Mn

coordination in the WOC is not known, theoretical considerations of trivalent Mn ions indicates a preference for penta coordination with either square planer or trigonal bipyramidal geometry (Åkesson *et al.*, 1994; Blomberg *et al.*, 1997a,b; Rotzinger, 1997). Situations of 5-coordinate Mn^{IV} centres could very well facilitate more labile oxo exchange rates.

4.2.2.4 Involvement of Calcium

A number of recent models for photosynthetic water oxidation have proposed a direct role for Ca^{2+} ions in the mechanism of the O-O bond formation, specifically as a substrate water holding site (Pecoraro *et al.*, 1998; Brudvig *et al.*, 1999; Siegbahn & Crabtree, 1999). Although spectroscopic evidence for the close proximity of a Ca^{2+} ion to the Mn_4 cluster is mounting (Noguchi *et al.*, 1995; Booth *et al.*, 1996; Latimer *et al.*, 1998; Cinco *et al.*, 1998) and one Ca^{2+} ion is known to be associated with oxygen evolution activity (Ädelroth *et al.*, 1995), the function of this ion in the reaction is far from clear. Early suggestions for the role of Ca^{2+} have included a substrate water holding site (Rutherford *et al.*, 1989) or in a type of gatekeeper function controlling accessibility/reactivity of the WOC (Tso *et al.*, 1991).

The substrate water exchange rates measured in this work appear to exclude Ca^{2+} ions as being involved in the role as a substrate binding site, at least in the S_3 state. The reason for excluding Ca^{2+} is that the rates of water ligand exchange rates at a Ca^{2+} site are exceedingly fast, i.e. 3×10^8 s^{-1}, and the exchange rate in the S_3 state is ~7 orders of magnitude slower. However, it is possible that Ca^{2+} is involved in binding the substrate water in the earlier S-states, i.e. S_0, S_1, or S_2, as there is a unresolved fast exchange.

4.2.3 Limitations in Accessibility

Another possible explanation for the measured ^{18}O exchange rates in the WOC of PSII is one of kinetic limitations due to diffusion or isotopic equilibration. In the first instance, the exchange is unlikely to be limited by solvent transport across the intact thylakoid vesicle. PSII membrane fragments which do not maintain the vesicular structure do not exhibit a faster exchange rate compared to thylakoids (Table 3.5). This conclusion is supported by the calculated water transport times of 1-2 ms into the lumen (Sharp & Yocum, 1981).

Nevertheless, the WOC is located within the protein domain away from the bulk solvent phase. Clearly a phenomenological water channel must exist, something akin to what is proposed for the cytochrome c oxidase (Iwata *et al.*, 1995; Tsukihara *et al.*, 1996).

Such a water channel may provide an important function in the optimisation of the water oxidation reaction (Wydrzynski *et al.*, 1996). However, the existence of possible water channels must await to be established with crystallographic techniques. Regardless, the question remains as to whether or not ^{18}O exchange is limited by the entry of the solvent water through the protein matrix or by the chemical exchange at the metal site. Clearly, the inability to resolve the fast phase of exchange in the S_0, S_1, and S_2 states could mean that one of the substrate water molecules enters the catalytic site in the S_3 state in which the resolvable fast phase reflects an accessibility barrier. There is some evidence to indicate that the S_3 state is less reactive to exogenous oxidants (hydrazine, hydroxylamine) than the S_2 state and this has been interpreted in terms of structural changes during the $S_2 \rightarrow S_3$ transition (Messinger *et al.*, 1991). There are, however, a number of reasons that make issues of accessibility unlikely to account for the exchange rates measured.

Firstly, the fast phase of exchange in the S_3 state is ~38 s^{-1} (Table 3.3). This implies a lifetime of ~27 ms at 10°C. Invoking *Fick's second law of diffusion* to obtain a distance associated with such a time it follows

$$x\ (\text{rms}) = 2\sqrt{(Dt/\pi)}$$

where a relevant diffusion coefficient (D) for water through a lipid is 10^{-9} m^2 s^{-1}. The average distance travelled in a time of 27 ms would be ~ 20 μm. This distance is too large and excludes simple diffusional limitations over the 10-20 Å into the WOC as contributing to our measured ^{18}O exchange reactions.

Secondly, integral water exchange rates in a number of proteins have been measured and determined to be very fast. Residence times for protein-bound water molecules range from 10^{-9}-10^{-3} s using NMR techniques. The majority of these water molecules exhibit residence times in the subnanosecond range and are attributed to surface water, but a small number are much longer lived (Otting *et al.*, 1991; Dötsch & Wider, 1995; Denisov & Halle, 1996a). The longer-lived water molecules appear to be buried within the protein and to correlate with crystallographically defined water (Denisov *et al.*, 1995). The magnitude of the fast phase of exchange in S_3 is slower than any measured water exchange process from within a protein by several orders of magnitude.

Thirdly, the NMR studies also indicate that the exchange of buried water molecule is related to the conformational changes and flexibility of the protein (Denisov *et al.*, 1996b) It seems unlikely that conformational changes are driving the fast phase of exchange the S_3 state for a number of reasons: 1) the activation energy for the fast exchange in S_3 is ~40 kJ

mol^{-1} (Table 3.4) which is quite high for a conformational/structural change; 2) numerous sample preparations (Table 3.5) and treatments (Tables 3.7; 3.8; 3.9) are unable to increase the fast phase of exchange; 3) the same treatments typically will affect both phases to similar degrees. For these reasons it would seem unlikely that the substrate accessibility is limited by accessibility into the protein.

4.3 On the Nature of Substrate binding

The discussion up to this point has covered details of water ligand exchange and summarised possible exchange mechanisms. In general, it is difficult to be precise about the nature of the exchange mechanism based on measurements of a single S-state. However, comparisons of isotope exchange between S-states is highly valuable and begins to place limitations on the mechanism involved.

A key finding in this study is that for all S-states (S_0, S_1, S_2 and S_3) the two substrate water molecules exhibit distinctly different behaviour. This observation suggests that the O-O bond is formed only after the S_3 state, in a concerted 4 electron mechanism. A second key finding is that there is **not** a sequential slowing in the exchange rates from $S_0 \rightarrow S_1 \rightarrow S_2$ which can be interpreted as a sequential $Mn^{II} \rightarrow Mn^{III} \rightarrow Mn^{IV}$ oxidation. The scheme below illustrates the relative changes in the rates for the two phases of exchange during the S-state cycle and the following discussion will endeavour to propose explanations for the observed behaviour.

	S_0	→	S_1	→	S_2	→	S_3
Site #1	Decrease (~1000)		Increase (~100)		No change		
Site #2	?		?		Decrease (>5)		

4.3.1 $S_0 \rightarrow S_1$ Transition

In the S_0 state, exchange of a single substrate water is resolved at 10 s^{-1} (Table 3.2, 3.3). The magnitude of this exchange rate is inconsistent with water ligand exchange originating at a Mn^{II} site which would be expected to be considerably faster (k_{ex} ~10^7 s^{-1}). The measured exchange, however, is potentially consistent with a water ligand bound to a Mn^{III} or Mn^{IV} site

(see section 4.2.1). Similarly, a slow phase of exchange is also resolvable in the S_1 state, but with a rate constant of ~0.02 s^{-1} (Table 3.2, 3.3). Thus, the net effect upon the $S_0 \rightarrow S_1$ transition is a slowing down in the measured exchange by a factor of 10^3 s^{-1}.

Current XANES measurements of the S_0 state (Roelofs *et al.*, 1996; Luzzolino *et al.*, 1998) and the discovery of the S_0 EPR signal (Åhrling *et al.*, 1997; Messinger *et al.*, 1997a) are consistent with the following oxidation assignments for the four Mn ions in the S_0 state: Mn^{II}, Mn^{III}, Mn^{IV}, Mn^{IV}. The XANES measurements also strongly support the $Mn^{II} \rightarrow Mn^{III}$ oxidation on the $S_0 \rightarrow S_1$ transition (Luzzolino *et al.*, 1998; Messinger *unpublished*). Although earlier UV measurements were initially interpreted in terms of a $Mn^{III} \rightarrow Mn^{IV}$ oxidation on $S_0 \rightarrow S_1$ (Lavergne, 1991), the UV changes are significantly different on this transition than on the $S_1 \rightarrow S_2$ and $S_2 \rightarrow S_3$ transitions and subsequent interpretations now consider that a $Mn^{III} \rightarrow Mn^{IV}$ oxidation on $S_0 \rightarrow S_1$ is less likely (Dekker, 1992). Thus, the $S_0 \rightarrow S_1$ transition is generally considered to be a $Mn^{II} \rightarrow Mn^{III}$ oxidation. The question becomes how can the magnitudes of the slow exchange measured for the S_0 and S_1 states be made compatible with the predicted Mn oxidation states.

A possible explanation for this exchange behaviour is that there is a Mn^{II} ion in S_0 which is indeed oxidised to Mn^{III} in the S_1 state. This Mn^{II} ion, however, would not bind the resolved substrate water molecule directly but its oxidation would influence the exchange properties of the substrate binding site, which may well be a ligand site on a Mn^{III} (minimally) or a Mn^{IV} centre. The slowing down of the exchange process would then result from a change in the primary coordination sphere of a substrate binding metal centre due to increased electron density from the neighbouring $Mn^{II} \rightarrow Mn^{III}$ oxidation. Such a suggestion implies that valence trapping of electrons does not occur during $S_0 \rightarrow S_1$ at room temperature. Examples of di μ-oxo Mn^{III} Mn^{IV} complexes exhibiting strong temperature dependence possibly can be used in support of this argument (Okuno & Nishida, 1996). Alternatively, the metal oxidation causes an increase in the p*K* of the complex and deprotonation of the substrate water itself.

It has been suggested that a μ-hydroxo bridge is deprotonated on the $S_0 \rightarrow S_1$ transition (Yachandra *et al.*, 1996; Limburg *et al.*, 1999). However, this case may also be unlikely since this type of deprotonation would tend to increase the electron withdrawing character of the bridge and consequently lead to faster water ligand exchange rates, unless the substrate molecule was in fact the μ-oxo bridge. Then the $Mn^{II} \rightarrow Mn^{III}$ oxidation

could account directly for the slowing down of in the ^{18}O exchange. As discussed earlier (Section 4.2.1.1), μ-oxo exchange at a Mn^{III} bridged dimer may in principle exhibit rates consistent with the observed k_{ex} ~0.02 s^{-1} given appropriate conditions of surrounding ligands.

Finally, some measurements of the water oxidation reaction have indicated that there may be long *relaxation* processes (seconds to hours) for the S_1 state which is suggested to interconvert in darkness between so-called 'active' and 'resting' forms (Beck *et al.,* 1985; Sivaraja *et al.,* 1989; Koulougliotis *et al.,* 1992), but possibly also for the S_0 state (Srinivasan & Sharp, 1986; Styring & Rutherford, 1988). However, it seems very unlikely that the observed exchange kinetics in the S_0 state arise from such phenomena as all samples are given an initial preflash to enrich [S_0]. In light of recent power saturation studies on the EPR signals (Peterson *et al., submitted*), a dynamic interconversion between different forms of the S-states during progressive cycling may occur but the nature of this phenomenon remains unclear.

4.3.2 $S_1 \rightarrow S_2$ Transition

XANES measurements (Roelofs *et al.,* 1996; Luzzolino *et al.,* 1998) and the nature of the multiline EPR signal favour the organisation of the Mn_4 cluster as an antiferromagnetically coupled Mn^{III}/Mn^{IV} dimer coupled to a second dimer of homogenous oxidation states of either Mn^{III}/Mn^{III} or Mn^{IV}/Mn^{IV} in the S_2 state. Although the latest interpretations suggest that the second pair of Mn ions exist in the higher oxidation state, the Mn^{III}/Mn^{III} assignment should not be ignored because the exact Mn coordination numbers are not known (Zheng & Dismukes, 1996) and because model Mn complexes exhibit some variations in edge energy position. Indeed, discussions with Dr R. Pace have raised the issue that the edge energy position may be strongly influenced by the O/N ratio of the primary coordination sphere.

The $S_1 \rightarrow S_2$ transition is commonly held to be an oxidation of $Mn^{III} \rightarrow Mn^{IV}$ resulting in the appearance of the associated EPR signals However, surprisingly the phase of exchange that is resolved in S_1 increases by a factor ~100 upon advancement to S_2 (Table 4.1), in contradiction to a formal oxidation increase of the Mn substrate binding site. Again, if the oxidation were to occur at a non substrate binding site coupled to a deprotonation event in one of the neighbouring ligands, then the increase in the rate can be explained (see Section 4.2.1). Examples of this situation can be seen with trivalent metal ions (Table 4.2) and the Cr^{III} hydrolytic dimer (Table 4.3). The effect of the deprotonation

is a labilisation of the primary coordination sphere resulting in increased ligand exchange. Here the proposed deprotonation of a μ-hydroxo bridge on the $S_0 \rightarrow S_1$ transition (Yachandra *et al.*, 1996; Limburg *et al.*, 1999) could be well consistent with this observation. The effect of bridge deprotonation is illustrated below. However, current EXAFS measurements can not be interpreted in terms of the distance change required for a deprotonation of a μ-oxo bridge on this transition (Yachandra *et al.*, 1996). One may speculate on the involvement of other ligands; for example, Noguchi *et al.*, (1995) have identified by FTIR measurements a change in the Mn ligation derived from a selective breakage of a carboxlyate bridge on $S_1 \rightarrow S_2$. In principle, such a structural change could have an effect on water ligand exchange rates similar to bridge deprotonation.

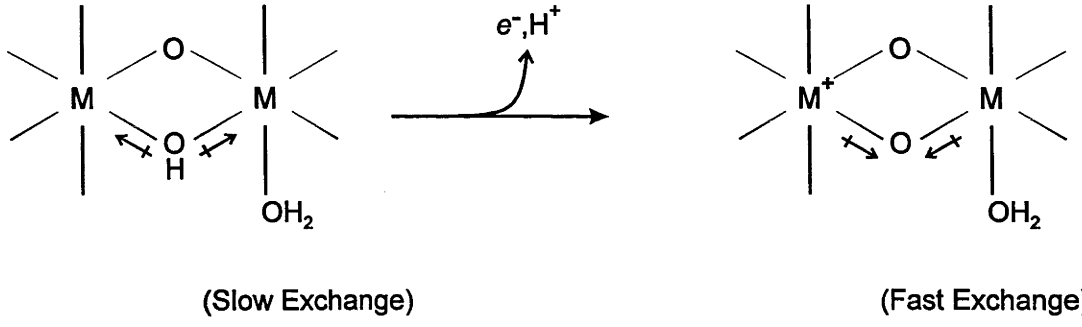

Scheme 4-3 Proposed bridge deprotonation event resulting in increased electron withdrawing character in the μ-oxo bridge. The net result is a reduced labilisation of the primary coordination sphere and faster water exchange rates.

4.3.3 $S_2 \rightarrow S_3$ Transition

The status for the Mn oxidation state changes associated with the $S_2 \rightarrow S_3$ transition is currently unclear. There are two groups undertaking XANES measurements of the S-states and their findings differ. The most recent publication (Luzzolino *et al.*, 1988) argues that there is a formal Mn oxidation increase on the $S_2 \rightarrow S_3$ transition. A second group argues that there is an oxidation of a non-Mn entity during this transition (Roelofs *et al.*, 1996; Messinger, *personal communication*). There are a variety of other measurements that support either one of these outcomes and the issue is far from resolved at this point.

The ^{18}O exchange behaviour upon the $S_2 \rightarrow S_3$ transition reveals two clear effects: 1) the slow exchanging substrate water molecule remains unchanged upon the $S_2 \rightarrow S_3$ transition; 2) the second substrate water molecule undergoes a slowing down in exchange

rate by a factor of 5 or greater. The substrate water molecule that is unchanged in exchange rate is presumably the same species that is resolved from the outset in the S_0 state. If one accepts that this species is a terminal water ligand bound to a Mn site that does not undergo oxidation on $S_0 \rightarrow S_1$ then there is also no evidence based from the exchange measurements for the advancement in formal oxidation of this site on the $S_1 \rightarrow S_2$ and $S_2 \rightarrow S_3$ transitions. The appearance of resolvable exchange kinetics for the second substrate water on the $S_2 \rightarrow S_3$ transition could correspond to what is interpreted by some as a $Mn^{III} \rightarrow Mn^{IV}$ oxidation state increase (Luzzolino *et al.*, 1998) or by the oxidation of a non-Mn site that results in a concomitant deprotonation of the substrate. We now have a situation in the S_3 state where there are two separate resolvable exchange rates which must be accounted for in terms of differences in Mn valence, i.e. Mn^{III} vs Mn^{IV} or differences in the ligation and labilisation of the primary coordination sphere of the Mn centres.

4.3.4 The S_3 State

To understand better the nature of the two separate substrate binding sites extensive, studies were performed on the S_3 state. Measurements from a variety of samples (thylakoid membranes, PSII membrane fragments, PSII cores from spinach and PSII cores from cyanobacteria) all consistently indicate that there are two separate sites in the S_3 state (Figure 3.8, 3.12). The fast and slow phases of exchange for all samples also consistently fit to the derived distribution of 57:43 based on the isotopic enrichment (Equation 2.1). The temperature dependence of the two phases in thylakoid membranes indicates that the substrate water molecule undergoing fast ^{18}O exchange has an activation energy of 39 ± 5 kJ mol^{-1} and the slow phase of exchange has an activation energy of 79 ± 6 kJ mol^{-1} at temperatures between 0-20°C and (assuming Arrhenius behaviour) (Figure 3.10; Table 3.4). Because of the difference in activation energies and the difference in the magnitudes of the two exchange rates, the two substrate water molecules are likely to be bound at two chemically distinct sites in the Mn_4 cluster. As the difference between the two exchange rates, $^{34}k_1$ and $^{34}k_2$, is not very large, Mn-substrate pair combinations differing by a formal oxidation state may be considered unlikely, unless countered by differences in protonation or ligation.

There are, however, small variations in the magnitudes of the exchange rates among the different sample preparations. The exchange rates for thylakoids exhibit the fastest exchange rates and the PSII cores the slowest (Table 3.5). The implication from this result

is that the substrate water is bound slightly more tightly in the PSII core preparations. However, the relative differences in rates, although they are measurable (differences by a factor of 2-3), are probably not all that significant with respect to the mechanism of exchange. In terms of energy, these differences represent effects in the order of 2-3 kJ mol^{-1} (Equation 3.5) which is consistent with small structural changes.

A number of small molecules inhibit O_2 evolution activity (Debus, 1992; Rutherford, 1992) potentially by competing with water at the substrate binding site. Given their accessibility to the Mn_4 cluster (Radmer & Ollinger, 1983) this is perhaps not surprising. Competitive ligands block water oxidation when their k_{OFF} rate is slower than the reaction turnover time. A commonly considered example of a competitive ligand is NH_3 which is isoelectronic with H_2O (Sandusky & Yocum, 1984; 1986). The NH_3 effects have been interpreted mechanistically as arising from the formation of a bridging imido group in the WOC (Beck & Brudvig, 1986; 1988; Brudvig & Beck, 1992) and are supported by ESEEM (Britt *et al.,* 1989) and EXAFS measurements (Dau *et al.,* 1995). It is clear, however, that the 50-100 mM NH_4Cl concentration ranges used in the above mentioned work result in only partial inhibition as S-state turnover continues and O_2 is evolved (Delrieu, 1976; Boussac *et al.,* 1990; Figure 3.21). The ^{18}O exchange measurements demonstrate that in the S_3 state (Table 3.10) the two substrate water molecules are not significantly affected by the presence of 100 mM NH_4Cl (~2 mM NH_3 free base). There is an overall slowing down of ~50% in the exchange rates and as discussed above this represents only a small energy difference of 2-3 kJ mol^{-1}. Based on the measurable exchange rates for the two substrate water molecules, NH_3 must have a k_{OFF} rate at the substrate binding site that is considerably slower than that of water, something less than 0.2 s^{-1}. Otherwise, sigmoidal kinetics would be observed. The following scheme can be used to consider the NH_3 interactions with the WOC. For the S_3 state NH_3 binding (k_{ON}) was estimated to be > 30 s (Boussac *et al.,* 1990) which is consistent with this model. The question whether or not NH_3 is interacts at a non-substrate site can not be established from the ^{18}O exchange data. However, that the exchange kinetics for the two substrate binding sites are affected proportionately by NH_3 suggests that small structural modifications to the catalytic site are involved.

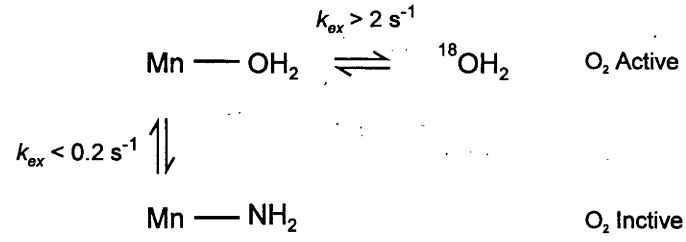

Scheme 4-4 **Substrate binding sites for the centres competent in O_2 evolution activity undergoing ligand exchange with NH_3. The time course of NH_3 exchange is considerably slower than that of water exchange to account for the net decrease in O_2 activity and the absence of sigmoidicity in the substrate water exchange kinetics**

Earlier studies of effects of ethylene glycol on the S_2 multiline Mn suggested that this molecule was able to gain access to the Mn_4 cluster in the WOC whereas sucrose could not (Kawamori *et al.,* 1989). Similarly, addition of ethylene glycol together with NH_3 (Beck & Brudvig, 1986) resulted in g =4.1 signals typical of untreated samples illuminated at 130 K (360 Gauss width, g ~4.1) whereas the addition of NH_3 in the presence of sucrose (Andréasson *et al.,* 1988; Ono & Inoue, 1988b) or in the absence of cyroprotectant (Boussac *et al.,* 1990) resulted in a narrower and shifted signal (~300 Guass width, g ~4.2). These findings suggest that ethylene glycol is able to interact closely with the Mn_4 cluster in the S_2 state and block NH_3 interactions resulting in the g =4.1 signal.

The addition of 30% ethylene glycol to PSII sample also has effects on the ^{18}O exchange rates. The measured exchange in the presence of 30% ethylene glycol show that the slow phase of exchange is decreased by about a factor of ~2.6 and that the fast phase is decreased by only a factor of ~1.2 relative to the control (Table 3.11). The difference in the fast phase of exchange is within the error and strongly suggests that ethylene glycol interacts only with one of the substrate binding sites. The nature of this interaction is curious as the two substrate water molecules, if bound to the Mn_4 cluster, are likely to be in close proximity in preparation for the O-O bond forming step. An explanation for this result may lie with regard to the dielectric constant of ethylene glycol, which is about half that of water, and possibly affects only one of the sites. This slowing in the exchange at one of the sites is unrelated to the steady-state rates of O_2 activity as there is no net effect of ethylene glycol on the O_2 yield or the Kok parameters (Table 3.6). Thus, small structural changes within the WOC may result in slower exchange kinetics without necessarily affecting the activity at the catalytic site. Future work is needed to determine more about this interaction.

The above experiments performed on the S_3 state suggest in general that subtle structural changes of the WOC can result in small effects on the binding affinity of the substrate water. Generally speaking, the exchange rates became slower after perturbation indicating that the substrate water becomes more tightly bound to the metal site. There was, however, one exception. Upon Sr^{2+} reconstitution of a Ca^{2+} depleted sample (Table 3.8), the ^{18}O exchange rate for slow phase of exchange ($^{34}k_1$, ^{36}k) specifically increases. The change in energy is quite small, however, in the order of ~1-2 kJ mol^{-1}, but the interactions between the substrate water and its binding site is clearly made weaker. In contrast, the fast phase of ^{18}O exchange decreases (Table 3.8). The nature of the Sr^{2+} interaction is unclear but is could reflect long range interactions by the Ca^{2+} binding site, similar to those which have been suggested to occur on the acceptor side of PSII (Andréasson *et al.*, 1995). Thus, the Ca^{2+} binding site may not necessarily be close to the substrate water binding site.

One of the active questions on the mechanism of photosynthetic water oxidation is what is the involvement of Cl^- ions in the reaction sequence. Many current models for water oxidation invoke a function for Cl^- in charge neutralisation in the higher S-states (Pecoraro *et al.*, 1998; Tommos & Babcock, 1998). Thus far, however, it has been exceedingly difficult to identify unambiguously the presence of Cl^- ions to the Mn_4 cluster. Magnetic resonance techniques are hampered due to the inhomogenous broadening of the EPR signal and the large Cl^- quadrupolar coupling while EXAFS measurements lack resolution (although a recent EXAFS measurement is now supportive of a Cl ligand to the Mn, see Conference Abstract, Fernandez *et al.*, 1998, *11th International Congress on Photosynthesis*, Hungary). Quantitative $^{36}Cl^-$ measurements do indicate that there is one Cl^- ion present per PSII which exchanges very slowly with $k_{ex} = 3 \times 10^{-4}$ s^{-1} (Lindberg *et al.*, 1993). Based on the magnitude of this Cl^- exchange rate it is attractive to suggest that it may be bound to a Mn^{III} or a Mn^{IV} ion.

The ^{18}O exchange measurements of Cl^- depleted PSII samples reported here are also somewhat ambiguous (Section 3.3.4) mainly because the amount of bound Cl^- is not precisely known; this indeed has been the problem with most of the Cl^- studies. The ^{18}O exchange rates in the Br^- reconstituted sample in comparison to the 'Cl depleted' sample exhibit relatively small changes of ~1.3 at most (Table 3.9). Comparisons of water exchange in Fe^{III}/Cr^{III} systems indicates that the substitution of Cl^- with Br^- can result in only minor changes in the exchange rates (Grant & Jordan, 1981; Xu *et al.*, 1985). Thus, the small differences in the exchange rates between the 'Cl depleted' sample and the Br^- reconstituted sample may well be consistent with the direct effect of a halogen at the Mn_4

cluster. Alternatively, the small differences the exchange may also be simply a consequence of minor structural changes within the WOC.

4.3.5 A H-Bonded Substrate Water Molecule

In an attempt to get information on the role of H-bonding, ^{18}O exchange in the S_3 state was measured in the presence of D_2O (Section 3.3.8). The results show that only the fast phase of exchange was affected, with a net increase in the rate (Table 3.12). The derived k_H/k_D ratio for the fast phase therefore is less than one (inverted) and by definition is indicative of a secondary isotope effect where a deuterated bond is more strongly bound in a transition state of the chemical exchange process (Cleland, 1995). Thus, it is likely that there is H-bonding to the substrate water molecule, which upon deuteration, becomes stronger and reduces the energy barrier for the transition state during the exchange reaction. The interesting issue in these results is again one of heterogeneity in the effects: only one substrate water molecule seems to be influenced by H-bonding while the other is not.

The pH dependence of the exchange rates in the S_3 state (Figure 3.26) indicates that the p*K*'s for the two substrate binding sites are outside of the pH 5-8 region. This result would favour the idea that the substrate water molecules are minimally monoprotonated, thus allowing for H-bonding interactions to occur with adjacent base(s). However, one can also consider the possibility of a terminal oxo ligand which interact with a nearby H-bond donor group. Terminal oxo ligands are now commonly considered as intermediates in the water oxidation reaction (Messinger *et al.*, 1995; Hoganson *et al.*, 1995; Wydrzynski *et al.*, 1996; Tommos & Babcock, 1998; Limburg *et al.*, 1999) and it is mechanistically attractive to consider Mn^{IV} as the site of the oxo ligand in the S_3 state. The exchange of a terminal oxo ligand with bulk water would be greatly facilitated by the presence of a H-bond (Scheme 4.2) as discussed earlier (Section 4.2.1.3).

The question is what is the species from which the H-bonding interaction is derived. One possibility is that the 'protonated peroxy species' suggested by Tommos & Babcock, (1998), i.e. Mn^{IV}-O-H...O=Mn^{IV}. A difficulty with this organisation is the need to exchange the oxo ligand on a time scale that is faster than the hydroxo species when both sites are Mn^{IV}. A second possibility is the H-bond interaction is derived from the redox active tyrosine Y_Z. At this point, the distance between Y_Z to the Mn_4 cluster remains somewhat controversial: some reports suggest the dipolar interaction is ~15-20 Å (Kodera *et al.*, 1995) while other reports suggest a much closer interaction of ~8 Å (Dorlet *et al.*,

1998; Peloquin *et al.*, 1998). Possible chemical and/or H-bond interactions between Y_Z and the Mn_4 cluster have been extrapolated from FTIR measurements (Noguchi *et al.*, 1997). However, there is also evidence to suggest H-bonding between Y_Z and adjacent amino acids (Hays *et al.*, 1998).

4.4 Mechanism of Substrate Activation and O-O Bond Formation

A number of models have recently appeared in the literature to account for the water oxidation reaction sequence. Unfortunately, none of the current models are entirely consistent with all of the exchange properties of the substrate water found in this work. Presented below is a summary of the data as a function of S-state which I will use in a phenomenological model to try to explain the ^{18}O exchange behaviour.

S_0 Exchange for one substrate water is ~14 s^{-1} while the other substrate water is either not present or exchanging too fast to measure.

S_1 Exchange for the first substrate water slows down to ~0.02 s^{-1} while the second substrate water is again either not present or exchanging too fast to measure.

S_2 Exchange for the first substrate water increases to ~2 s^{-1} while the second substrate water is still either not present or exchanging too fast to measure.

S_3 Two substrate exchange rates are resolvable: the first remains unchanged compared to S_2 at ~2 s^{-1} while the second appears at ~38 s^{-1}. The exchange rates, activation energies and H-bonding interactions are significantly different for the two substrate water binding sites in this S-state.

The magnitude of the exchange rates and their S-state dependence strongly supports the involvement of two Mn ions as the binding sites for the substrate water. To account for the changes in exchange rates, three principle interpretations are invoked: 1) Mn-centred oxidation events and/or substrate deprotonation events result in a decrease in the exchange rates, and 2) chemical deprotonation of metal ligands binding adjacent to the substrate water results in an increase in the exchange rates, 3) H-bonding facilitates exchange.

From the S-state behaviour in the ^{18}O exchange rate, a sequential oxidation of a Mn binding site or a step-wise deprotonation of substrate ligand is difficult to accommodate. Rather, the data suggest, particularly for the substrate molecule whose exchange can be measured throughout the S-states, that substrate water and Mn binding centre may have

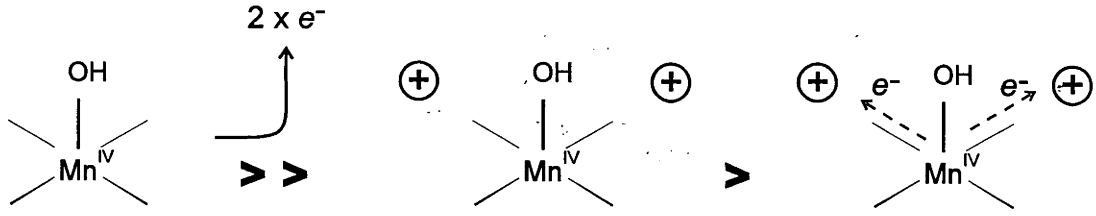

Scheme 4-5 **A *spectator* role of the substrate water molecule bound at a Mn^{IV} site.**

only a *spectator* role up to the S_3 state. This scenario is envisaged in Scheme 4.5 where the substrate water is bound to a Mn^{IV} ion and the oxidation charge is stored on the other Mn ions or in the surrounding protein matrix. The key step in the O-O bond formation would thus be the concerted transfer of the electrons from the bound substrate water to the stored oxidation charges during the last step.

Information on the rate limiting step of O-O bond formation has been studied by a combination of kinetic and isotopic means. Measurements of the O_2 release step indicate that there is only a small k_H/k_D effect of ~1.4 during the S_3-S_4-S_0 transition (Sinclair & Arnason, 1974; Krohs & Metzner, 1990) and measurements of ^{18}O discrimination for O_2 evolution derive a negligible isotopic discrimination (Δ = -0.06 ‰ for O_2 evolution (Guy et al., 1993) while respiration for example exhibits a Δ of ~25 ‰ (Lane & Dole, 1956)). At first glance, the small k_H/k_D effect and ^{18}O discrimination suggest that the limiting step for O_2 evolution reaction has a very low zero-point energy difference and would potentially argue against bond breakage chemistry as being involved in the rate limiting step. But kinetic isotope values are diminished in so-called three-centred interactions (Kresge, 1977) and current concepts for water oxidation now consider that proton-coupled electron transfers are involved, to support a H abstraction mechanism (Lydakis-Simantiris *et al.*, 1997). However, it is well known that the electron transfer step from the Mn to the tyrosine Y_Z^{OX} on the S_3-S_4-S_0 transition is considerably slower than all three preceding electron transfer steps combined (Babcock *et al.*, 1976; Razeghifard *et al.*, 1997) and has a ~100 μs lag phase (Rappaport *et al.*, 1994; Haumann *et al.*, 1997; Razeghifard & Pace *submitted*). The lag phase might suggest that the $S_3 \rightarrow S_4$ transition is limited by the final withdrawal of an electron from the Mn centre or from the substrate water itself. Recent proposals for the O-O bond formation have invoked a Mn^V intermediate in the S_4 state (Pecoraro *et al.*, 1998; Limburg *et al.*, 1999). It is possible to consider that some sort of intermediate state, such as $Mn^{IV}{\equiv}O^+ \Leftrightarrow Mn^V{=}O$ (Messinger *et al.*, 1995; Wydrzynski *et al.*,

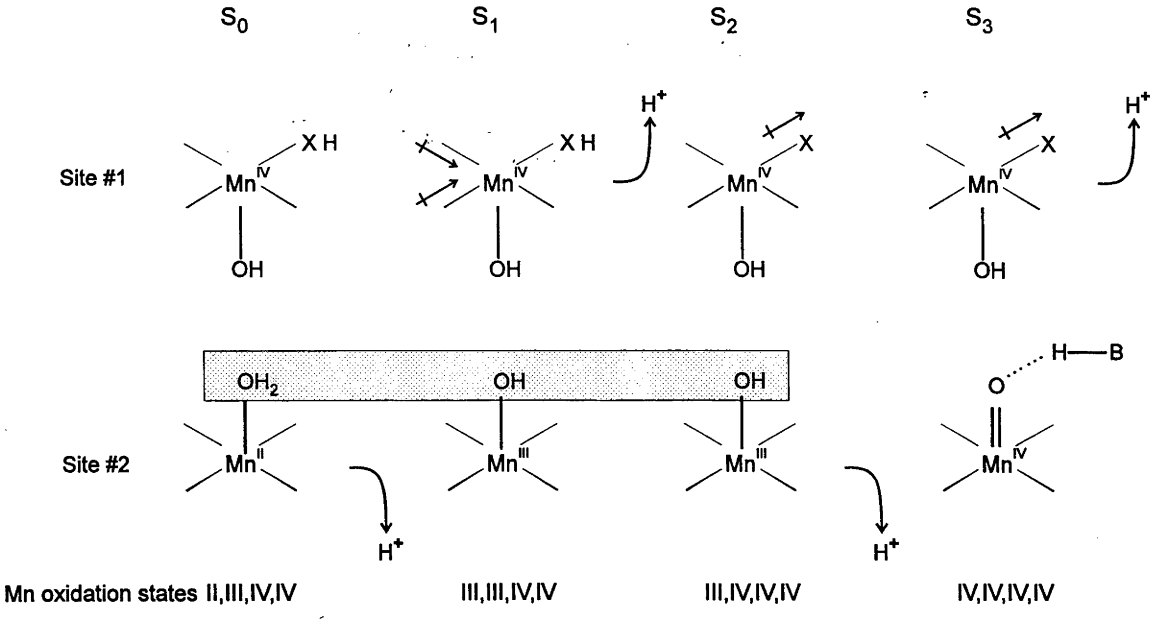

Scheme 4-6 Phenomenological scheme to account for the ^{18}O exchange behaviour of the substrate water molecules. The grey fill represents water exchange unresolved in these measurements. See text for details.

1996) accounts for the lag phase and the delay is electron transfer from the Mn^{IV} ion species before the final O-O bond generating step.

To account for the exchange behaviour of the two substrate water molecules the following phenomenological model can therefore be considered. The S_3 state clearly exhibits two separate exchange phases whose kinetics are different but not greatly so when compared to the changes that occur over the S-state advancements. Thus, the S_3 state is considered to be arranged with two Mn^{IV} centres: site #1, which binds the substrate as a hydroxyl ligand, and site #2, which binds the substrate as a H-bonded oxo ligand. Site #1 would represent the slow exchange phase in the S_3 state and constitute the Mn centre that does not undergo any formal oxidation state change, while site #2 would represent the fast exchange phase and exhibit the interactions with a nearby H donor group. The sites are illustrated in Scheme 4.6.

During the $S_0 \rightarrow S_1$ transition, site #1 would experience an increase in electron density due to the formal oxidation increase at site #2, thus accounting for a slowing down in the exchange rate. During the $S_1 \rightarrow S_2$ transition, site #1 would then undergo a chemical deprotonation of an adjacent ligand which would cause an increase in the substrate water exchange rate. During $S_2 \rightarrow S_3$ no change would occur at this site.

Site #2 is predicted to undergo the metal centred oxidations and is fully reduced to Mn^{II} in S_0 to account for the XANES measurements (Yachandra *et al.*, 1996; Luzzolino *et al.*, 1998; Messinger, *personal communication*). As such, the substrate would most likely be bound as a whole water molecule and undergo very rapid exchange. During the $S_0 \rightarrow S_1$ transition site #2 is oxidised formally to a Mn^{III} with a deprotonation event, but the bound substrate water would still be in very fast exchange. On the $S_1 \rightarrow S_2$ transition two situations may be possible. One is that there is a formal oxidation increase at site #2 to Mn^{IV}. But the bound substrate would still be in very fast exchange because of ligand arrangements and the formation of H-bonding. Alternatively, the oxidation on the $S_1 \rightarrow S_2$ transition occurs at another location in the complex and the bound substrate remains in fast exchange as in the S_1 state. During the $S_2 \rightarrow S_3$ transition, according to the first possibility, an oxidation elsewhere in the complex would have to occur to maintain Mn^{IV} at site #2 but which promotes the formation of a terminal oxo ligand as the activation step for this substrate molecule. According to the second possibility, there would be a formal oxidation from Mn^{III} to Mn^{IV} which then activates the bound substrate molecule to a terminal oxo ligand.

On the final $S_3 \rightarrow S_4 \rightarrow S_0$ transition, the *spectator* substrate bound to site #1 would be activated by electron movement out of the site thereby activating it to another terminal oxo ligand. The O-O bond formation step would then rapidly follow from the condensation of the two terminal oxo ligands at sites #1 and #2 and the dioxygen product would consequentially be released

4.5 Future Research Directions

I wish to conclude the thesis by noting that the model presented above is merely phenomenological. Considerably more chemical details in the overall reaction scheme are needed before the true nature of the S-state transitions can be determined. If the substrate water is involved in a spectator role then further characterisation of the two binding sites in terms of their formal oxidation states and ligand nature need to be determined. The question of whether or not the substrate water in fast exchange is present in the S_0, S_1, and S_2 states also needs to be addressed, possibly by NMR techniques. Finally, identification of the ligands, possibly via low frequency FTIR measurements is needed to clarify the nature of the substrate water.

The immediate extensions to the ^{18}O exchange studies could include a vast array of measurements as a function of S-state. One key piece of missing data is the activation energy for S_0 state. Further recent improvements in the instrumentation at RSBS have been made that would facilitate this measurement (i.e. the purchase of a new Micromass mass spectrometer with multiple channel and improved S/N). Additional measurements on the pH dependence of the exchange in all of the S-state would be of considerable value in order to help establish the nature of the bound substrate water molecules. Other important possible measurements include a detailed examination of the interactions of Sr^{2+} reconstituted samples, particularly in relation to the recent the suggestion that the ligation to Ca^{2+} changes upon the $S_1 \rightarrow S_2$ transition (Noguchi *et al.*, 1996). The issue too of Cl^- involvement as a function of S-state needs to be addressed in combination with the use of $^{36}Cl^-$ to quantify anion binding. It would also be very important to examine site-directed mutants in cyanobacteria to get more information on the role of the protein environment surrounding the catalytic site, although an obvious requirements here is that only O_2 evolving systems can be measured. Of primary importance in an interpretation of the present results are representative exchange rate measurements of model Mn complexes. A particularly good example for studying the terminal ligand exchange rates (are the $Mn_2L_2^{0,+}$ dimers (L = 2-hydroxy-1,3-bis(3,5-H_2-salicylideneamino)propane (Caudle & Pecoraro, 1997). Other Mn dimers including the classic 2,2'-bipyridine, would be of interest to examine μ-oxo exchange rates.

REFERENCES

Ädelroth, P., Lindberg, K., & Andréasson, L-E. (1995) Studies of Ca^{2+} binding in spinach photosystem II using $^{45}Ca^{2+}$. *Biochemistry 34,* 9021-9027.

Ahlbrink, R., Haumann, M., Cherepanov, D., Bögershausen, O., Mulkidjanian, A., & Junge, W. (1998) Function of tyrosine Z in water oxidation by photosystem II: electrostatical promoter instead of hydrogen abstracter. *Biochemistry 37,* 1131-1142.

Åhrling, K. A., & Pace, R. J. (1995) Simulation of the S_2 state multiline electron paramagnetic resonance signals of photosystem II: A multifrequency approach. *Biophys. J. 68,* 2081-2090.

Åhrling, K. A., Peterson, S., & Styring, S. (1997) An oscillating manganese electron paramagnetic resonance signal from the S_0 state of the oxygen evolving complex in photosystem II. *Biochemistry 36,* 13148-13152.

Åhrling, K. A., Smith, P. J., & Pace, R. J. (1998) Nature of the Mn centers in photosystem II. Modelling and behaviour fo the g = 4 resonances and related signals. *J. Am. Chem. Soc. 120,* 13202-13214.

Åhrling, K. A., & Styring, S. (1999) The manganese cluster in photosystem II investigated by EPR spectroscopy. In *Probing Photosynthesis: Mechanism, Regulation and Adaptation* (M. Yunus, U. Pathre, & P. Mohanty, eds.) (*in press*) Taylor & Francis, London, UK

Åkerlund, H-E., Jansson, C., & Andersson, B. (1982) Reconstitution of photosynthetic water splitting in inside-out thylakoid vesicals and identification of a participating polypeptide. *Biochim. Biophys. Acta 681,* 1-10.

Åkesson, R., Pettersson, L. G. M., Sandström, M., & Wahlgren, U., (1994) Theoretical study on water-exchange reactions of the divalent and trivalent metal ions of the first transition period. *J. Am. Chem. Soc. 116,* 8705-8713.

Allakhverdiev, S. I., Yruela, I., Picorel, R., & Klimov, V. V. (1997) Bicarbonate is an essential constituent of the water-oxidising complex of photosystem II. *Proc. Natl. Acad. Sci. USA 94,* 5050-5054.

Ananyev, G., & Klimov, V. (1989) Interaction of the luminol-peroxidase system with manganese of the water oxidising complex of photosystem II. *Biochemistry (USSR) 54,* 1587-1597.

Ananyev, G., & Dismukes, G. C. (1997) Calcium induces binding and formation of a spin-coupled dimanganese (II,II) center in the apo-water oxidation complex of

photosystem II as a precursor to the functional tetra-Mn/Ca cluster. *Biochemistry 36,* 11342-11350.

Andréasson, L-E., Hansson Ö., & von Schenck, K. (1988) The interaction of ammonia with the photosynthetic oxygen-evolving system. *Biochim. Biophys. Acta 936,* 351-360.

Andréasson, L-E., Vass, I., & Styring, S. (1995) Calcium ion depletion modifies the electron transfer on both the donor and acceptor sides in photosystem II from spinach. *Biochim. Biophys. Acta 1230,* 155-164.

Araga, C., Akabori, K., Sasaki, J., Maeda, A., Shiina, Y., & Toyoshima, Y. (1993) Functional reconstitution of the primary quinone acceptor, Q_A, in the photosystem II core complexes. *Biochim. Biophys. Acta 1142,* 36-42.

Armstrong, W. H., (1992) Polynuclear manganese complexes as models for the photosystem II water oxidation catalyst. In *Manganese redox enzymes* (V. L. Pecoraro, ed.) pp. 261-286, VCH Publishers, New York.

Artz, K., Williams, J. C., Allen, J. P., Fendzian, F., Rautter, J. R., & Lubitz, W. (1997) Relationship between the oxidation potential and electron spin density of the primary electron donor in reaction centers from *Rhodobacter sphaeroides. Proc. Natl. Acad. Sci. USA 94,* 13582-13587.

Aurangzeb, N., Hulme, C. E., McAuliffe, C. A., Pritchard, R. G., Watkinson, M., Bermejo, M. R., Garcia-Deide, A., Rey, M., Sanmartin, J., & Sousa, A. (1994) Crystallographic characterisation of a possible model for photosystem II. *J. Chem. Soc., Chem. Commun. 1994,* 1153-1155.

Babcock, G. T., Blankenship, R. E., & Sauer, K. (1976) Reaction kinetics for positive charge accumulation on the water side of chloroplast Photosystem II. *FEBS Lett. 61,* 286-289.

Bader, K. P., Thibault, P., & Schmid, G. H. (1987) Study on the properties of the S_3-state by mass spectrometry in the filamentous cyanobacterium *Oscillatoria chalybea. Biochim. Biophys. Acta 893,* 564-571.

Beck, W. F., de Paula, J. C., & Brudvig, G. W. (1985) Active and resting states of the O_2-evolving complex of photosystem II. *Biochemistry 24,* 3035-3043.

Beck, W. F., & Brudvig, G. W. (1986) Binding of amines to the O_2-evolving center of photosystem II. *Biochemistry 25,* 6479-6486.

Beck, W. F., de Paula, J. C., & Brudvig, G. W. (1986) Ammonia binds to the manganese site of the O_2-evolving complex of photosystem II in the S_2 state. *J. Am. Chem. Soc. 108,* 4018-4022.

Beck, W. F., & Brudvig, G. W. (1988) Resolution of the paradox of ammonia and hydroxylamine as substrate analogues for the water oxidising reaction catalysed by photosystem II. *J Am. Chem. Soc. 110,* 1517-1523.

Berg, S. P., & Seibert, M. (1987) Is functional manganese involved in hydrogen-peroxide-stimulated anomalous oxygen evolution in $CaCl_2$-washed photosystem II membranes? *Photosynth. Res. 13,* 3-17.

Bernadou, J., Fabiano, A-S., Robert, A., & Meunier, B. (1994) "Redox tautomerism" in high-valent-metal-oxo-aquo complexes. Origin of the oxygen atom in epoxidation reactions catalysed by water soluble metalloporphyrins. *J. Am. Chem. Soc. 116,* 9375-9376.

Berthold, D. A., Babcock, G. T., & Yocum, C. F. (1981) A highly resolved, oxygen-evolving photosystem II preparation from spinach thylakoid membranes. *FEBS Lett. 13,* 231-233.

Berthomieu, C., Hienerwadel, R., Boussac, A., Breton, J., & Diner, B. A. (1998) Hydrogen bonding of redox-active tyrosine Z of photosystem II probed by FTIR difference spectroscopy. *Biochemistry 37,* 10547-10553.

Blomberg, M. R. A., & Siegbahn, P. E. M. (1997a) A comparative study of high-spin manganese and iron complexes. *Theor. Chem. Acc. 97,* 72-80.

Blomberg, M. R. A., Siegbahn, P. E. M., Styring, S., Babcock, G. T., Åkermark, B. & Korall, P. (1997b) A quantum chemical study of hydrogen abstraction from manganese-coordinated water by a tyrosyl radical: a model for water oxidation in photosystem II. *J. Am. Chem. Soc. 119,* 8285-8292.

Booth, P. J., Rutherford, A. W., & Boussac, A. (1996) Location of the calcium binding site in photosystem II: A Mn^{2+} substitution study. *Biochim. Biophys. Acta 1277,* 127-134.

Bouges, B. (1971) Action de faibles concentrations d'hydroxylamine sur emission d'oxygene des algues Chlorella et des chloroplasts d'épinards. *Biochim. Biophys. Acta 234,* 103-112.

Bouges-Bocquet, B. (1973) Limiting steps in photosystem II an water decomposition in *Chlorella* and spinach chloroplasts. *Biochim. Biophys. Acta 292,* 772-785.

Boussac, A., & Rutherford, A. W. (1988) Nature of the inhibition of the oxygen-evolving enzyme of Photosystem II induced by NaCl washing and reversed by the addition of Ca^{2+} and Sr^{2+}. *Biochemistry 27,* 3476-3483.

Boussac, A., Zimmermann, J. L., & Rutherford, A. W. (1989) EPR signals from modified charge accumulation states of the oxygen evolving enzyme in Ca^{2+} deficient Photosystem II. *Biochemistry 28,* 8984-8989.

Boussac, A., & Rutherford, A. W., & Styring, S. (1990) Interaction of ammonia with respect with the water splitting enzyme of photosystem II. *Biochemistry 29,* 24-32.

Boussac, A., & Rutherford, A. W. (1992a) The involvement of Ca^{2+} in the Ca^{2+}-effect on photosystem II oxygen evolution. *Photosynth. Res. 32,* 207-209.

Boussac, A., Sétif, P., & Rutherford, A. W. (1992b) Inhibition of tyrosine Z photooxidation after formation of the S_3-state in Ca^{2+} depleted and Cl^- depleted photosystem II. *Biochemistry 31,* 1224-1234.

Boussac, A. & Rutherford, A. W. (1994) The oxygen-evolution enzyme: effects of calcium and chloride ions. *Biochem. Soc. Trans. 22,* 352-358.

Boussac, A. (1995) Exchange of chloride by bromide in the manganese photosystem II complex as studied by cw- and pulsed-EPR. *Chem. Phys. 194,* 409-418.

Bögershausen, O., Haumann, M., & Junge, W. (1996) Photosynthetic oxygen evolution: H/D isotope effects and the coupling between electrons and proton transfer during transitions $S_2 \rightarrow S_3$ and $S_3 \rightarrow S_4 \rightarrow S_0$. *Ber. Bunsenges. Phys. Chem. 100,* 1987-1992.

Brettel, K., Schlodder, E. and Witt, H. T. (1984) Nanosecond reduction kinetics of photooxidised chlorophyll a_{II} (P-680) in single flashes as a probe for the electron pathway, H^+-release and charge accumulation in the O_2- evolving complex *Biochim. Biophys. Acta 766,* 403-415.

Bricker., T. M. (1992) Oxygen evolution in the absence of the 33 kilodalton manganese-stabilising protein. *Biochemistry 31,* 4623-4628.

Britt, D. R., Zimmermann, J.-L., Sauer, K., & Klein M. P. (1989) Ammonia binds to the catalytic Mn of the oxygen-evolving complex of photosystem II: evidence by electron spin-echo envelope modulation spectroscopy. *J. Am. Chem. Soc. 111,* 3522-3532.

Britt, D. R., Derose, V. J., Yachandra, V. K., Kim, D. H., Sauer, K., & Klein M. P. (1990) Pulsed EPR studies of the manganese center of the oxygen-evolving complex of

photosystem II. In *Current Research in Photosynthesis*, Vol. 1 (M. Baltscheffsky, ed.) pp. 769-772, Kluwer Academic Publishers, The Netherlands.

Britt, D. R. (1996) Oxygen evolution. In *Oxygenic Photosynthesis: The Light Reactions* (D. R. Ort & C. F. Yocum, eds.) pp. 137-164, Kluwer, Dordrecht, The Netherlands.

Brudvig, G. W., & Beck, W. F. (1992) Oxidation-reduction and ligand substitution reactions. In *Manganese Redox Enzymes* (V. L. Pecoraro, ed.) pp. 119-140, VCH Publishers, New York.

Burnap, R. L., & Sherman, L. A. (1991) Deletion mutagenesis in *Synechocystis* sp. PCC 6803 indicates that the Mn-stabilising protein of photosystem II is not essential for O_2 evolution. *Biochemistry 30,* 440-446.

Cammarata, K. V., & Cheniae, G. M. (1987) Studies on 17, 24 kD depleted photosystem II membranes. *Plant Physiol. 84,* 587-595.

Carroll, J. M., & Norton, J. R. (1992) Protonation of a bridging oxo ligand is slow. *J. Am. Chem. Soc. 114,* 8744-8745.

Casey, J. L., & Sauer, K. (1984) EPR detection of a cryogenically photo-generated intermediate in photosynthetic oxygen evolution. *Biochim. Biophys. Acta 767,* 21-28.

Caudle, T., & Pecoraro, V. L. (1997) Thermodynamic viability of hydrogen atom transfer from water coordinated to the oxygen-evolving complex of photosystem II. *J. Am. Chem. Soc. 119,* 3415-3416.

Chen, C., Kazimir, J., & Cheniae, G. M (1995) Calcium modulates the photoassembly of photosystem II Mn_4 - cluster by preventing ligation of non-functional high-valency states of manganese. *Biochemistry 34,* 13511-13526.

Cinco, R. M., Robblee, J. H., Rompel, A., Fernandez, C., Yachandra, V. K., Sauer, K., & Klein, M. P. (1998) Strontium EXAFS reveales the proximity of calcium to the manganese cluster of oxygen-evolving photosystem II. *J. Phys. Chem. B 102,* 8248-8256.

Cleland, W. W. (1995) Isotope effects: Determination of enzyme transition state structure. In *Methods in Enzymology: Enzyme kinetics and mechanism, Vol. 249* (D. L. Purich, ed.) pp. 341-373, Academic Press, Inc., New York.

Comba, P., & Merbach, A. (1987) The titanyl question revisited. *Inorg. Chem. 26,* 1315-1323.

Covington, A. K., Robinson, R. A., & Bates, R. G. (1966) The ionisation constant of deuterium oxide from 5 to 50°. *J. Phys. Chem. 70,* 3820-3824.

Crimp, S. L., Spiccia, L., Krouse, H. R., & Swaddle, T. W. (1994) Early stages of the hydrolysis of chromium(III) in aqueous solution. 9. Kinetics of water exchange on the hydrolytic dimer. *Inorg. Chem. 33,* 465-470.

Czernuszewicz, R. S., Su, Y. O., Stern, M. K., Macor, K. A., Kim. D., Groves, J. T., Spiro, T. G. (1988) Oxomanganese(IV) porphyrins identified by resonance raman and infrared spectroscopy: Weak bonds and the stability of the half-filled t_{2g} subshell. *J. Am. Chem. Soc. 110,* 4158-4165.

Dau, H. (1994) Molecular mechanisms and quantitative models of variable photosystem II fluorescence. *Photochem. Photobiol. 60,* 1-23.

Dau, H., Andrews, J. C., Roelofs, T. A., Latimer, M. J., Liang, W., Yachandra, V. K., Sauer, K., & Klein, M. P. (1995) Structural consequences of ammonia binding to the manganese center of the photosynthetic oxygen-evolving complex: An X-ray absorption spectroscopy study of isotropic and oriented photosystem II particles. *Biochemistry 34,* 5274-5287.

Debé, C. E., Wright, D. W., Pal, S., Bonitatebus, P. J., & Armstrong, W. H. (1998) Tetranuclear manganese-oxo aggregates relevant to the photosynthetic water oxidation center. Crystal structure, spectroscopic properties and reactivity of adamantane-shaped $[Mn_4O_6(bpea)_4]^{4+}$ and the reduced mixed-valance analog $[Mn_4O_6(bpea)_4]^{3+}$. *J. Am. Chem. Soc. 120,* 3704-3716.

Debus, R. J. (1992) The manganese and calcium ions of photosynthetic oxygen evolution. *Biochim. Biophys. Acta 1102,* 269-352.

Delrieu, M.-J. (1976) Inhibition by ammonium chloride of the oxygen yield of photosynthesis. *Biochim. Biophys. Acta 440,* 176-188.

Dekker, J. P. (1992) Optical studies on the oxygen-evolving complex of photosystem II. In *Manganese Redox Enzymes* (V. L. Pecoraro, ed.) pp. 85-103, VCH Publishers, New York.

Denisov, V. P., Halle, B., Peters, J., & Hörlein, H. D. (1995) Residence times of the buried water molecules in bovine pancreatic trypsin inhibitor and its G36S mutant. *Biochemistry 34,* 9046-9051.

Denisov, V. P., & Halle, B. (1996a) Protein hydration dynamics in aqueous solution. *Faraday Discuss. 103,* 227-244.

Denisov, V. P., Peters, J., Hörlein, H. D., & Halle, B. (1996b) Using buried water molecules to explore the energy landscape of proteins. *Nature Struct. Biol. 3,* 505-509.

Dexheimer, S. L., & Klein, M. P. (1992) Detection of a paramagnetic intermediate in the photosynthetic oxygen-evolving complex. *J. Am. Chem. Soc. 114,* 2821-2826.

Diner, B. (1974) Cooperatively between photosystem II centres at the level of primary electron transfer. *Biochim. Biophys. Acta 368,* 371-385.

Diner, B. (1975) Dependence of the turnover and deactivation reactions of photosystem II on the redox state of the pool A varied under anaerobic conditions. In *Proceedings of the third international congress on photosynthesis* (M. Avron, ed.) pp 589-601, Elsevier, Amsterdam, The Netherlands.

Diner, B., & Babcock, G. T. (1996) Photosystem II. In *Oxygenic Photosynthesis: The Light Reactions* (D. R. Ort & C. F. Yocum, eds.) pp. 213-247, Kluwer, Dordrecht, The Netherlands.

Dismukes, G. C., & Siderer, Y. (1981) Intermediates of a polynuclear manganese center involved in photosynthetic water oxidation. *Proc. Natl. Acad. Sci. USA 78,* 274-278.

Dismukes, G. C. (1996) Manganese enzymes with binuclear active sites. *Chem. Rev. 96,* 2909-2926.

Dittmer, J., & Dau, H. (1997) On the influence of multiple scattering contributions to the extended x-ray absorption fine structure (EXAFS) spectra of the photosystem II manganese complex. *Ber. Bunsenges. Phys. Chem. 100,* 1993-1998.

Dorlet, P., Di Valentin, M., Babcock, G. T., & McCracken, J. L. (1998) Interaction of $Y_Z^{\bullet}$ with its environment in acetate-treated photosystem II membranes and reaction center cores. *J. Phys. Chem. B 102,* 8239-8247.

Dötsch, V., & Wider, G. (1995) Exchange rates of internal water molecules in proteins measured using pulsed field gradients. *J. Am. Chem. Soc. 117,* 6064-6070.

Drljaca, A., Spiccia, L., Krouse, H. R., & Swaddle, T. W. (1996) Kinetics of water exchange on the dihydroxo-bridged rhodium (III) hydrolytic dimer. *Inorg. Chem. 35,* 985-990.

Drljaca, A., Zahl, A., & van Eldik, R. (1998) High-pressure oxygen-17 NMR study on the dihydroxo-bridged rhodium (III) hydrolytic dimer. Mechanistic evidence for a limiting dissociative water exchange pathways. *Inorg. Chem. 37,* 3948-3953.

Ducommun, Y., Newman K. E., & Merbach, A. E. (1980) High-pressure ^{17}O NMR evidence for a gradual mechanistic changeover from I_a to I_d for water exchange on divalent octahedral metal ions going from manganese(II) to nickel(II). *Inorg. Chem. 19,* 3696-3703.

Eaton-Rye, J. J., & Vermaas, W. F. J. (1991) Oligonucleotide-directed mutagenesis of *psbB*, the gene encoding CP47, employing a deletion strain of the cyanobacterium *Synechocystis* sp. 6803. *Plant Mol. Biol. 17,* 1165-1177.

Eigen, M. (1963) Fast elementary steps in chemical reaction mechanisms. *Pure Appl. Chem. 6,* 97-115.

Farkas, D. L., & Malkin, S. (1979) Cold storage of isolated class c chloroplasts: Optimal conditions for stabilisation of photosynthetic activities. *Plant. Physiol. 64,* 942-947.

Fiege, R., Zweygart, W., Bittl, R., Adir, N., Renger, G., & Lubitz, W. (1996) EPR and ENDOR studies on the water oxidising complex of Photosystem II. *Photosynth. Res. 48,* 227-237.

Forbrush, B., Kok, B., & McGloin, M. (1971) Cooperation of charges in photosynthetic O_2 evolution-II. Damping of flash yield oscillation, deactivation. *Photochem. Photobiol. 14,* 307-321.

Ghanotakis, D.F, Babcock, G. T., & Yocum, C. F. (1984) Calcium reconstitutes high rates of oxygen evolution in polypeptide depleted photosystem II preparations. *FEBS Lett. 167,* 127-130.

Ghanotakis, D. F., Demetriou, D. M., & Yocum, C. F. (1987) Isolation and characterisation of an oxygen-evolving Photosystem II reaction centre core preparation and a 28 kDa chl *a*-binding protein. *Biochim. Biophys. Acta 891,* 15-21.

Gilchrist, M. L., Ball, J. A., Randall, D. W., & Britt, R. D. (1995) Proximity of the manganese cluster of photosystem II to the redox-active tyrosine Y_Z. *Proc. Natl. Acad. Sci. USA 92,* 9545-9549.

Glasoe, P. K., & Long, F. A. (1960) Use of glass electrodes to measure acidities in deuterium oxide. *J Phys. Chem. 64,* 188-190.

Govindjee, & van Rensen, J. J. S. (1993) Photosystem II reaction centre and biocarbonate. In *The Photosynthetic Reaction Centre, Vol 1* (J. Deisenhoffer & J Norris, eds.) pp. 357-389. Academic Press, New York.

Grant, M., & Jordan, R. B. (1981) Kinetics of solvent water exchange in iron(III). *Inorg. Chem. 20,* 55-60.

Greenfield, S. R., Seibert, M., Govindjee, & Wasielewski, M. R. (1997) Direct measurment of the effective rate constant for primary charge separation in isolated photosystem II reaction centers. *J Phys. Chem. 101,* 2251-2255.

Groves, J. T., & Stern, M. K. (1988) Synthesis, characterisation, and reactivity of oxomanganese(IV) porphyrin complexes. *J. Am. Chem. Soc. 110,* 8628-8638.

Guy, R. G., Fogel, M. L., & Berry, J. A. (1993) Photosynthetic fractionation of the stable isotopes of oxygen and carbon. *Plant Physiology 101,* 37-47.

Haddy, A., Aasa, R., & Andréasson L-E. (1989) S-band EPR studies of the S_2 state multiline signal from the photosynthetic oxygen-evolving complex. *Biochemistry 28,* 6954-6959.

Hallén, S., & Nilsson, T. (1992) Proton transfer during the reaction between fully reduced cytochrome c oxidase and dioxygen: pH and deuterium isotope effects. *Biochemistry 31,* 11853-11859.

Hansson, Ö., Andréasson, L-E., & Vänngård, T. (1986) Oxygen from water is coordinated to manganese in the S_2 state of photosystem II. *FEBS Lett. 195,* 151-154.

Hansson, Ö., & Wydrzynski, T. (1990) Current perceptions in photosystem II. *Photosynth. Res. 23,* 131-162.

Hashimoto, S., Tatsuno, Y., & Kitagawa, T. (1986a) Resonance raman evidence for oxygen exchange between the Fe^{IV}=O heme and bulk water during enzymic catalysis of horseradish peroxidase and its reaction with the heme-linked ionization. *Proc. Natl. Acad. Sci. USA 83,* 2417-2421.

Hashimoto, S., Teraoka, J., Inubushi, T., & Kitagawa, T. (1986b) Resonance raman study on cytochrome *c* peroxidase and its intermediate. *J. Biol. Chem. 261,* 11110-11118.

Hastings, G., Durrant, J. R., Barber, J., Porter, G., & Klug, D. R. (1993) Observation of pheophytin reduction in photosystem two reaction centers using femtosecond transient absorption spectroscopy. *Biochemistry 31,* 7638-7647.

Haumann, M., & Junge, W. (1994) Extent and rate of proton release by photosynthetic water oxidation is thylakoids: Electrostatic relaxation versus chemical production. *Biochemistry 33,* 864-872.

Haumann, M. & Junge, W. (1996a) Protons and charges. In *Oxygenic Photosynthesis: The Light Reactions* (D. R. Ort & C. F. Yocum, eds.) pp. 165-193, Kluwer, Dordrecht, The Netherlands.

Haumann, M., Drevenstedt, W., Hundelt, M., & Junge, W. (1996b) Photosystem II of green plants. Oxidation and deprotonation of the same component (Histidine?) on the $S_1^* \Rightarrow S_2^*$ in chloride depleted centres as on the $S_2 \Rightarrow S_3$ in controls. *Biochim. Biophys. Acta 1273,* 237-250.

Haumann, M., Bögershausen, O., Cherepanov, D., Ahlbrink, R., & Junge, W. (1997) Photosynthetic oxygen evolution: H/D isotope effects and the coupling between

electron and proton transfer during the redox reaction at the oxidising side of photosystem II. *Photosynth. Res. 51,* 193-208.

Hays, A.-M., Vassiliev, I. R., Goldbeck, J. H., & Debus, R. J. (1998) Role of D1-His190 in proton-coupled electron transfer reactions in photosystem II: A chemical complementation study. *Biochemistry 37,* 11352-11365.

Hillier, W., & Wydrzynski, T. (1993) Increases in peroxide formation by the photosystem II oxygen evolving reactions upon removal of the extrinsic 16, 22 and 33 kDa proteins are reversed by $CaCl_2$ addition. *Photosynth. Res. 38,* 417-424.

Hillier, W., Lukins, P., Seibert, M., & Wydrzynski, T. (1997) Photochemical reactions of photosystem II in ethylene glycol. *Biochemistry 36,* 76-85.

Hoch, G., & Kok, B. (1963) A mass spectrometer inlet system for sampling gases dissolved in liquid phase. *Arch. Biochem. Biophys. 101,* 160-170.

Hoganson, C. W., & Babcock, G. T. (1997) A metalloradical mechanism for the generation of oxygen from water in photosynthesis. *Science 277,* 1953-1956.

Homann, P. H. (1988) The chloride and calcium requirement of photosynthetic water oxidation: effects of pH. *Biochim. Biophys. Acta 934,* 1-13.

Hundelt, M., Haumann, M., & Junge, W. (1997) Cofactor X of photosynthetic water oxidation: Electron transfer, proton release, and electrogenic behaviour in chloride-depleted photosystem II. *Biochim. Biophys. Acta 1321,* 47-60.

Hurst, J. K., Zhou, J., & Lei, Y. (1992) Pathways for water oxidation catalysed by the $[(bpy)_2Ru(OH_2)]_2O^{4+}$ ion. *Inorg. Chem. 31,* 1010-1017.

Ikeuchi, M., Yuasa, M., & Inoue, Y. (1985) Simple and discrete isolation of an O_2 evolving PSII reaction center complex retaining Mn and the 33 kDa protein. *FEBS Lett. 185,* 316-322.

Ikeuchi, M., & Inoue, Y. (1988) A new 4.8-kDa polypeptide intrinsic to the PSII reaction center, as revealed by modified SDS-PAGE with improved resolution of low-molecular-weight proteins. *Plant Cell Physiol. 29,* 1233-1239.

Ikeuchi, M., Takio, K., & Inoue, Y. (1989) N-terminal sequencing of photosystem II low-molecular-mass proteins. 5 and 4.1 kDa components of the O_2-evolving core comples from higher plants. *FEBS Lett. 242,* 263-269.

Iwata, S., Ostermeier, C., Ludwig, B., & Michel, H. (1995) Structure at 2.8 Å resolution of cytochrome c oxidase from *Parancoccus denitrificans. Nature (UK) 376,* 660-669.

Johnson, M. D., & Murmann, R. K. (1983) Isotopic ^{18}O exchange between $VO^{2+}(aq)$ and water. *Inorg. Chem. 22,* 1068-1072.

Joliot, P, Barieri, G. & Chabaud, R. (1969) Un nouveau modéle des centres photochimique du systém II. *Photochem. Photobiol. 10,* 309-329.

Jursinic, P. A., & Dennenberg, R. J. (1990) Oxygen release in leaf discs and thylakoids of peas and photosystem II fragments of spinach. *Biochim. Biophys. Acta 1020,* 195-206.

Karge, M., Irrgang, K-D., & Renger, G. (1997) Analysis of the reaction coordinate of photosynthetic water oxidation by kinetic measurements of 355 nm absorption changes at different temperatures in photosystem II preparations suspended in either H_2O or D_2O. *Biochemistry 36,* 8904-8913.

Kawamori, A., Inai, T., Ono, T., & Inoue, Y. (1989) ENDOR study on the positions of hydrogens close to the manganese cluster in S_2 state of photosystem II. *FEBS Lett. 254,* 219-223.

Kelley, P. M., & Izawa, S. (1978) The role of chloride ion in photosystem II: I. Effects of chloride ion on Photosystem II electron transport and on hydroxylamine inhibition. *Biochim. Biophys. Acta 502,* 198-210.

Kitamura, K., Ozawa, S., Shiina, T., & Toyoshima, Y. (1994) L protein, encoded by *psbL,* restores normal functioning of the primary quinone acceptor, Q_A, in isolated D1/D2/CP47/Cytb-559/I photosystem II reaction center core complex. *FEBS Lett. 354,* 113-116.

Klimov, V. V., Allakhverdiev, S. I., Demeter, S., & Krasnovsky, A. A. (1979) Photoreduction of pheophytin in photosystem 2 of chloroplasts as a function of redox potential of the medium. *Dokl. Akad. Nauk. SSSR 249,* 227-230.

Klimov, V., Ananyev, G., Zastryzhnaya, O., Wydrzynski, T., & Renger, G. (1993) Photoproduction of hydrogen peroxide in Photosystem II membrane fragments: A comparison of four signals. *Photosynth. Res. 38,* 409-416

Klug D. R., Rech, T., Joseph, M., Barber, J., Durrant, J. R., & Porter, G., (1995) Primary processes in isolated Photosystem II reaction centers probed by magic angle transient absorption spectroscopy. *Chem. Phys. 194,* 433-442.

Kodera, Y., Hara, H., Astashkin, A. V., Kawamori, A., & Ono, T.-A. (1995) EPR study of trapped tyrosine Z^+ in Ca-depleted photosystem II. *Biochim. Biophys. Acta 1232,* 43-51.

Kok B., Forbush B., & McGloin, M. (1970) Cooperation of charges in photosynthetic O_2 evolution-1. A linear four step mechanism. *Photochem. Photobiol. 11,* 457-475.

Kok, B., & Velthuys, B. R. (1977) Present status of the O_2 evolving model. In *Research in Photobiology* (A. Castellani, ed.) pp.111-119, Plenum Press, New York.

Koulougliotis, D., Hirsh, D. J., & Bridvig, G. W. (1992) The O_2 evolving center of photosystem II is diamagnetic in the S_1 resting state. *J. Am. Chem. Soc. 114,* 8322-8323.

Kramarz, K. W., & Norton, J. R. (1994) Slow proton-transfer reactions in organometallic and bioinorganic chemistry. In *Progress in Inorganic Chemistry, Vol 42* (K. D. Karlin, ed.) pp. 1-65, John Wiley & Sons, Inc., New York.

Kresge, A. J. (1977) Magnitude of primary hydrogen isotope effects. In *Isotope effects on enzyme-catalysed reactions* (W. W. Cleland, M. H. O'Leary & D. B. Northrop, eds.) pp. 37-63, University Park Press, Baltimore.

Krieger, A., Rutherford, A. W., & Johnson, G. N. (1995) On the determination of redox midpoint potential of the primary quinone electron acceptor, Q_A, in photosystem II. *Biochim. Biophys. Acta 1229,* 193-201.

Krishtalik, L. I. (1990) Activation energy of photosynthetic oxygen evolution: an attempt at theoretical analysis. *Bioelectrochem. Bioenerg. 23,* 249-263.

Krohs, U., & Metzner, H. (1990) Overall kinetics of photosystem II: pH dependence and deuterium isotope effect. *Bioelectrochem. Bioenerg. 23,* 141-152.

Kuhn, M. G., & Vermaas, W. F. J. (1993) Deletion mutations in a long hydrophilic loop in the photosystem II chlorophyll-binding protein CP43 in the cyanobacterium *Synechocystis* sp. PPC 6803. *Plant Mol. Biol. 23,* 123-133.

Kusunoki, M., Ono T.-A., Noguchi, T., Inoue, Y., & Oyanagi, H. (1993) Manganese K-edge x-ray absorption spectra of the cycling S-states in the photosynthetic oxygen-evolving system. *Photosynth Res. 38,* 331-339.

Kuwabara, T., & Murata, N. (1982) Inactivation of photosynthetic oxygen evolution and concomitant release of three polypeptides in the photosystem II particles of spinach chloroplasts. *Plant Cell Physiol. 23,* 533-539.

Kuwabara, T., & Murata, N. (1983) Inactivation of photosynthetic oxygen evolution and concomitant release of three polypeptides in the photosystem II particles of spinach chloroplasts. *Plant Cell Physiol. 24,* 741-747.

Kuwabara, T., Miyao, M., Murata, T., Murata, N. (1985) The functioning of 33-kDa protein in the photosynthetic oxygen-evolving system studied by reconstitution experiments. *Biochim. Biophys. Acta 806,* 283-289.

Lane, G. A., & Dole, M. (1956) Fractionation of oxygen isotopes during respiration. *Science 123,* 574-576.

Latimer, M. J., DeRose, V. J., Mukerji, I., Yachandra, V. K., Sauer, K., & Klein, M. P. (1995) Evidence for the proximity of calcium to the manganese cluster of photosystem II: determination by X-ray absorption spectroscopy. *Biochemistry 34,* 10898-10909.

Latimer, M. J., DeRose, V. J., Yachandra, V. K., Sauer, K., & Klein, M. P. (1998) Structural effects of calcium depletion on the manganese cluster of photosystem II: Determination by x-ray absorption spectroscopy. *J. Phys. Chem. B 102,* 8275-8265.

Laurenczy, G., Rapaport, I., Zbinden, D., & Merbach, A. E., (1991) Variable-pressure oxygen-17 NMR study of water exchange on hexaaquarhodium(III) *Mag. Res. Chem. 29,* S45-51.

Lavergne, J. (1991) Improved UV-visible spectra of the S-transitions in the photosynthetic oxygen-evolving system. *Biochim. Biophys. Acta 1060,* 175-188

Lavergne, J. & Junge, W. (1993) Proton release during the redox cycle of the water oxidase. *Photosynth. Res. 38,* 279-296.

Lavorel, J. (1992) Determination of the photosynthetic oxygen release time by amperometry. *Biochim. Biophys. Acta 1101,* 33-40.

Limburg, J., Szalai, V. A., & brudvig, G. W. (1999) A mechanistic and structural model for the formation and reactivity of a Mn^{V}=O species in photosynthetic water oxidation. *J. Chem. Soc., Dalton Trans. (in press).*

Lincoln, S. F. & Merbach, A. E. (1995) Substitution reactions of solvated metal ions. *Adv. Inorg Chem. 42,* 1-88.

Lindberg, K., Wydrzynski, T., Vängård, T., & Andréasson, LE. (1990) Slow release of chloride from $^{36}Cl^-$ labelled photosystem II membranes. *FEBS Lett. 264,* 153-155.

Lindberg, K., Vängård, T., & Andréasson, LE. (1993) Studies of the slowly exchanging chloride in Photosystem II membranes. *Photosynth. Res. 38,* 401-408.

Lindberg, K., & Andréasson, LE. (1996) A one-site, two-state model for the binding of anions in photosystem II. *Biochemistry 35,* 14259-14267.

Lubbers, K., Drevenstedt, W., & Junge, W. (1993) Chloride depletion of photosynthetic water oxidase. *FEBS Lett. 336,* 304-308.

Luzzolino, L., Dittmer, J., Dörner, W., Meyer-Klaucke, W., & Dau, H. (1998) X-ray absorption spectroscopy on layered photosystem II membrane particles suggest manganese oxidation of the oxygen-evolving complex for the S_0-S_1 , S_1-S_2 and S_2-S_3 transitions of the water oxidation cycle. *Biochemistry 37,* 17112-17119.

Lydakis-Simantiris, N., Ghanotakis, D. F., & Babcock, G. T. (1997) Kinetic isotope effects on the reduction of the Y_Z radical in oxygen evolving and tris-washed photosystem II membranes by time-resolved EPR. *Biochim. Biophys. Acta 1322,* 129-140.

Makino, R., Uno, T., Nishimura, Y., Lizuka, T., Tsuboi, M., Ishimura, Y. (1986) Coordination structures and reactivities of compound II in iron and manganese horseradish peroxidase. *J. Biol. Chem. 261,* 8376-8382.

Mayes, S. R., Cook, K. M., Self, S. J., Zhang, Z., & Barber, J. (1991) Deletion of the gene encoding photosystem II 33 kDa protein from *Synechocystis* sp. PCC 6803 does not inactivate water-splitting but increases vulnerability to photoinhibition. *Biochim. Biophys. Acta 1060,* 1-12.

Mayfield, S. P., Bennoun, P., & Rochaix, J-D. (1987) Expression of the nuclear encoded OEE1 protein is required for oxygen evolution and stability of photosystem II particles in *Chlamydomonas reinhardtii. EMBO J. 6,* 313-318.

Messinger, J., Wacker, U., & Renger, G. (1991) Unusually low reactivity of the water oxidase in redox state S_3 toward exogenous reductants. Analysis of the NH_2OH- and NH_2NH_2-induced modifications of flash induced oxygen evolution in isolated spinach thylakoids. *Biochemistry 30,* 7852-7862.

Messinger, J., Schröder, W. P., & Renger, G. (1993) Structure-Function relations in Photosystem II. Effects of temperature and chaotropic agents on the period four oscillations of flash-induced oxygen evolution. *Biochemistry 32,* 7658-7668.

Messinger, J, Badger, M., & Wydrzynski, T. (1995) Detection of *one* slowly exchanging substrate water molecule in the S_3 state of Photosystem II. *Proc. Natl. Acad. Sci. USA 92,* 3209-3213.

Messinger, J. Robblee, J. H., Yu, W. O., Sauer, K., Yachandra, V. K., & Klein, M. P. (1997a) The S_0 state of the oxygen-evolving complex in photosystem II is paramagnetic: detection of an EPR multiline signal. *J. Am. Chem. Soc. 119,* 11349-11350.

Messinger, J., Seaton, G., Wydrzynski, T., Wacker, U., & Renger, G. (1997b) S_{-3} state of the water oxidase in Photosystem II. *Biochemistry 23,* 6862-6873.

Meyer, B., Schlodder, E., Dekker, J. P., & Witt, H. T. (1989) O_2 evolution and Chl a_{II}^+ ($P\text{-}680^+$) nanosecond reduction kinetics in single flashes as a function of pH. *Biochim. Biophys. Acta 974,* 36-43.

Michel, H., & Deisenhofer, J. (1988) Relevance of the photosynthetic reaction center from purple bacteria to the structure of photosystem II. *Biochemistry 27,* 1-7.

Nagatsuka, T., Fukuhara, S., Akabori, K., Toyoshima, Y. (1991) Disintegration and reconstitution of photosystem II reaction centre core complex. II*. Possible involvement of low-molecular-mass proteins in the functioning of Q_A in the PSII reaction center. *Biochim. Biophys. Acta 1057,* 223-231.

Nam, W. & Valentine, J. S. (1993) Reevaluation of the significance of ^{18}O incorporation in metal complex-catalysed oxygenation reactions carried out in the presence of $H_2{}^{18}O$. *J. Am. Chem. Soc. 115,* 1772-1778.

Nanba, O., & Satoh, K. (1987) Isolation of a photosystem II reaction center consisting of D-1 and D-2 polypeptides and cytochrome b-559. *Proc. Natl. Acad. Sci. USA 84,* 109-112.

Naruta, Y., Sasayama, M.-a., & Sasaki, T. (1994) Oxygen evolution by oxidation of water wth manganese porphyrin dimers. *Angew. Chem. Int. Ed. Engl. 33,* 1839-1841.

Nick, R. J., Ray, G. B., Fish, K. M., Spiro, T. G., & Groves, J. T. (1991) Evidence for a weak Mn=O bond and a Non-porphyrin radical in manganese-substituted horseradish peroxidase compound I. *J. Am. Chem. Soc. 113,* 1838-1840.

Nouguchi, T., Ono, T-A., & Inoue, Y. (1995) Direct detection of a carboxylate bridge between Mn and Ca^{2+} in the photosynthetic oxygen-evolving center by means of fourier transform infrared spectroscopy. *Biochim. Biophys. Acta 1228,* 189-200.

Nouguchi, T., Inoue, Y., & Tang, X.-S. (1997) Structural coupling between the oxygen-evolving Mn cluster and a tyrosine residue in photosystem II as revealed by fourier transform infrared spectroscopy. *Biochemistry 36,* 14705-14711.

Nugent, J. H. A. (1987) Water binding to the oxygen-evolving system of chloroplasts; effects of isotope substitution on the S_2 state of the EPR spectrum. *Biochim. Biophys. Acta 893,* 184-189.

Nuijs, A. M., van Gorkom, H. J., Plijter, J. J., & Duysens, L. M. N. (1986) Primary charge separation and excitation of chlorophyll a in photosystem II particles from spinach as studies by picosecond absorbance-difference spectroscopy. *Biochim. Biophys. Acta 848,* 167-175.

Okuno, T., & Nishida, Y. (1996) Electron delocalisation in binuclear manganese (III/IV) complexes with di μ-oxo bridges. *Polyhedron 15,* 1509-1515.

Ono, T-A., & Inoue, Y. (1983) Mn-preserving extraction of the 33-, 24- and 16-kDa proteins from O_2-evolving PSII particles by divalent salt washing. *FEBS Lett. 164,* 255-259.

Ono, T-A., & Inoue, Y. (1984) Ca^{2+}-dependent restoration of O_2-evolving activity in $CaCl_2$-washed PSII particles depleted of 33, 24 and 16 kDa proteins. *FEBS Lett. 168,* 281-286.

Ono, T-A., & Inoue, Y. (1988a) Discrete extraction of the Ca atom functional for O_2 evolution in higher plant photosystem II by a simple low pH treatment. *FEBS Lett. 227,* 147-152.

Ono, T-A., & Inoue, Y. (1988b) Abnormal S-state turnovers in NH_3-binding Mn centers of photosynthetic O_2 evolving system. *Arch. Biochem. Biophys. 264,* 82-92.

Ono, T., Noguchi, T., Inoue, Y., Kusunoki, M., Matsushita, Oyanagi, H. (1992) X-ray detection of the period-four cycling of the manganese cluster in photosynthetic water oxidising enzyme. *Science 258,* 1335-1337.

Ono, T., Zimmermann, J. L., Inoue, Y., & Rutherford, A. W. (1986) EPR evidance for a modified S-state transition in chloride-depleted Photosystem II. *Biochim. Biophys. Acta 851,* 193-201.

Otting, G., Liepinsh, E., & Wuthrich, K. (1991) Protein hydration in aqueous solution. *Science 254,* 974-980.

Pauly, S., Schlodder, E., & Witt, H. Y. (1992) The influence of salts on charge separation ($P680^+Q_A^-$) and water oxidation of photosystem II complexes from cyanobacteria: active and inactive conformational states of photosystem II. *Biochim. Biophys. Acta 1099,* 203-210.

Pecoraro, V. L., Baldwin, M. J., & Gleasco, A. (1994) Interactions of manganese with dioxygen and its reduced derivatives. *Chem. Rev. 94,* 807-826.

Pecoraro, V. L., Baldwin, M. J., Caudle, M. T., Hsieh, W-Y., & Law, N. A. (1998) A proposal for water oxidation in photosystem II. *Pure & Appl. Chem. 70,* 925-929.

Peloquin, J. M., Campbell, K. A., & Britt, R. D. (1998) Mn-55 pulsed ENDOR demonstrate that the photosystem II split EPR signal arises from a magnetically-coupled mangano-tyrosyl complex. *J. Am. Chem. Soc.* 120, 6840-6841.

Penner-Hahn, J. E. (1998) Structural characterisation of the Mn site in the photosynthetic oxygen-evolving complex. In *Structure and Bonding, Vol. 90* (H. A. O. Hill, P. J. Sadler, & A. J. Thomson, eds.) pp. 1-36, Springer Verlag, Berlin.

Peterson, S., Åhrling, K. A., & Styring, S. (1999) The EPR signals from the S_0 and S_2 states of the Mn cluster in photosystem II are different. (*submitted*)

Petrouleas, V., & Diner, B. A. (1986) Identification of Q_{400}, a high-potential electron acceptor of photosystem II with the iron of the quinone-iron acceptor complex. *Biochim. Biophys. Acta 849,* 264-275.

Philbrick, J. B., Diner, B. A., & Zilinskas, B. A. (1991) Construction and characterisation of cyanobacterial mutants lacking the manganese-stabilising polypeptide of photosystem II. *J. Biol. Chem. 266,* 13370-13376.

Preston, C., & Seibert, M. (1991) Protease treatments of photosystem II membrane fragments reveal that there are four separate high-affinity Mn-binding sites. *Biochemistry 30,* 9625-9633.

Radmer, R. J., & Kok, B. (1976) Photoreduction of O_2 primes and replaces CO_2 assimilation. *Plant Physiol. 58,* 336-340.

Radmer, R., & Ollinger, O. (1980) Isotopic composition of the photosynthetic O_2 flash yields in the presence of $H_2{}^{18}O$ and $HC^{18}O_3^-$. *FEBS Lett. 110,* 57-61.

Radmer, R,. & Ollinger, O. (1983) Topography of the O_2-evolving site determined with water analogs. *FEBS Lett. 152,* 39-43.

Radmer, R., & Ollinger, O. (1986) Do the higher oxidation states of the photosynthetic O_2-evolving system contain bound H_2O? *FEBS Lett. 195,* 285-289.

Rapaport, I., Helm., L., Merbach, A. E., Berhard, P., & Ludi, A. (1988) Variable-temperature and variable-pressure NMR kinetic study of solvent exchange on $Ru(H_2O)_6^{3+}$, and $Ru(CH_3CN)_6^{2+}$. *Inorg. Chem. 27,* 873-879.

Rappaport, F., Blanchard-Desce, M., & Lavergne, J. (1994) Kinetics of electron transfer and electrochemical change during the redox transitions of the photosynthetic oxygen-evolving complex. *Biochim. Biophys. Acta 1184,* 178-192.

Razeghifard, M. R., Klughammer, C., & Pace, R. J. (1997) Electron paramagnetic resonance kinetic studies on the S-states in spinach thylakoids. *Biochemistry 36,* 86-92.

Razeghifard, M. R., & Pace, R. J. (1998) EPR kinetic studies of oxygen release in thylakoids and PSII membranes: an intermediate in the S_3 to S_0 transition. *(submitted)*

Renger, G. (1997) Mechanistic and structural aspects of photosynthetic water oxidation. *Physiologia Plant. 100,* 828-841.

Rhee, K-H., Morris, E. P., Barber, J., & Kühlbrandt (1998) Three-dimensional structure of the plant Photosystem II at 8-Å resolution. *Nature 396,* 283-286.

Rich, P. R. (1996) Electron transfer complexes coupled to ion translocation. In *Protein electron transfer* (D. S. Bendall, ed.) pp. 217-248, BIOS Scientific Publishers Ltd, Oxford, UK.

Richens, D. T., Helm, L., Pittet, P.-A., Merbach, A. E., Nicoló, F., & Chapuis, G. (1989) Crystal structure of and mechanism of water exchange on $[Mo_3O_4(OH_2)_9]^{4+}$ from x-ray and oxygen-17 NMR studies. *Inorg. Chem. 28,* 1394-1402.

Riggs-Gelasco, P. J., Mei, R., Ghanotakis, D. F., Yocum, C. F., & Penner-Hahn, J. E. (1996) X-ray absorption spectroscopy of calcium-substituted derivatives of the oxygen-evolving complex of photosystem II. *J. Am. Chem. Soc. 118,* 2400-2410.

Robinson, H. H., & Crofts, A. R. (1983) Kinetics on the oxidation-reduction reactions of the photosystem II quinone acceptor complex, and the pathways for deactivation. *FEBS Lett. 153,* 221-226.

Roelofs, T. A., Liang, W., Latimer, M. J., Cinco, R. M., Rompel, A., Andrews, J. C., Sauer, K., Yachandra, V. K., & Klein M. P. (1996) Oxidation states of the manganese cluster during the flash-induced S-state cycle of the photosynthetic oxygen-evolving complex. *Proc. Natl. Acad. Sci. USA 93,* 3335-3340.

Rotzinger, F. P. (1997) Mechanism of water exchange for the di- and trivalent metal hexaaqua ions of the first transition series. *J. Am. Chem. Soc. 119,* 5230-5238.

Rutherford, A. W., Renger, G., Koike, H., & Inoue, Y. (1984) Thermoluminescence as a probe for photosystem II. The redox and protonation states of the secondary acceptor quinone and the O_2-evolving enzyme. *Biochim. Biophys. Acta 767,* 548-556

Rutherford, A. W. (1989) Photosystem II, the water splitting enzyme. *TIBS 14,* 227-232.

Rutherford, A. W. (1992) Oxygen evolution. In *The Photosystems: Structure, Function and Molecular Biology* (J. Barber, ed.) pp. 179-229, Elsevier Science Publishers, Amsterdam, The Netherlands.

Satoh, K., Ohno, T., & Katoh, S. (1985) An oxygen-evolving complex with a simple subunit structure – 'a water-plastoquinone oxidoreductase' – from the thermophylic cyanobacterium *Synechococcus* sp. *FEBS Lett. 180,* 326-330.

Satoh, K. (1996) Photosystem II reaction center. In *Oxygenic Photosynthesis: The Light Reactions* (D. R. Ort & C. F. Yocum, eds.) pp. 193-211, Kluwer, Dordrecht, The Netherlands.

Schatz, G. H., Brock, H., & Holzwarth, A. R. (1987) Picosecond kinetics of fluorescence and absorbance changes in photosystem II particles excited at low photon density. *Proc. Natl. Acad. Sci. USA 54,* 397-405.

Sandusky, P. O., & Yocum, C. F. (1984) The chloride requirement for photosynthetic oxygen evolution: Analysis of the effects of chloride and other anions on amine inhibition of the oxygen-evolving complex. *Biochim. Biophys. Acta 766,* 603-611.

Sandusky, P. O., & Yocum, C. F. (1986) The chloride requirement for photosynthetic oxygen evolution: Factors effecting the nucleophilic displacement of chloride from the oxygen evolving complex. *Biochim. Biophys. Acta 849,* 85-93.

Scheiner, S., & Cuma, M. (1996) Relative stability of hydrogen and deuterium bonds. *J. Am. Chem. Soc. 118,* 1511-1521.

Schiller, H., Dittmer, J., Luzzolino, L., Dörner, W., Meyer-Klaucke, W., Solé, V. A., Nolting, H.-F., & Dau, H. (1998) Structure and orientation of the oxygen-evolving Manganese complex of green algae and higher plants investigated by x-ray absorption linear dichroism spectroscopy on orientated photosystem II membrane particles. *Biochemistry 37,* 7340-7350.

Schowen, K. B., & Schowen, R. L. (1982) Solvent isotope effects on enzyme systems. In *Methods in Enzymology: Enzyme kinetics and mechanism,* Vol. 87 (D. L. Purich, ed.) pp. 551-606, Academic Press, Inc., New York.

Schröder, W. P. and Åkerlund, H-E. (1986) H_2O_2 accessibility to the Photosystem II donor side in protein-depleted inside-out thylakoids measured as flash induced oxygen production. *Biochim. Biophys. Acta 848,* 359-363.

Seidler, A. (1996) The extrinsic polypeptides of photosystem II. *Biochim. Biophys. Acta 1277,* 35-60.

Sharp, R. R., & Yocum, C. F. (1980) The kinetics of water exchange across the chloroplast membrane. *Biochim. Biophys. Acta 592,* 169-184.

Sharp, R. R. (1992) Proton NMR relaxation due to the photosynthetic oxygen-evolving center. In *Manganese Redox Enzymes* (V. L. Pecoraro, ed..) pp. 177-196, VCH Publishers, New York.

Sheats, J. E., Czernuszewicz, R. S., Dismukes, G. C., Rheingold, A. L., Peteouleas, V., Stubbe, J., Armstrong, W. H., Beer, R. H., & Lippard, S. J. (1987) Binuclear manganese (III) complexes of potential biological significance. *J. Am. Chem. Soc. 109,* 1435-1444.

Shen, J-R., Satoh, K., & Katoh, S. (1988) Isolation of an oxygen evolving Photosystem II preparation containing only one tightly bound calcium atom from a chlorophyll b-deficient mutant of rice. *Biochim. Biophys. Acta 936,* 386-393.

Shen, J-R., & Katoh, S. (1991) Inactivation and calcium-dependent reactivation of oxygen evolution in photosystem II preparations treated at pH 3.0 or with high concentrations of NaCl. *Plant Cell Physiol, 32,* 439-446.

Shen, J-R., & Inoue, Y. (1993) Binding and functional properties of the two new extrinsic components, Cytochrome *c*-550 and a 12 kDa protein, in cyanobacterial photosystem II. *Biochemistry 32,* 1825-1832.

Shen, J-R., Burnap, R. L., & Inoue, Y. (1995) An independent role of cytochrome *c*-550 in cyanobacterial photosystem II as revealed by double-deletion mutagenesis of the *psb*O and *psb*V genes in *Synechocystis* sp. PCC 6803. *Biochemistry 34,* 12661-12668.

Shi, L. X., & Schroder, W. P. (1997) Composition and topological studies of the *psb* W protein in spinach thylakoid membrane. *Photosynth. Res. 53,* 45-53.

Siegbahn, P. E. M., & Crabtree, R. H. (1999) Manganese oxyl radical intermediates and O-O bond formation in photosynthetic oxygen evolution and a proposed role for the calcium cofactor of photosystem II. *J. Am. Chem. Soc. 121,* 117-127.

Sinclair, J., Arnason, T., (1974) Studies on a thermal reaction associated with photosynthetic oxygen evolution. *Biochim. Biophys. Acta 368,* 393-400.

Sivaraja, M., Philo, J. S., Lary, J., & Dismukes, G. C. (1989) Photosynthetic oxygen evolution: changes in magnetism of the water-oxidising enzyme. *J. Am. Chem. Soc. 111,* 3221-3225.

Sjöberg, B.-M., Loehr, T. M., & Sanders-Loehr, J. (1982) Raman spectral evidence for a μ-oxo bridge in the binuclear iron center of ribonucleotide reductase. *Biochemistry 21,* 96-102.

Smith, P. J., & Pace, R. J. (1996) Evidence for two forms of the $g = 4.1$ signal in the S_2 state of photosystem II. Two magnetically isolated manganese dimers. *Biochim. Biophys. Acta 1275,* 213-220.

Srinivasan, A. N., & Sharp, R. R. (1986) Flash-induced enhancements in the proton NMR relaxation rate of photosystem II particles: response to flash trains of 1-5 flashes. *Biochim. Biophys. Acta 851,* 369-376.

Styring, S., & Rutherford, A. W. (1987) In the oxygen-evolving complex of photosystem II the S_0 state is oxidised to the S_1 state by D^+ (signal II_{slow}) *Biochemistry 26,* 2401-2405.

Styring, S., & Rutherford, A. W. (1988) The microwave power saturation of SII_{slow} varies with redox state of the oxygen-evolving complex in photosystem II. *Biochemistry 27,* 4915-4933.

Svensson, B., Etchebest, C., Tuffery, P., van Kan, P., Smith, J., & Styring, S. (1996) A model for the photosystem II reaction center core including the structure of the primary donor P-680. *Biochemistry 35,* 10060-10068.

Tamura, N., Inoue, H., & Inoue, Y. (1990) Inactivation of the water-oxidising complex by exogenous reductants in PSII membranes depleted of extrinsic proteins. *Plant Cell Physiol. 31,* 469-477.

Tang, X-S., & Satoh, K. (1985) The oxygen-evolving photosystem II core complex. *FEBS Lett. 179,* 60-64.

Tang, X-S., Fushimi, K., Satoh, K. (1990) D1-D2 complex of the Photosystem II reaction center from spinach: isolation and partial characterisation. *FEBS Lett. 273,* 257-260.

Tang, X-S., Sivaraja, M., & Dismukes, G. C. (1993) Protein and substrate coordination to the manganese cluster in the photosynthetic water oxidising complex: ^{15}N and ^{1}H ENDOR spectroscopy of the S_2 state multiline signal in the thermophilic cyanobacterium *Synechococcus elongatus. J. Am. Chem. Soc. 115,* 2382-2389.

Tang, X-S., Diner, B. A., Larsen, B. S., Gilchrist jr. M. L., Lorigan, G. A., & Britt, R. D. (1994) Identification of histidine at the catalytic site of the photosynthetic oxygen-evolving complex. *Proc. Natl. Acad. Sci. USA 91,* 704-708.

Thompson, R. L., Lee, S., Geib, S. J., & Cooper, N. J. (1993) Intramolecular bridge/terminal oxo exchange within $[Mo^{V}_2O_3]^{4+}$ complexes containing linear oxo bridges. *Inorg. Chem. 32,* 6067-6075.

Tolman, W. B. (1997) Making and breaking the dioxygen bond: New insights from studies of synthetic copper complexes. *Acc. Chem Res. 30,* 227-237.

Tommos, C., & Babcock, G. T. (1998) Oxygen production in nature: a light-driven metalloradical enzyme process. *Acc. Chem Res. 31,* 18-25.

Tommos, C., McCracken, J., Styring, S., & Babcock, G. T. (1998) Stepwise disintegration of the photosynthetic oxygen-evolving complex. *J. Am. Chem. Soc. 120,* 10441-10452.

Tso, J., Sivaraja, M., & Dismukes, G. C. (1991) Calcium limits substrate accessibility or reactivity at the manganese cluster in photosynthetic water oxidation. *Biochemistry 30,* 4734-4739.

Tsukihara, T., Aoyama, H., Yamashita, E., Tomizaki, T., Yamaguchi, H., Shinzawa-Itoh, K., Nakashima, R., Yaono, R., & Yoshikawa, S. (1996) The whole structure of the 13-subunit oxidized cytochrome c oxidase at 2.8 Å. *Science 272,* 1136-1144.

Turconi, S., MacLachlan, D., J., Bratt, P., J., Nugent, J., H., A., & Evans, M., C., W. (1997) Analysis of the interaction of water with the manganese cluster of photosystem II using isotopically labelled water. *Biochemistry 36,* 879-885.

van Leeuwen, P. J., Nieveen, M. C., van de Meent, E. J., Dekker, J. P., & van Gorkom, H. J. (1991) Rapid and simple isolation of pure Photosystem II core and reaction centre particles from spinach. *Photosynth. Res. 28,* 149-153.

Vermaas, W. F. J., Renger, G., & Dohnt, G. (1984) The reduction of the oxygen-evolving system in chloroplasts by thylakoid components. *Biochim. Biophys. Acta 764,* 194-202.

Wasielewski, M. R., Johnson, D. G., Seibert, M., & Govindjee (1989) Determination of the primary charge separation rate in isolated photosystem II reaction centers with 500-fs time resolution. *Proc. Natl. Acad. Sci. USA 86,* 524-528.

Wincencjusz, H., van Gorkom, H. J., & Yocum, C. F. (1997) The photosynthetic oxygen evolving complex requires chloride for its redox state S_2-S_3 and S_3-S_0 transitions but not for S_0-S_1 or S_1-S_2 transitions. *Biochemistry 36,* 3663-3670.

Witt, H. T. (1996) Primary reaction of oxygenic photosynthesis. *Ber. Bunsenges. Phys. Chem. 100,* 1923-1942.

Wydrzynski, T., Zumbulyadis, N., Schmidt, P. G., Gutowsky, H. S., & Govindjee, (1976) Proton relaxation and charge accumulation during oxygen evolution in photosynthesis. *Proc. Natl. Acad. Sci. USA 73,* 1196-1198.

Wydrzynski, T., Marks, S. B., Schmidt, P. G., Govindjee, & Gutowsky, H. S. (1978) Nuclear magnetic relaxation by the manganese in aqueous suspension of chloroplasts. *Biochemistry 17,* 2155-2162.

Wydrzynski, T., & Renger, G. (1986) On the interpretation of the NMR water-proton relaxivity of photosynthetic membrane samples: ramifications in the use of EDTA. *Biochim. Biophys. Acta 851,* 65-74.

Wydrzynski, T. Baumgart, F., MacMillan, F., & Renger, G. (1990) Is there a direct chloride cofactor requirement in the oxygen-evolving reactions of Photosystem II? *Photosynth. Res. 25,* 59-72.

Wydrzynski, T., Hillier, W., & Messinger, J. (1996) On the functional significance of substrate accessibility in the photosynthetic water oxidation mechanism. *Physiol. Plant. 96,* 342-350.

Xiong, J., Subraminiam, S., & Govindjee, (1998) A knowledge-based three dimensional model of the photosystem II reaction centre of *Chlamydomonas reinhardtii. Photosynth. Res. 56,* 229-254.

Xu., F.-C., Krouse, H. R., & Swaddle, T., W., (1985) Conjugate base pathway for water exchange on aqueous chromium (III): Variable-pressure and -temperature kinetic study. *Inorg. Chem. 24,* 267-270.

Yachandra, V. K., Guiles, R. D., Sauer, K., & Klein, M. P. (1986) The state of manganese in the photosynthetic apparatus. 5. The chloride effect in photosynthetic oxygen evolution. Is halide coordinated to the EPR-active manganese in the O_2-evolving complex? Studies of the substructure of the low-temperature multiline EPR signal. *Biochim. Biophys. Acta 850,* 333-342.

Yachandra, V. K., Sauer, K., & Klein, M. P. (1996) Manganese cluster in photosynthesis: where plants oxidise water to dioxygen. *Chem. Rev. 96,* 2927-2950.

Yamaguchi, K. & Sawyer, D. T. (1985) Redox chemistry of the mononuclear tris(picolinato)-, tris(acetylacetibati)-, and tris(8-quinolato) manganese(III) complexes: reaction mimics for the water oxidation cofactor in photosystem II. *Inog. Chem. 24,* 971-976.

Yamauchi, T., Mino, H., Matsukawa, T., Kawamori, A., & Ono, T. (1997) Parallel polarization electron paramagnetic resonance studies of the S_1-state manganese cluster in the photosynthetic oxygen evolving complex. *Biochemistry 36,* 7520-7526.

Yonetani, T., & Asakura, T., (1969) Studies on cytochrome c peroxidase. *J. Biol. Chem. 244,* 4580-4588.

Yruela, I., Allakhverdiev, S. I., Ibarra, J. V., & Klimov, V. V. (1998) Bicarbonate binding to the water-oxidising complex in the photosystem II. A fourier transform infrared spectroscopy study. *FEBS lett. 425,* 396-400.

Zheng, M., & Dismukes, G. C. (1996) Orbital configurations of the valance electrons, ligand field symmetry, and manganese oxidation states of the photosynthetic water complex: Analysis of the S_2 state multiline signals. *Inorg. chem. 35,* 3307-3319.

Zimmermann, J-L., & Rutherford, A. W. (1984) EPR studies of the oxygen-evolving enzyme of photosystem II. *Biochim. Biophys. Acta 767,* 160-167.